Winter 2019

ESTIMATION OF MEASUREMENT UNCERTAINTY OF SEAFLOOR ACOUSTIC BACKSCATTER

Mashkoor Malik
University of New Hampshire, Durham

Follow this and additional works at: https://scholars.unh.edu/dissertation

ESTIMATION OF MEASUREMENT UNCERTAINTY OF SEAFLOOR ACOUSTIC
BACKSCATTER

BY

MASHKOOR MALIK

BSc (Hons.) Marine Sciences, Karachi University, Pakistan, 1998

MS Ocean Engineering (Ocean Mapping), University of New Hampshire, USA, 2005

DISSERTATION

Submitted to the University of New Hampshire

In Partial Fulfillment of

The Requirements for the Degree of

Doctor of Philosophy

In

Earth and Environmental Sciences

December 2019

ESTIMATION OF MEASUREMENT UNCERTAINTY OF SEAFLOOR
ACOUSTIC BACKSCATTER

BY

MASHKOOR MALIK

This dissertation was examined and approved in partial fulfillment of the requirements

for the degree of PhD in Earth and Environmental Sciences by:

Dissertation Director, Dr. Larry Mayer
Professor, Earth Sciences, Director Center for Coastal &
Ocean Mapping, University of New Hampshire, Durham,
NH, USA

Dr. Brian Calder, Research Professor, Ocean
Engineering, Center for Coastal & Ocean Mapping,
University of New Hampshire, Durham, NH, USA

Dr. Anthony Lyons, Research Professor, Ocean
Engineering, Center for Coastal & Ocean Mapping,
University of New Hampshire, Durham, NH, USA

Dr. Xavier Lurton, Research Engineer, French Research
Institute for Exploration of the Sea (IFREMER), Brest,
France

Dr. Thomas Weber, Associate Professor, Mechanical
Engineering, Center for Coastal & Ocean Mapping,
University of New Hampshire, Durham, NH, USA

On 17 October 2019

Approval signatures are on file with the University of New Hampshire Graduate School.

DEDICATION

To my family and teachers

ACKNOWLEDGEMENTS

TABLE OF CONTENTS

LIST OF TABLES

LIST OF FIGURES

ABSTRACT

ESTIMATION OF MEASUREMENT UNCERTAINTY OF SEAFLOOR ACOUSTIC
BACKSCATTER

by

Mashkoor Malik

University of New Hampshire, December 2019

In the last three decades, Multibeam echo sounders (MBES) have become the tool of choice to study the seafloor. MBES collects two distinct types of data: bathymetry that provides topographic details of the seafloor and backscatter that has the potential to characterize the seafloor. While the uncertainty associated with MBE bathymetry has been well studied, the uncertainty in MBES backscatter measurement has received relatively little attention, hindering the improvements in quantitative analysis of backscatter data. Both acquisition and processing stages can introduce uncertainty in the final seafloor backscatter products. Application of well-established uncertainty quantification principles to seafloor backscatter data is challenging for several reasons: the uncertainty sources are not well known, they vary on a case-by-case basis, and standards do not exist for acquisition and processing. This dissertation focuses on assessing uncertainty in backscatter measurements and is comprised of four separate but related studies that identify and address the challenges of uncertainty quantification of backscatter measurements. The first study (Lucieer et al., 2018) which is presented as background, describes an end users' survey identifying key uses and challenges of backscatter data acquisition and processing. The study identified that consistency and repeatability of backscatter measurements is a major constraint in the use and re-use of backscatter. The second study (Malik et al., 2018), identified the sources of uncertainty and categorized them as significant or insignificant based on various use cases. The most significant sources of uncertainty were found to be inherent statistical fluctuations in the backscatter measurement, calibration uncertainty, seafloor slope and water column absorption estimation. While calibration uncertainty remains the main issue in advancing the quantitative use of the backscatter, the other sources were also shown to cause large uncertainties. These include non-standardized methods used to account for

seafloor slope and absorption, and data interpretation errors due to missing background information about the processing procedures. With a comprehensive list of uncertainty sources established, two uncertainty sources, seafloor slope and processing errors, were examined further in the third (Malik, 2019) and the fourth (Malik et al., submitted) study respectively. Seafloor slope corrections are important to correct for both the area insonified and the incidence angle. Both of these corrections are adversely affected if seafloor slope corrections are not applied. Even in cases where the seafloor slope is used, further uncertainty can occur if the highest resolution bathymetry is not used. The results from this study showed that for the purpose of accurate slope corrections, the spatial scale of backscatter data should be selected based on the best available bathymetry. The majority of end users depend on third-party software solutions to process the backscatter data. The fourth study evaluated the output of three commonly used software packages after inputting the same data set and found that there were significant differences in the outputs. This issue was addressed by working closely with software developers to explore options to make the processing chain more transparent. Two intermediate processing stages were proposed and implemented in three commonly used software tools. However, due to proprietary restrictions, it was not possible to know the full details of the software processing packages. Differing outputs likely result, in part, from the different approaches used by the various software packages to read the raw data. Quality assessment and uncertainty quantification of MBES backscatter measurements is still at an early stage and further work is required to develop data acquisition and processing standards to improve consistency in the backscatter acquisition and processing.

Publications:

Lucieer, V.; Roche, M.; Degrendele, K.; Malik, M.; Dolan, M.; Lamarche, G. User expectations for multibeam echo sounders backscatter strength data-looking back into the future. *Mar. Geophys. Res.* **2018**, *39*, 23–40. doi:10.1007/s11001-017-9316-5.

Malik, M.; Lurton, X.; Mayer, L. A framework to quantify uncertainties of seafloor backscatter from swath mapping echosounders. *Mar. Geophys. Res.* **2018**, *39*, 151–168. doi.org/10.1007/s11001-018-9346-7.

Malik, M. Sources and Impacts of Bottom Slope Uncertainty on Estimation of Seafloor Backscatter from Swath Sonars. *Geosciences* **2019**, *9*, 183. doi: 10.3390/geosciences9040183.

Malik, M.; Schimel, A.; Masetti, G.; Roche, M.; Deunf, J.L.; Dolan, M.; Beaudoin, J.; Augustin, J.M.; Hamilton, T.; Parnum, I. Results from the first phase of the Backscatter Software Inter-comparison Project. *Geosciences*. ***Submitted***.

CHAPTER 1

1 INTRODUCTION

Characterization of the seafloor through descriptions of its topography, composition, sediment type, and the presence or absence of living organisms has long been of interest to a broad range of marine scientists [1–3]. Historically, seafloor characterization has relied on direct (e.g., grab samples, cores) and indirect sampling methods (e.g., photographs and video) to determine sediment size, density, and material properties [4–6]. These methods are time-consuming and are representative of just the sites where the samples are taken. In contrast, acoustic seafloor mapping offers broad areal coverage, and the potential for becoming an efficient mechanism for remotely describing seafloor properties.

Early sonar systems were first developed to detect icebergs, and during World War I to detect submarines. Their potential use for studying the seafloor was soon realized, and several types of single-beam echo sounders and sidescan sonars were developed [7]. The first commercial multibeam sonar system (Seabeam), was developed and operated in the late 1970s [8] for bathymetric applications and attempts to use multibeam sonars to characterize the seafloor soon followed [9,10]. Further improvements in hydrographic multibeam sonar technology have focused on improving spatial resolution by increasing the number of beams and decreasing beamwidth, improving the accuracy of the depth measurements, and improving data handling, recording, and processing [11,12]. Most multibeam sonars can provide two fundamental types of data: seafloor depth and seafloor/water column backscatter. While multibeam sonars estimate depth by determining the time of flight of an acoustic pulse transmitted by the sonar at various angles to and from the seafloor, the backscatter is the amount of acoustic energy scattered back from seafloor

and water column targets. The ability of multibeam sonar to provide co-located depth and backscatter data with high spatial resolution over large areal coverage (typically swath width as much as 3–6 times water depth) and the ability to provide precise depth measurements (< 0.1 % of water depth e.g., <5 cm vertical resolution in <100 m water depth) makes multibeam sonar an ideal tool for mapping the seafloor [13] and studying ocean processes [1,14,15]. Water column backscatter from multibeam sonars has also been used in fisheries studies [16] and to detect water column anomalies, such as gas seeps [17,18].

Depths derived from multibeam sonar echo sounders (MBES) have found use in many bathymetric applications, including mapping for nautical charts, port management, and military applications [12,19,20]. On the other hand, seafloor backscatter data have the potential to offer insights into the surficial properties of the seafloor (e.g., sediment type, epifauna, etc.) that are not easily inferred from bathymetric maps. Recognizing the potential of seafloor backscatter data to infer geo-acoustical properties of the seafloor, these data have been used in geological studies [21], ecological monitoring [22,23], offshore oil and gas exploration, surveying of telecommunication and power cable routes, military applications, and habitat mapping [24] with the primary purpose of the backscatter data to infer sediment type.

The complexity of the processes responsible for seafloor backscatter has made the use of backscatter to directly characterize sediment type a difficult task and has led to much research aimed at understanding of interaction of sound with the seafloor. Seafloor backscatter is known to show strong dependence on acoustic frequency, angle of insonification (i.e., angle of incidence) [19,25,26] as well as the geo-acoustical properties of the seafloor. The primary goal of backscatter data processing for seafloor characterization is to remove the effects unrelated to the geo-acoustic properties (such as instrumental, and environmental effects) in order to provide backscatter that is dependent only on the geo-acoustical properties of the seafloor that can then be correlated with its physical properties (e.g., sediment grain size). There is a large body of research that has attempted to correlate the laboratory measurements of the acoustic parameters that can be measured with a sonar (e.g., reflectivity, attenuation) with the laboratory measurements of

2

physical properties of seafloor that are of interest to seafloor researchers (e.g., grain size, porosity, etc.) [27–31]. However, the studies of correlations between physical parameters and remotely measured acoustic parameters need, at minimum, backscatter observations that are consistent, repeatable and above all, accurate.

Quantitative backscatter measurements are critical to advance inversion techniques. From a modeling perspective, reliable backscatter data are essential for the inversion of backscatter data to quantitatively infer physical parameters or to simply compare the measured values with results from theoretical modeling. Although inversion techniques to characterize the seafloor quantitatively have been developing rapidly [32–35], the uncertainty quantification in remote sensing in general, and seafloor backscatter in particular, is a relatively new concept [36–38]. The last two decades have seen a shift from qualitative to more quantitative treatment of backscatter supported by improvement in backscatter data acquisition and processing. With the improved quality of the seafloor backscatter measurements and processing there is a renewed effort to satisfy a broader community of marine scientists as well as those who seek to analyze backscatter data quantitatively [39]. To fulfil this increasing need, however, a better understanding of uncertainty in observed seafloor backscatter measurement is required.

MBES seafloor backscatter uncertainty has been addressed only on a limited basis, mostly in the context of seafloor backscatter variation [26], the comparison of different data sets collected over the same seafloor (see [40]), and efforts to remove observed artifacts in backscatter mosaics [41]. To analyze backscatter data for seafloor characterization, the data must undergo several corrections and adjustments related to the sonar system and survey conditions, including geometric, environmental, and hardware settings. However, the question of what is the overall uncertainty of the seafloor backscatter, after some (or all) corrections and adjustments have been made, remains mostly unanswered. If hardware and environmental adjustments are not fully known, repeated MBES surveys often provide different results even when using the same MBES model [42]. One difficulty is to appropriately calibrate the sonar system used for echo level measurement. Although fisheries sonars have developed detailed calibration routines, calibration data sets for hydrographic MBES (i.e., quantitative measurements of gain,

3

source level, beam width etc.) continue to be difficult to obtain [43–45]. For monitoring applications, comparisons between surveys conducted at different times or by different MBES are needed. Without a detailed knowledge of uncertainty causes and magnitudes, ambiguities arise as to whether the measurement differences represent actual changes in seafloor conditions (e.g., composition vegetation or morphology) or an artifact of unaccounted uncertainty (e.g., changes in system behavior). Additionally, the MBES backscatter measurement process relies on corrections for environmental variables (e.g., seafloor slope and absorption through water column) that may or may not be well known during data acquisition. The accuracy with which these parameters are measured or estimated and the way they are compensated for during post processing will have an impact on the uncertainty of the final backscatter measurement. If appropriate corrections are not correctly or accurately applied, the backscatter measurements reported by the MBES can be highly inaccurate and errors up to 10 dB are not uncommon.

Data acquisition protocols and post-processing steps also vary for different commercial multibeam systems as well as for commercial backscatter processing software products. Unpacking the assumptions used during data acquisition, often requires removing the adjustments and corrections used during data acquisition and replacing them with more accurate and complete adjustments [46]. Thus, there are several potential sources of backscatter uncertainty related to every aspect of backscatter measurement, from data acquisition to the processing stage. Recognizing these challenges and need to improve the consistency of backscatter acquisition and processing, an international working group was launched in 2013. The Backscatter Working Group (BSWG) consists of academic researchers, hardware and software manufacturers and end users. The BSWG compiled their detailed guidelines in a report published in 2015 [15], focused on identifying challenges faced by the backscatter user community. The collaborative model put forward through BSWG participants also influenced this dissertation since one key outcome of BSWG was realization that seafloor backscatter issues will only be solved by working in a cooperative fashion. Two of the studies reported in this dissertation were directly initiated through the BSWG (Chapter 2, 5). Among several recommendations of the working group included improvement in the accuracy and consistency of the backscatter data acquisition

and processing. Identification and categorization of these uncertainty sources is the first step towards improving the backscatter data quality. *The overall goal of this dissertation is to establish approaches for estimating the uncertainty of hydrographic multibeam sonar derived seafloor backscatter through the identification and quantified analysis of the key uncertainty parameters and processes.*

1.1. <u>Organization of the Dissertation</u>

The main body of this document is divided into four chapters (Chapter 2-5) consisting of four stand-alone research papers that have been or will be published:

Chapter 2: Lucieer, V., M. Roche, K. Degrendele, M. Malik, M. Dolan and G. Lamarche (2018). User expectations for multibeam echo sounders backscatter strength data-looking back into the future. *Marine Geophysical Research*, June 2018, Volume 39, Issue 1–2, pp 23–40.

Chapter 3: Malik, M., X. Lurton, and L. Mayer (2018). A framework to quantify uncertainties of seafloor backscatter from swath mapping echosounders. *Marine Geophysical Research*, June 2018, Volume 39, Issue 1–2, pp 151–168.

Chapter 4: Malik, M. (2019). Sources and Impacts of Bottom Slope Uncertainty on Estimation of Seafloor Backscatter from Swath Sonars. *Geosciences*, *9*(4), 183.

Chapter 5: Malik, M.; Schimel, A.; Masetti, G.; Roche, M.; Deunf, J.L.; Dolan, M.; Beaudoin, J.; Augustin, J.M.; Hamilton, T.; Parnum, I. Results from the first phase of the Backscatter Software Inter-comparison Project. *Geosciences. Submitted.*

Chapter 2 provides the background and context for this dissertation by offering insights into the needs of seafloor backscatter users. This study relies on a user survey conducted under the auspices of the Backscatter Working Group (BSWG) [39]. The goal of this survey was to understand diversity of backscatter users, their unique requirements in terms of accuracy and resolution of the backscatter, and their intended use of backscatter. In the absence of a uniform methodology to determine the accuracy of backscatter, the users have been using backscatter as a discovery tool for which comparison among repeated measurements may not be critical. The results of the user survey determined that the lack of backscatter quality assessment is a constraint on standardizing backscatter acquisition and processing as well as the use of backscatter for monitoring applications

where repeated backscatter measurements need to be compared. The users, multibeam manufacturers and multibeam software developers have a shared responsibility to respond to the need to improve backscatter accuracy. Continuing work to understand user needs will bring the diverse applications to adopt a minimum multibeam backscatter standard that is useful for the broader backscatter user community. My contribution to this study included support in design and revision of the questionnaire, analysis of the user survey results, and writing of the manuscript. This study clearly showed that while seafloor backscatter mapping as a qualitative tool has been successful, the users face numerous difficulties while using seafloor backscatter quantitatively. The uncertainty in backscatter surveys was found to be a major hindrance in utilizing seafloor backscatter where repeated surveys or quantitative use of backscatter is required.

Chapter 3 takes a first-order approach to identifying the most significant sources of seafloor backscatter uncertainty. Identification of the significant uncertainty sources and their relative magnitudes provides an initial framework to develop approaches to identifying and evaluating the uncertainty of MBES-derived backscatter. The systematic uncertainty that may result from various commonly used assumptions, data acquisition, and processing methodologies is discussed, and the impact of the uncertainty sources is evaluated. Four major uncertainty components were identified: random fluctuations in the echo level, transmission loss, seafloor slope, and calibration. It was shown that the statistical uncertainty of backscatter can be controlled by averaging a number of samples into a mean echo level with the understanding that increasing this number degrades resolution and thus a trade-off has to be made between resolution and uncertainty. In contrast, the uncertainty stemming from inaccurate values of MBES characteristics can reach unpredictable and unacceptable magnitudes if appropriate calibration operations have not been conducted. The transmission loss uncertainty is almost exclusively due to the absorption coefficient estimation, the inaccurate estimation of which can have a significant impact on the backscatter level estimation. However, the combination of the measurement of temperature and salinity values over the full water column with appropriate procedures for compensation can keep the impact of the absorption coefficient

within acceptable limits. Uncertainty related to seafloor slope and processing methodology are further expanded in Chapters 4 and 5 respectively.

Chapter 4 breaks down the uncertainty sources for seafloor slope into their subcomponents. This study explores the impact of uncertainty in our knowledge of local seafloor slope on the overall accuracy of the backscatter measurement. Amongst the various sources of slope uncertainty studied here, the impacts of bathymetric uncertainty and scale were identified as the major causes. Bottom slope affects two important corrections needed for estimating seafloor backscatter: (1) the insonified area, and (2) the seafloor incidence angle. The impacts of these slope-related uncertainty sources were quantified for a shallow-water multibeam survey. The results show that the most significant uncertainty in backscatter data arises when seafloor slope is not accounted for or when low-resolution bathymetry is used to estimate seafloor slope. This effect is even more pronounced for rough seafloors. A standard method of seafloor slope correction is proposed to achieve repeatable and accurate backscatter results. Additionally, a standard data package including metadata describing the slope corrections applied, needs to accompany backscatter results, and should include details of the slope estimation method and resolution of bathymetry used. As most of the processing tools currently available are proprietary, end users cannot effectively compare the impact of the choice of various available processing methods.

Chapter 5 summarizes the key results of uncertainty that can be introduced in backscatter products due to the differences in processing approaches. In close collaboration with the software vendors, the methodology proposed by Schimel et al. [41] was adapted to produce results from backscatter intermediate processing stages (denoted BL_0, BL_1 etc. – see [41]). The analysis found that output from these intermediate processing stages are currently not consistent across the software developers. The two stages that were assessed during this study included BL_0: data as read from the raw data files using snippets (also referred to as full time series) within beams and BL_3: data after radiometric corrections but before removal of angular dependence for generating a backscatter mosaic. Software developers applied the required corrections in their processing methodologies and provided data in Beam – Ping configuration with BL_0 and BL_3 reported for each beam along with

incidence angle. The differences in BL_0 indicate that proprietary software developers have adopted different approaches to read the raw data. Without complete knowledge of algorithms used by the software developers, it is not possible to describe the exact nature of the differences in reading of raw data for BL_0 data, but having identified that the results are different between software packages, suggests that this is a plausible cause of the differences observed between backscatter mosaics in earlier studies. This preliminary study has shown the applicability and usefulness of access to the output intermediate processing stages for inter-comparison of proprietary software without requiring the software vendors to disclose their proprietary algorithms. Hence, although the scope of this study has been limited to developing a method to understand the differences between the software products, this study suggests that it is critical for sonar manufacturers, commercial and academic software developers, and end users to work together to develop methods that can improve the consistency of backscatter processing. This study offers a first step towards implementation of previously proposed processing protocols. Provided software developers offer the results from their intermediate processing stages, it can be envisioned that data test benches can be developed to aid end users in accessing the processing options available currently in processing tools.

Chapter 6 summarizes the key results of the study and discusses their implications in the context of seafloor characterization. The limitations of this effort are outlined along with the prospective recommendations for future work needed to improve the estimation of uncertainty of seafloor backscatter measurements.

CHAPTER 2

USER EXPECTATIONS FOR MULTIBEAM ECHO SOUNDERS BACKSCATTER STRENGTH DATA-LOOKING BACK INTO THE FUTURE

Abstract With the ability of multibeam echo sounders (MBES) to measure backscatter strength (BS) as a function of true angle of insonification across the seafloor, came a new recognition of the potential of backscatter measurements to remotely characterize the properties of the seafloor. Advances in transducer design, digital electronics, signal processing capabilities, navigation, and graphic display devices, have improved the resolution and particularly the dynamic range available to sonar and processing software manufacturers. Alongside these improvements the expectations of what the data can deliver has also grown. In this paper, we identify these user-expectations and explore how MBES backscatter is utilized by different communities involved in marine seabed research at present, and the aspirations that these communities have for the data in the future. The results presented here are based on a user survey conducted by the GeoHab (Marine Geological and Biological Habitat Mapping) association. This paper summarizes the different processing procedures employed to extract useful information from MBES backscatter data and the various intentions for which the user community collect the data.

We show how a range of backscatter output products are generated from the different processing procedures, and how these results are taken up by different scientific disciplines, and also identify common constraints in handling MBES BS data. Finally, we outline our expectations for the future of this unique and important data source for seafloor mapping and characterization.

2.1. <u>Introduction</u>

The applications for multibeam echosounder (MBES) backscatter data have grown exponentially in the past 30 years since it was first presented as a potential data source for characterizing the seafloor in 1985 by [1]. This paper presents a short review of data use, informed from the results of a survey conducted in 2014 by the International Marine Geological and Biological Habitat Mapping (GeoHab) forum (GeoHab: http://geohab. org/) [the survey can be found at: http://geohab.org/bswg/bswg_participation/userneeds/ (last accessed 28/03/2017)]. This survey revealed both the specific details regarding the current utility of backscatter within the user-community and the range of intended future application areas, which may help shape the future evolution of the technology. The utility of backscatter data can be summarized into two main categories; mapping the seafloor for (a) exploration and (b) monitoring implying different levels of technical constraints. This paper follows on from the report "Backscatter measurements by seafloor-mapping sonars: guidelines and recommendations"[15].

Historically, backscatter data were collected by sonars and interpreted with qualitative descriptive methods [47]. Relevant information would have been extracted by hand-drawing lines around features of interest in the imagery often displayed as a 'waterfall' or backscatter 'mosaic'. Qualitative data extraction existed prior to the development of image processing software that was able to deal with the nature of highly textured backscatter imagery (e.g., large artefacts at nadir, intensively speckled images, acoustic shadows). The outputs of such analysis would have been single-scale interpreted maps which, although basic, would have still provided a wealth of information regarding the continuous nature of benthic substrates or features of interest [48]. Although sidescan sonar may still be a tool of choice for some of the applications, MBES is now becoming

the primary tool for morphological as well as geological and biological mapping and interpretation of the seabed.

Over the last decade or so backscatter data has been commonly recorded during MBES surveys, regardless of their primary purpose. Prior to this backscatter was often seen as a secondary product to bathymetry data, and relatively seldom logged. The upward trend in interest in backscatter data has coincided with substantial improvements in general MBES performance in terms of measurement accuracy and resolution. Improvements in backscatter data quality have come from the multiple and simultaneous advantages of (a) precise co-registration of backscatter with the MBES bathymetry data set, (b) optimal signal-to-noise ratio imposed from bathymetry measurements; and (c) an increased resolution of the physical measurements, leading to a higher resolution products. As seafloor backscatter imagery has improved and the scales of features that are able to be defined become smaller and more spatially accurate, the users' needs and diversity of applications has expanded in a variety of disciplines; ocean science; geoscience [14,49,50] and biology [51], fisheries research and species distribution modelling [52], hydrocarbon detection [53], offshore construction [54] and coastal engineering [55]. This expansion has also coincided with backscatter processing methods becoming quantitative and the classification of MBES backscatter data becoming more robust [38,56]. The uptake may also be related to commercially available backscatter processing software offering greater diversity and more "user friendly" interfaces whereby "end products" can be easily integrated into mapping projects. The characteristics of these improvements, alongside the variety of digital export formats through which the data can now be accessed, have shown how backscatter data has increased to becoming a valuable asset for data users as they seek to image, understand and monitor the seafloor environment.

The past 10 years have seen an increase in MBES data collection (Figure 2.1) and access to data via web-based data portals and a decrease in the costs of survey [57,58].
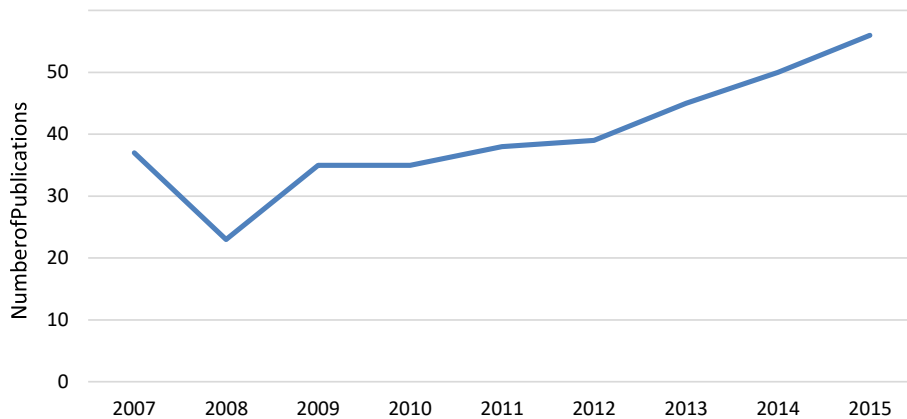
Figure 2.1: Published articles with "acoustic backscatter" in the title between 2007 and 2015. Source: Web of Science.

As the multibeam user group expands beyond traditional hydrographic applications, there has been an outburst of techniques used to collect and process backscatter data. This was clearly identified by the GeoHab association who saw a need to develop protocols for standardizing backscatter acquisition, processing and dissemination. Selecting the appropriate methodology for moving backscatter data through the pipeline from acquisition to seafloor maps has been identified as a major hurdle in moving towards quantitative backscatter measurements of the seafloor. The working group mandated by the GeoHab association identified that before recommendations could be designed for standardizing methods for operations and data handling of backscatter, it was pertinent to try and understand how, where and why backscatter data are being collected. To assess the expectation of users of backscatter data and capture the diversity of applications, a 'user survey' was conducted in 2014 through the Geohab forum.

2.1.1. <u>Design of the user survey</u>

The survey was designed using Survey Monkey (surveymonkey.com) and included 11 sections with each section having between 1 and 7 questions. Most questions included a list of typical answers with drop down menus or tick-off lists to facilitate the interpretation of the results, and an open field was available for unlisted options and questions where categorization was not possible (software usage, organization names etc.).

The survey was distributed by the Backscatter Working Group (http://geohab.org/BSWG/) via email to professional networks (such as LinkedIn' and the Geohab Facebook page) and industry mailing groups. The survey was available for 3 months between May and July 2014.

2.1.2. <u>Results of the user survey</u>

A total of 97 responses were received representing a 10% response rate from the email sent, which considering the specificity of the topic and short time for answering we consider acceptable. The responses were represented by 41% from civilian government agencies, 24% from universities, 31% from private companies and the remaining 4% from government defense agencies.

Within the last 5 years the marine zones of interest where backscatter data has been the most utilized is the near shore coastal zone (<50 m water depth) to identify marine habitats (specifically reef systems, Figure 2.2a). The features of interest were dominated by marine habitats and reefs in particular, followed by wrecks and seagrass (Figure 2.2b). Data currency (Figure 2.2c) (date of data collection) seemed of less relevance to users as long as it was collected within the past 10 years (which is likely when the greatest advances in backscatter data collection have developed). The resolution of the gridded data was preferred to be at 1 m [for a common resolution for coastal research and to correspond to the near shore and coastal requirement of (a) and 10 m for areas >100 m depth (Figure 2.2d)].

The need for higher resolution data for benthic habitat mapping is supported by the literature through an increase in publications for the period 1995–2014 (Figure 2.3), and the number of cases that address scale [59]. Approximately a third of the articles and reviews used the term "scale" in the title, abstract or keywords, with 22% for "spatial scale", <5% for "multiple scales" and 1% for "multiscale"; these numbers are much lower than in landscape ecology-related publications, where scale is still considered as being insufficiently described [60].

The wide variety of background disciplines of the backscatter user community offers an opportunity to expand the use of backscatter but also presents a serious challenge. One of the difficulties for establishing standards for MBES backscatter data acquisition

and processing for such a group, is the diversity of expertise of the users and their associated acoustic and technical knowledge required for appropriate backscatter interpretation. Not only is this the result of user training but also of user experience with backscatter data. In the survey we specifically asked "how many years people had been working with backscatter data" with the results showing that the majority of users had 2–5 years of experience (30.5%) followed by 6–10 years of experience (28%), 11–20 years of experience (24.4%), more than 20 years of experience (12.5%) and <1 year (4.8%). This corresponds with the increase in the literature of backscatter being improved and implemented in research studies (Figure 2.4). The diversity of the user group also hints at the scientists using backscatter data may not be trained in acoustics and may lack a full understanding of the factors that affect backscatter data or how to optimize the data for subsequent analysis. These results correspond to an increase in the number of disciplines that have cited work or published studies on MBES backscatter data in the past 5 years (Figure 2.4).
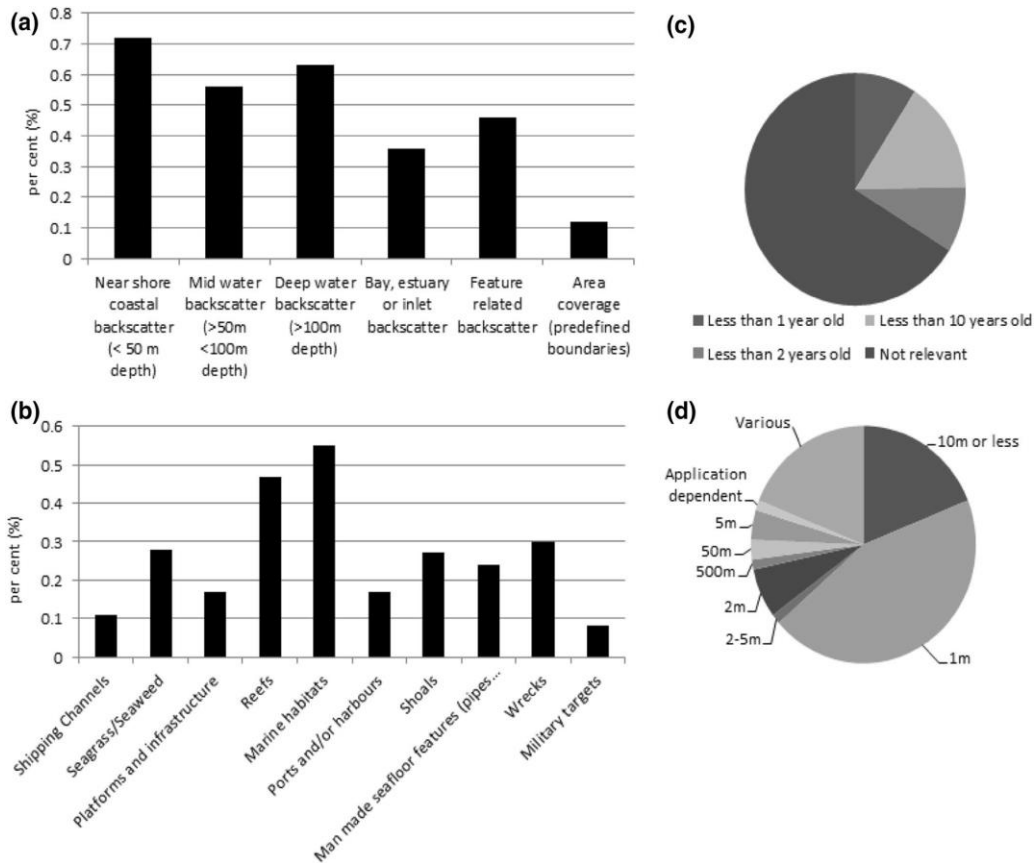
Figure 2.2: (a) Survey response to 'What are the marine zones of interest for your work unit within the last 5 years?' (b) Survey response to 'What are the main backscatter features of interest?' (c) Survey response to "What data currency important to your surveying application" and (d) Survey response to 'When gridded, what resolution of data do you mostly require?'

2.1.3. Users' expectations

Users' expectations were derived from S5 ("problems with using backscatter"), S7 ("Current data needs") and S8 ("What is your expectation of backscatter data in the next 5–10 years?"), and in part from S4Qc ("What problems have you found with obtaining backscatter data?"). The survey also provided a synopsis of the diversity of primary roles that MBES backscatter data underpins through S1 and S2 (Figure 2.5). S1Qd ("What are the primary roles of your work unit?") provides an insight in the primary applications that backscatter data are presented as a fundamental data source for. The top three applications were (a) seafloor type mapping (16%), (b) marine habitat mapping (14%) and (c)

15

bathymetric survey for hydrography only (no further analysis) (10%). These three primary applications are dominated by two disciplines—geology and biology. The ability to use processing methods (either signal or image processing) to discriminate between different seafloors substrates and seafloor habitats at specific spatial resolutions, in addition to improved classification accuracy was highlighted as the key expectation of both disciplines. The realization of this expectation is dependent on the spatial and radiometric resolution of the MBES backscatter data and this will be further discussed in "Mapping for monitoring".

Marine geologists typically use MBES backscatter data to aid in the interpretation of surficial seabed sediments [61–63]. As mentioned earlier, traditionally this had been done using only the amplitude information from MBES backscatter mosaics, together with expert interpretation, following the method already in standard use for interpretation of side-scan data. The interpretation of the MBES backscatter was guided by available ground truth information (video, sediment grabs) and any other available information on the geology of the area. Employing this traditional workflow, the expert would be able to accommodate for variations in backscatter data quality, and/or differences between MBES backscatter dB levels between surveys covering the study area.

Central to the discussion of utilization of backscatter data is a need to understand the diversity of needs of the users of backscatter data. These users collect backscatter data for a variety of reasons ranging from the primary roles identified in Figure 2.5 and can belong to either one of two motivational groups (a) mapping for exploration— where backscatter data are collected as a single survey without any duplication of data over the site or (b) mapping for monitoring—which refers to multiple surveys over the same seabed where the objective is to be able to understand changes on the seafloor.
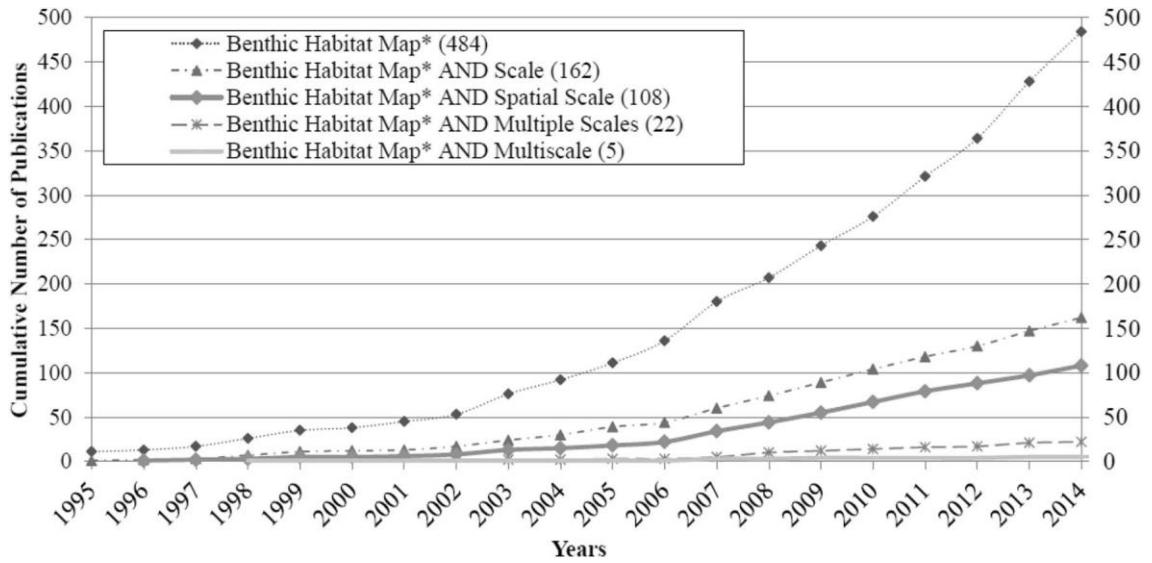
Figure 2.3: Cumulative number of publications (articles or reviews) mentioning specific keywords (see key) in their title, abstract or keywords, by the end of 2014 [59]. Source: Scopus
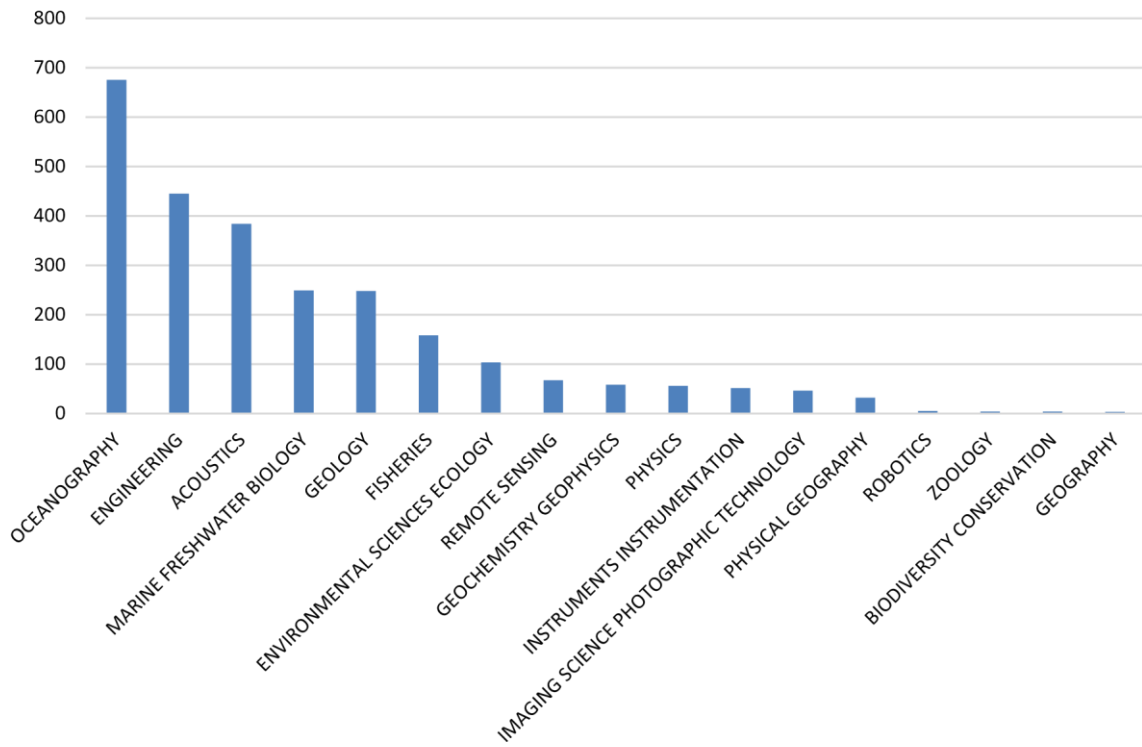
Figure 2.4: Increase in number of disciplines publishing MBES acoustic backscatter in their titles between 2010 and 2015. Source: Web of Science

2.1.4. <u>Mapping for exploration (single pass survey)</u>

The backscatter intensity value (in dB) will vary depending on the acoustic processing method (see [64–66]). In terms of 'mapping for exploration' the stability and precision of the backscatter measurement is of a lower demand due to the end-user objectives of only acquiring one-time series over the survey region.
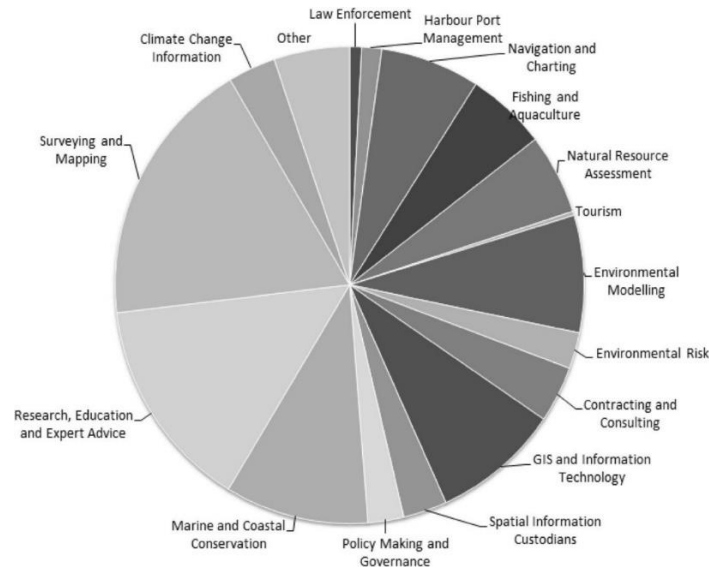
Figure 2.5: Survey response to Q2(d) "What is the primary role of your work unit that utilizes backscatter data?"

In the responses to S2Qd (Figure 2.2) the majority of applications do not require repeated backscatter surveys. These applications typically require only a relative measure of BS level as compared to the applications that require an absolute dB scale, i.e., a value that is calibrated, accurate and stable and can be compared from one survey to another.

In the first row of Figure 2.6A, a schematic of backscatter data is shown as the black line with the true value of backscatter shown as the red line. The backscatter from a homogenous seafloor is expected to show consistent values from repeated measurements validating the stability of the backscatter swath with time. Even if the backscatter shows stable values, backscatter data may be inaccurate. We identified the three survey 'levels', B–D (Figure 2.6) to correspond to single survey mapping for exploration and repeat survey mapping for habitat assessment and benthic monitoring. These are compared in the

following section in terms of the different needs for stability and accuracy of measurements. Backscatter data collected from a single survey with no planned intention to constitute a long-term time series of data nor to compare them later with data from the same (or different) MBES systems, are suitable for exploration purposes (Figure 2.6, left column), as users focus primarily on data processing techniques that allow them to obtain a high contrast, artefact-free backscatter image that can be used to identify and classify substrate boundaries between different types of seabed and/or habitats. In mapping for exploration the resolution and scale of the data being generated is inherently adapted to meet the objectives of the survey; there is usually no planned ongoing program to collect data at the same location in the immediate future. In applications of mapping for exploration the MBES data will form part of the dataset including seabed survey videos, sediment grabs/cores and sub-bottom profile information that may all be simultaneously (or subsequently) collected. These surveys are common to benthic habitat mapping programs that are exploring the seafloor for the first time aiming to collect integrated data on species habitats and facies distribution. In this configuration the MBES backscatter data would be valued for the descriptive image it gives of the seafloor. So backscatter data recorded in such a context is more unlikely to be quantitatively analyzed (such as using angular response curves). Mapping for exploration relies on the visual quality requirements of the backscatter (which is ensured by MBES backscatter stability), rather than on the accuracy in intensity levels. Within this approach a coarser resolution is sufficient for the mapping purpose.

2.1.5. <u>Mapping for monitoring (calibrated-absolute level-multiple pass comparison map)</u>

Prior to raising the expectation that backscatter data can be used for monitoring, a strict evaluation of the multiple sources of variation that can affect the mean backscatter level from one measurement to another is mandatory. Mapping for monitoring objectives require successive measurements of backscatter at the same site under evaluation, in order to observe objectively the sedimentary backscatter over medium to long term time scales (months to years).
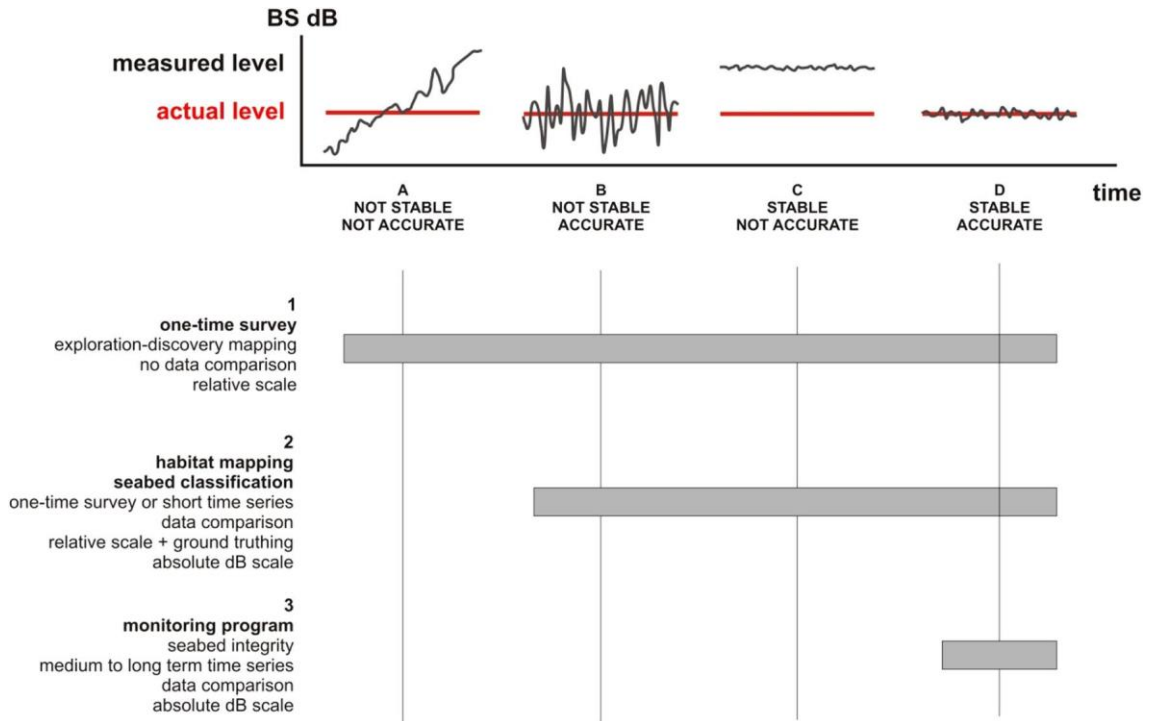
Figure 2.6: Levels of stability and accuracy required for MBES backscatter measurements according to final objectives (single survey, habitat mapping, monitoring program). Image adapted from National Instruments Tutorial http://www.ni.com/tutorial/14705/en/ last accessed 09/03/2017

The vast majority of users who use backscatter to perform habitat mapping (either coupled with or without data classification at control samples) lies somewhere between the two poles A and D of Figure 2.6.

It is important to emphasize that some sources of variations in the backscatter data may cause discrepancies in the reflectivity image that are not obvious in the data [67]. In order to use backscatter for monitoring changes in the nature of the seabed, potential external sources of variation must first be clarified. The first type of variation is related to data acquisition and includes hardware impact causes such as aging antennas, antenna surface condition, potential (but not measured) influence of water column (turbidity, bubbles etc.), platform motion, direction of navigation in relation with seabed morphology, erroneous calibration and biofouling of the transducer head [14,68]. The second type of variation relates to post-processing and includes inconsistency in post-processing software

and workflows. Therefore, for backscatter data to be utilized for monitoring, users need to address three critical issues:

- improving the stability of the collected dB values of backscatter. This requires strict monitoring and control of variability and sources causing variability in the data;

- ensuring repeatability of the measurements by a quantitative comparison between different surveys over a reference surface [the bathymetric equivalent is referred to as a '*patch test*' see Gueriot et al. [69].

- maintaining an estimate of accuracy that informs about usability of measurements to detect changes in the seabed environment despite the measurement uncertainty.

The requirement to compare data acquired by a MBES over time at one specific location by the same sensor will be determined by the particular application. However, there is a strong argument for scientists to work with calibrated MBES systems; as more data are collected and a need arises for data to be (a) merged to generate large geographic coverages, (b) calibrated so that the data can support future data comparison, (c) able to detect natural or human caused changes on the seabed in areas where the data may not have been collected for this purpose. Calibrated backscatter has the potential to serve multiple current and future users and therefore it makes the data more valuable and a better research investment. However, to get calibrated backscatter values, efforts and decisions are required prior to data acquisition possibly causing a prohibitive increase of the survey costs [68]. Also, as the accuracy requirements are not well understood, the users have no way to gauge additional amount of efforts versus benefit of improved accuracy.

The required backscatter accuracy for discrimination of sediment classes can be appraised using the Applied Physics Laboratory (APL) model which "employs a mixture of theory and data fitting and use the same set of bottom parameters" [70]. Figure 2.7 shows, for an acoustic system at 100 kHz, the APL model results for the relationship between the backscatter level and the grazing angle for different sediment types. For each sediment type, the strong angular dependence of backscatter causes a very high dispersion of measurements (15–25 dB across the 0°–80° angle range). The average difference

21

between the mean backscatter levels of the different sediment types is 2 dB for the entire angular range and 3 dB for the most discriminating angular part, from 30° to 60° grazing angle. In terms of accuracy, it may be considered that 1 dB (half of the mean difference) is the order of magnitude of the accuracy necessary to discriminate the classes of sediments from their mean backscatter response in the grazing angle sector of 30°–60°. Hence, 1 dB level of accuracy should be ensured and certified in the technical specification of a MBES system and possibly in the future, within the metadata of MBES output products (see nomenclature proposed by Lurton et al. [15]).

Figure 2.7: Backscatter strength (BS) versus grazing angle for different classes of sediment at 100 kHz. From: University of Washington Applied Physics Laboratory, high-frequency ocean environmental acoustic models, APL-UW TR 9407AEAS 9501, October 1994. Data encoded in Excel to plot the XY graph. Source: Chap. 3 in [15].

The accuracy of BS measurements remains a key issue for the confidence of MBES users' mapping for monitoring [71]. This complex issue is not currently resolved and there is no formal backscatter quality 'scale' (such as IHO standards for bathymetry) and therefore no standardization in reliability for the dB values. For the different backscatter user communities, the development of a total propagation error model for backscatter, based on a rigorous metrological approach, is necessary to objectify the meaning of their backscatter measurements. However, each user can pragmatically assess the variance of its own MBES regarding the backscatter level by performing repeated measures on a same seabed area under stable conditions. Backscatter variance on a short term (e.g., tide cycle)

estimated by this way with shallow water MBES is found to be extremely low (standard deviation of successive backscatter mean levels <0.2 dB for 30°–50° beams) demonstrating that the 1-dB required accuracy could be ensured in routine by shallow water MBES (e.g., [67]).

Post-acquisition corrections depend on the assumptions used during acquisition and attempt to correct for them. If these assumptions are not properly known or not documented, then it may not be possible to implement informed decisions to the data in the processing stage. The standardization of processing algorithms across hardware and software vendors is also a real challenge for using the backscatter to monitor seabed sediment variations. High variations in quality and dB levels between data from various processing software seriously hamper the possibilities of exchange and comparison of backscatter data among geoscientists (Figure 2.8). This has important consequences for users interested in long-term monitoring of the seafloor.
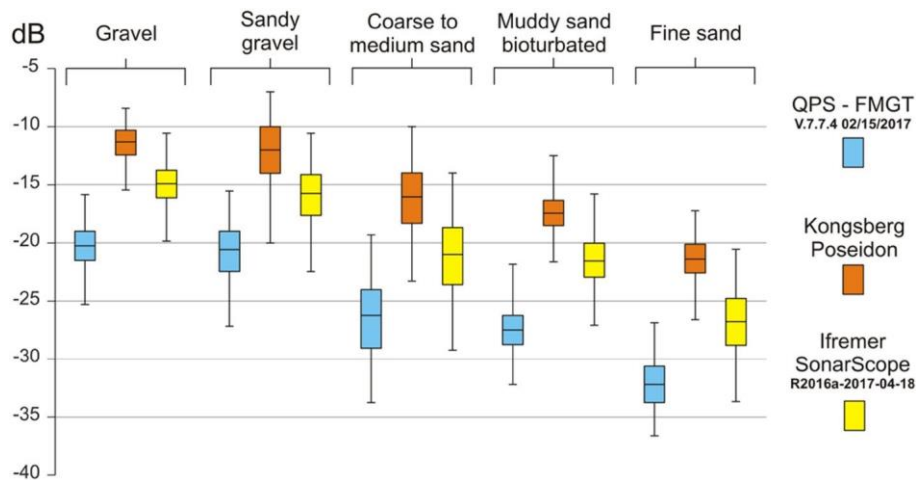
Figure 2.8: Comparison between three commercially available processing software using the same dataset from the Flemish sandbanks region from a Kongsberg EM3002D MBES on RV *Belgica*. Data from campaign 0906–26/02/2009; Processing: Geocoder: 1 × 1 m mosaic using beam time series and defaults settings (Tx/Rx power gain correction, beam pattern correction, calibrated backscatter range and AVG correction); Kongsberg Maritime Poseidon: 1 × 1 m mosaic using beam averaged BS, 2D interpolating filter set on 3, footprint size set on 50%, histogram correction 100%; SonarScope: 1 × 1 m mosaic using beam averaged backscatter, global compensation using BS versus Tx angle mean curve; boxplots computed for each mosaic (same area for each sediment type).

Besides differences in processing protocols, various known and unknown environmental factors can affect the consistency and accuracy of backscatter during data acquisition. Water column properties (e.g., salinity, temperature) and conditions (e.g., bubbles, turbidity, vessel motion) will affect the backscatter values at the transducer interface recorded by a MBES system (even with a calibrated MBES). This is a major issue in coastal areas where changes occur rapidly both in time and space, but can equally be a problem in deep water under rough sea states. To fulfil monitoring requirements, it is absolutely necessary to answer the question: "*how does the mean backscatter amplitude variation, from one survey to another, reflect the significant changes in the seabed properties and are not a result of changes in the conditions of the water column?*". Increased turbidity during changing currents near the seafloor, biological migration, increased occurrence of microbubbles at the sea surface due to wind are few examples of the complexity of modelling the water column variations and their effects on backscatter.

Repeated surveys with a multidisciplinary approach combining MBES and ADCP measurements, optical measurements of sediment load near the seabed, turbidity sensor chains rising into the water column and seawater sampling should be organized in the future in order to assess the influence of the water column on the backscatter measurement at a given location and time. While the precise quantitative effects of environmental parameters are often unknown, monitoring the backscatter data as it is being acquired may indicate if these environmental factors are deteriorating backscatter data quality beyond expected accuracy. For monitoring applications, it should be mandatory that an absolute calibration be followed by regular control of the stability of the mean measured backscatter level. This should be completed and recorded on a reference site and documented by the multiple sources of variation that can affect the mean backscatter level.

2.1.6. Backscatter spatial resolution expected by users?

It appeared from the survey that many users had an expectation for the minimum spatial resolution that they should be able to achieve given a particular water depth (Figure 2.2d). In this section we aim to highlight the discourse between this expectation and what is reasonable to expect in reality and emphasize the significance of BS values.

24

Several criteria can be used to define the spatial resolution of the final BS mosaic. A 'rule of thumb' is to consider that the average resolution of the mosaic must, as far as possible, reflect the actual average spatial resolution as defined by the along and across specific dimensions of the signal footprint. However, even for one given sounder, the footprint extent depends on the measurement configuration (water depth, angle) [19]. The BS time series i.e., the successive echo intensities returned from a finite area of the seafloor inside the beam footprint vary depending on, (a) the pulse length, (b) the beam width along- and across-track, and (c) the slant range (see the Ocean Mapping Group/HydroMetrica course for further details http://www. omg.unb.ca/mbc/). Therefore, the intrinsic spatial resolution of a MBES is not constant. Selection of mosaic resolution therefore should not exceed the maximum footprint size. BS data from modern MBES using a large number of narrow beams (+300), shorter pulse lengths and very high ping rate (50 Hz), can be used to generate mosaics with resolution up to tens of centimeters. However, during the mosaicking process an artificial decrease of the image sampling step can create a misleading impression of extreme resolution.

Besides, the size of the footprint (beam width + water depth) determined by the specific parameters of the system additional factors needs to be considered also while selecting the optimal spatial resolution of the backscatter. Important considerations that users should be aware of with regards to their MBES backscatter data include:

- The optimal cell-size for the backscatter mosaic depends on scale of the output map and the resolution required for the survey. For example, with a scale of 1:10,000, 1 mm on paper corresponds to 10 m on the ground. Since the human eye can perceive around 1/2 mm, a resolution of 5 m is sufficient in this case, and it is not necessary to compute mosaics with finer resolutions even if the initial data allows it. Yet, despite this evidence there seem to be a real push for obtaining the highest possible resolution of backscatter (and bathymetry) data from many users even though it does not directly fit their primary survey purpose. This may often satisfy demand for potential re-use of the data (e.g., for related scientific study) rather than for pure mapping activities.

- When considering the backscatter *mean* level it is not necessary to compute mosaics with a very small grid size (e.g., 0.5×0.5 m). These expectations are comparable to the space-borne radar domain where satellites operate both Synthetic Aperture Radar SAR (meter- or less-resolution for very detailed imaging) and scatterometer (kilometer resolution for averaged BS) for very different applications.

- The spatial resolution of the final products dictates how many backscatter samples will be used to compute average backscatter values. As backscatter is a stochastic process, the inherent variability of the backscatter samples can be as high as 5.57 dB, the standard deviation for a Rayleigh-distribution of the sample amplitudes [26] even in absence of heterogeneity of the seafloor. Therefore, better accuracy of averaged backscatter values can be obtained using a higher number of samples which will be inversely proportional to the resolution.

2.2. Processing procedures

The "Design of the user survey " section of the Questionnaire explored the processing procedures employed by backscatter users. Although it is difficult to include representative studies from every different backscatter application revealed in the survey, some of the well-known methods used for backscatter seafloor discrimination (based on the level of BS) are compiled in Table 2.1. Processing procedures can be broadly divided into *signal processing* and *image processing* methods [64]. Signal processing focuses on data represented in angular or time space where the raw amplitude of returned signals is preserved. With image processing methods the backscatter is modified (flattened by averaging) to produce smooth-looking image mosaics. Here we describe the common 'users' concerns with products from either of the two processing procedures.

Table 2.1. A synopsis of the different processing method for seafloor Backscatter Strength (BS).

Measure of MBES BS	Computed from	Studies that have used this method
Angular response [signal processing]	Averaging N pings over the swath and comparing with theoretical models	[32,72]
Angular response after segmentation based on mosaics [signal processing]	Angular range analysis extracts features from mean BS angular curves and compares with theoretical models	[31,73]
Statistical analysis of angular curves [signal processing]	Linear discriminate analysis /Principal component analysis/ clustering	[74,75]
Angular response characteristics within n° of angular curve [signal processing]	Mean intensity, BS mean slope, second derivative,	[76]
BS fluctuations as a function of incidence angle [signal processing]	Shape factor of K-distribution	[77,78]
Mosaic analysis / Thematic clustering [signal processing]	Averaging NxN grid cells obtained after normalizing at a particular angle and segmenting areas with similar mean BS	[49,79]
Power spectral methods [signal processing]	Power spectral classification works specifically along the ping azimuth, deliberately avoiding high grazing angle data and can be used to attempt to classify multiple sediment types within a single swath.	[80–82]
Textural methods such as Gray-Level co-occurrence matrices (GLCM) [image processing]	Image segmentation of changes in textural values from the derived BS image.	[50,83–86]
Mosaic: Bayesian approach [image processing]	Analysis of distribution of the BS	[23]
Fractal analysis [image processing]	Analysis for modelling topographic relief based on 2-D spatial spectrum analysis that confines the variety of modelling spectra within a single class of fractal spectra. The shape of a fractal spectrum is defined by only two parameters, which are a fractal dimension, and a cut-off wavenumber that determines the roughness correlation length. In the general case of an anisotropic surface, the cut-off wavenumber is different along X and Y directions.	[87,88]
Probability density function (PDF) [image processing]	Used as a posteriori for outlier detection.	[9,89,90]
Hybrid techniques [image and signal processing]	Using a combination of the above techniques along with the features extracted from the seafloor bathymetric data e.g., slope, rugosity	[91]

The signal processing approach uses the parameters (shape, amplitude, angular variations etc.) of the seafloor returned echo. Its output may be presented in the time domain or the angular domain. Time-domain signal processing has been widely used in single beam echo sounders where the energy of the first and second return from the seafloor (E1 and E2) is used to characterize the seafloor but has not gained popularity for MBES [92]. The majority of users rather rely on angular variations of the backscatter. The angular dependence curve can be corrupted if appropriate geometric and radiometric corrections are not accurately applied (Figure 2.9). Significant changes in the amplitude or the shape of the angular response can be the result of incorrect corrections related to time varying gain (TVG), seafloor slope corrections and adjustments for transmit and receive characteristics of the sonar. To generate a stable backscatter angular curve, several swaths (or pings) are averaged together taking care to avoid averaging angular curves collected over more than one seafloor type. Segmented areas of backscatter mosaics can be used as an aid in the selection of the swaths or parts of the angular curve to be used in the averaging process thus avoiding contamination of the backscatter from different seafloor types. The correction of the backscatter angular response, either overall or in sectors (Figure 2.10) will drastically reduce the strong along-track artefacts.
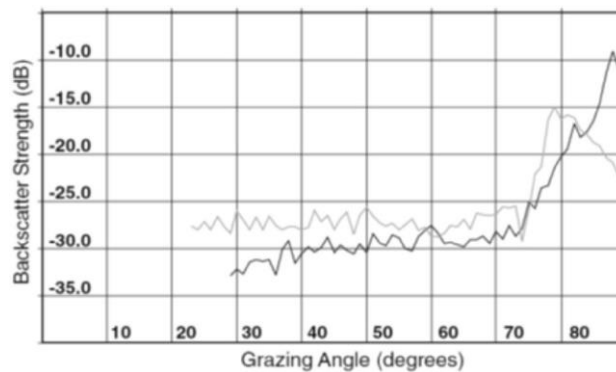
Figure 2.9: BS angular response of a small patch on the seafloor, acquired by a Simrad EM3000 multibeam sonar. The *grey line* shows the original observation and the *black solid line* the BS angular response after all the geometric and radiometric corrections were applied. Note that the seafloor had a considerable slope, so that the maximum BS in the original observation was not at nadir but at a grazing angle of 80°. Figure from Fonseca and Mayer [31].

Angular response curves can be compared to modelled seafloor angular response curves or be classified using ground truth data to characterize the seafloor into various classes (Figure 2.7). Further processing may be required to simplify this procedure by extracting features that can be used more easily as an input to inversion models. For example Fonseca et al. [73] divided backscatter angular response curves into near, far and outer response (Figure 2.11). Lamarche et al. [49] used a heuristical model with a small number (4 or 6) of input parameters usable as descriptors of the angular shape and correlated to the seabed interface characteristics.
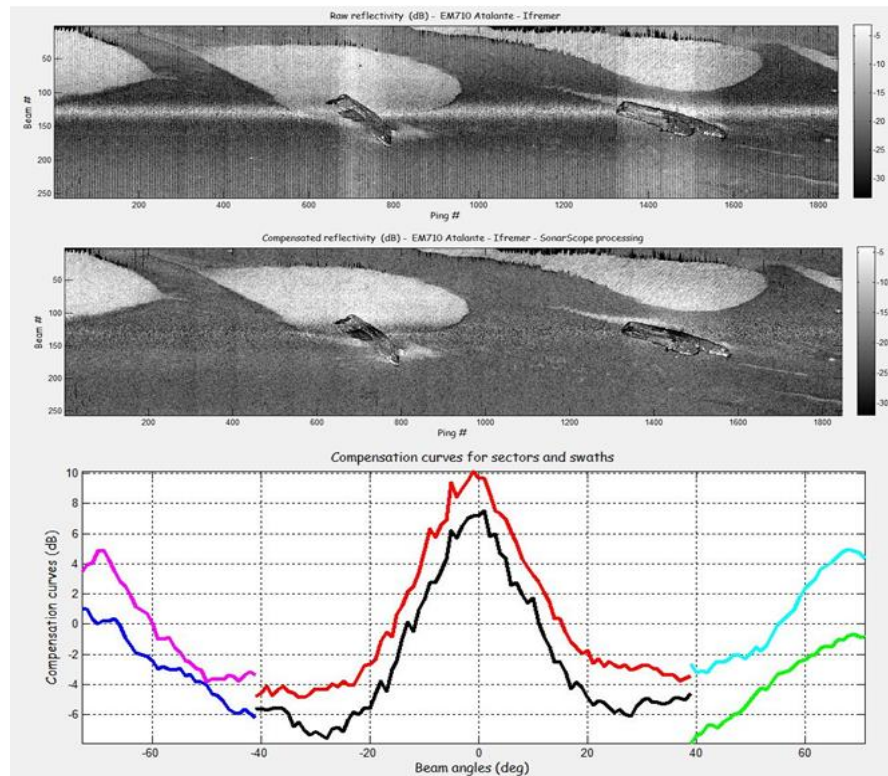
Figure 2.10: Correction of BS angular response and beam pattern. *Top* raw data; *middle* after correction; *bottom* applied compensation for the different sectors. Data from EM710 of RV *Atalante* (Ifremer), BS processed with Ifremer SonarScope® software (from Jean-Marie Augustin, unpublished)
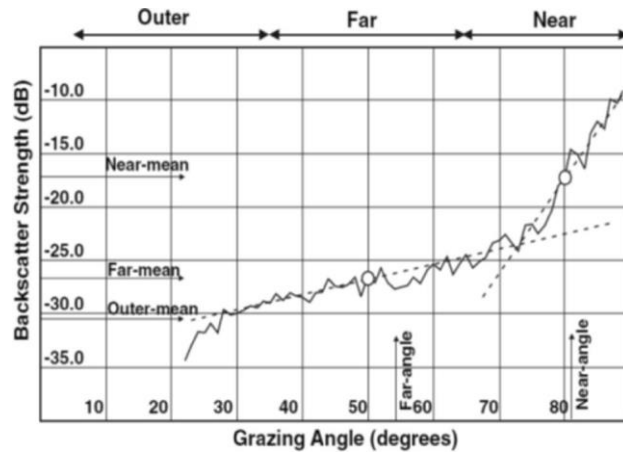
Figure 2.11: An example of extraction of the parameters to be used in acoustic inversion processing from Fonseca et al. [35]. The *dashed line* at the near-range defines the near-slope and the near-intercept (*white circle*). Similarly, the *dashed line* at the far range defines the far-slope and the white circle the far-intercept. The *arrows* on the *left side* of the graph show the calculated dB levels for the near-mean, far-mean and outer-mean, and the *arrows* on the *bottom* the near-angle and the far-angle.

Image processing refers to any form of signal processing for which the input is an image, such as a MBES grid with cell values in db. First an image needs to be obtained that is free of the angular variations in the across-track direction due to the inherent property of angular variation of the backscatter. This is achieved most commonly by normalizing the angular curve by the backscatter reported at a single value, usually at 45° [15,49]. The normalized backscatter response is then used to produce mosaics of backscatter (backscatter grids with cell values in dB). The results of image processing may be either a classified map or a set of characteristics or parameters related to the image. Most image-processing techniques consider the image as a two-dimensional signal and apply standard signal-processing techniques to it. These signal processing algorithms are utilized to extract features of interest from the image such as geological facies, geomorphological topographies or patterns and textures representing different physical habitat types.

A MBES backscatter image defined by geographic coordinates is considered to be a function of two real variables, for example, $a(x,y)$ with a as the amplitude (e.g., dB-value at a particular angle of incidence) of the image at the real coordinate position (x,y). A backscatter image or mosaic may be considered to contain characteristic sub-images

sometimes referred to as regions-of-interest. In a sophisticated image processing system it should be possible to apply specific image processing operations to identify discrete regions in a hierarchical manner when smaller regions within regions can be labelled. This has been reported on in the literature and is a novel advancement in acoustic backscatter processing (Figure 2.12) [50,86,93]. The utility of image processing is predicted to expand in the future with the implementation of both image and signal processing tools and procedures in commercially available software and with it the realization that image processing can provide quantitative characterization of the seafloor [94].
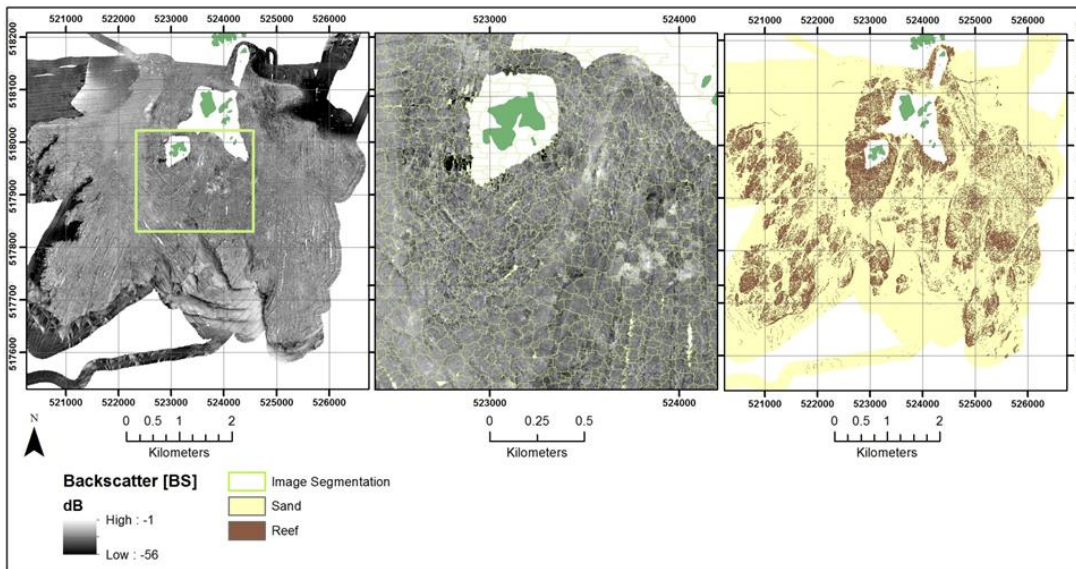
Figure 2.12: An example of image segmentation of MBES backscatter. (a) MBES backscatter image, (b) image segmentation shown by green outlines, (c) image classification of segments based on object textural and spatial parameters (slope, rugosity etc.) [95].

2.2.1. What data formats do users expect backscatter data to be in?

In the users survey it was asked what format different disciplines preferred to access backscatter data. The most common response was as a 'raster mosaic of the backscatter amplitude value' (25 responses). A raster mosaic can be stored in many data formats, usually dependent on the processing software employed or the data formats in common use within the user's institute. Some of these formats are now largely outdated and it would seem desirable today that in the purpose of data compatibility backscatter data are rid of the restrictions of any proprietary data format. For example, ArcGIS grid format has been

in widespread use for data integration among the scientific community; however more flexible, non-proprietary, formats such as georeferenced floating point .tif raster grids, which permit lossless data compression, or NetCDF (see "Data storage and processing speed" section) may be more favorable standards for the future. For data exchange there will no doubt also be a long-term demand for simple text files giving position coordinates and backscatter value (xyz files).

A data format that erases all previous corrections and reverts to the raw unprocessed signal would be appropriate. All processing steps need to be described in this format. Currently the only way to be able to return to the raw backscatter values is to maintain the original data backup: for Kongsberg systems, the *.all* format combines all recorded data (including backscatter) with the survey parameters. The preservation of all the corrections on the BS data set (a format that enables recovery of raw data) will mean a host of ancillary data will need to be available to enable corrections of the data in the future.

2.3. Current Challenges for users of backscatter data

The backscatter user survey comprehensively summarized the current challenges that backscatter users experience. These challenges ranged from data storage and processing speeds, skills and expertise to acquire, process and analyze the data, a lack of software to handle specific needs for information extraction from backscatter data and processing limitations either by software or computation limitations within their organization.

2.3.1. Data storage and processing speed

Many of the users commented that one of the major challenges with backscatter data was the costs associated with the 'acquisition storage' and 'backup storage' required for the large volume of backscatter data acquired by high-resolution MBES. One of the major problems this creates for future reference is the impossibility to archive the corrected backscatter data with the sounding values. When the data are retrieved there may be a lack of understanding of the influence of the acquisition settings from the original data. It was acknowledged by some users that the changes to the NetCDF support in the mosaic data set could significantly help in overcoming this limitation. At present it was noted that current IT technology and infrastructure is not ready to handle the large data volumes of

raw and processed data from water column backscatter and seafloor backscatter in a user-friendly manner. This severely affected processing speed and ability to perform even basic analyses on such large data sets. Although this may be seen as an institutional or funding issue rather than technological it was identified in more than 20 responses in the survey (Figure 2.13).
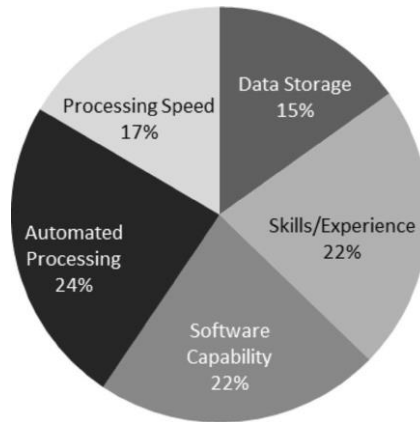
Figure 2.13: Challenges that the users work unit had with working with backscatter data in the past 5 years. Percentage values represent number of respondents per question

2.3.2. Skills and expertise

Another major limitation highlighted by the user survey was that backscatter utility was often hampered by contractors and processing staff not being properly trained in acquiring backscatter data and that training courses (from various companies) focus almost exclusively on bathymetric processing in their curriculum. This lack of expertise has compounding issues in the field as poor training can lead to surveyors constantly adjusting sonar settings during acquisition, which can severely affect the quality of the backscatter measurements during post-processing. Few researchers or surveyors have been properly taught to fully understand the implications of the sensitivities of backscatter data and therefore little standardization is being imposed by the survey industry, research, or other institutions in conducting MBES surveys including backscatter data. As yet no generic standard operating procedures for MBES data acquisition exists which incorporate the need to acquire good backscatter data contrarily to what has been established for bathymetry.

2.3.3. <u>Software and Processing</u>

Survey responses commonly mentioned that the current evolution of software and the compatibility of data between software platforms is improving and this is assisting with the increasing use of backscatter data. The limitation regarding software was mentioned in relation to both acquisition software packages and processing software packages and that sometimes the data formats between the different platforms were not compatible in the recent past. The majority of users in the survey used the following software: Sonarscope®, QPS Fledermaus®, ArcGIS®, CARIS® and MB System. From this list only Sonarscope®, QPS Fledermaus®, CARIS® and MB System are able to provide some level of backscatter data processing while ArcGIS provides image analysis only once backscatter image has been produced by the earlier listed software tools. Amongst the four backscatter processing tools, users can apply backscatter corrections and produce mosaics (image processing) with various levels of signal processing available. One survey question asked about the variety of ways that backscatter data was used as an ancillary data source and the responses ranged from; visualization for distribution maps (image processing), analysis for boundaries (image/signal processing) and as input to sediment and habitat classification map (signal processing). There was equal utility of users relying on both image processing and signal processing to draw out information from their backscatter data.

For some users, the costs of processing software(s) both to purchase and to maintain ongoing licenses was a severe limitation to their abilities to improve backscatter processing within their industry. Some users mentioned that there was a lack of "platform independent" solutions to handle backscatter processing issues. This was identified by a number of users and an example was given that few software packages were able to quantitatively handle navigation correction. In some instance there were problems with file compatibility between the software and the sonar output files so that navigation issues could not be corrected. In many instances user responses in the questionnaire said that the software documentation for both acquisition and processing packages was very poor in relation to MBES backscatter data handling. This was noted in addition to "inappropriate or missing specifications of technical details from manufacturers".

Many of the questionnaire participants said that the software parameters in relation to automated MBES backscatter processing were "not properly *tuned* by users which resulted in less than ideal corrections being applied and therefore unsatisfactory results". There was little confidence in the automated MBES backscatter processing algorithms provided by software companies in that the results were deemed unstable or "still in beta-testing mode" although they were commercially available. Many of the users commented on the need for "human intervention" at all stages of the automatic processing workflows where 'adjustments' were often required and that other steps appeared to be a 'black box'.

Many of the users noted that, although the limitations for acquiring, processing and analyzing BS data were going through a period of great transition, recent advances especially made by CARIS® and QPS Fledermaus® have made the process a little simpler especially with regard to cleaning artefacts from the data (nadir effect) and navigational uncertainties.

2.4. <u>Discussion</u>

The major outcome from this study has been to give the marine acoustics community a voice to identify the major concerns and limitations they have with wanting to employ backscatter data in their research. There was no doubt in the community that these data will continue to be useful, and, in time, better understood which in turn will add inherent value to backscatter data.

Stability and accuracy remain the top issues for backscatter data and its derived products. We analyzed the requirements for the users using image processing and signal processing approaches. Although the two user groups differed in their approach to utilize the backscatter data and the final products that they developed, stability and accuracy issues equally affected both groups.

These top issues are related to the greatest concerns to the backscatter user's communities—that being the 'lack of calibration required for optimizing backscatter data', the lack of standardization methods available for referencing and the ongoing struggles with the large data volumes (relevant to both data storage and time required for processing).

Issues of standardized interpretation of backscatter within and between surveys for both geological and biological interpretation demand a pathway forward for new

workflows for MBES backscatter processing. Many applications of habitat mapping make use of some form of classification or modelling and will often integrate backscatter data directly or indirectly in this process. Standardized data are essential for this workflow. Data quality and signal levels/properties that differ between surveys instruments within a same study area lead to poor classification/modelling results and weaken the usefulness of backscatter data for habitat mapping.

In the past where several frequencies of MBES have been used within a mapping area, the interpreter would be aware of the differences in penetration and scattering mechanisms arising from e.g., shallow water and deep water echosounders, since these will not necessarily affect the dB levels, but would have been referred to in order to aid in backscatter interpretation. Today the traditional qualitative methods are becoming obsolete as the data sets become larger and image-processing techniques begin to offer comparatively consistent and improved interpretation. In contrast to only differentiating the major sediment classes of sediment type, benthic habitat mapping (i.e., mapping that integrates the biological properties of the seabed with the seabed facies) has benefited in particular from advances in automated methods for processing BS data. Partly this may be because it is often not feasible to collect biological data over the same vast expanse as surficial sediment backscatter data, and that inference and extrapolation are required from a very small and well-understood area of seabed, which was led by predictive mapping methods based on quantitative modelling. We now see the growth in automated classification and extraction of quantitative descriptors of the backscatter amplitude, or signal properties being used to interpret and classify BS data e.g., texture measures [63,96] and estimates of geotechnical properties [15].

The user survey did not adequately capture from the user community as whether the BS data they employed was collected 'in-house' or obtained through contract work, or from incidental backscatter data collected as 'by catch' during bathymetric surveys. Although the backscatter data acquisition and processing techniques are at their nascent, in the last 10 years they have been developed to an extent where with additional and appropriate resources (trained personnel), equipment (calibrated sonars) and diligence

(times of surveys, environmental considerations) reasonable and useful backscatter products can be generated.

The question remains as to whether these additional resources are justified where the primary purpose of the multibeam survey is not to collect backscatter but to collect bathymetric data. It can be argued confidently that the majority of multibeam sonar users emphasize bathymetric data collection as compared to seafloor and water column backscatter. In areas where no mapping data exist, bathymetric data are as equally important to satisfy the needs of different applications. In rough weather, for example, where the bathymetric data quality can still be acceptable should these surveys stop collecting data if the backscatter quality is being compromised? A major issue for maintaining the backscatter data quality is that there are no 'easy to use' quality metrics for backscatter data. Whilst bathymetric data quality in terms of stability and accuracy can be confirmed using a host of available methods (e.g., patch test, lead line); the backscatter comparison is challenging as the parameters that control the seafloor backscatter quality are difficult to quantify or are ill-defined and there are no easy-to-deploy at-sea methods that can provide confidence during the acquisition that high-quality backscatter data are being acquired.

The metrics used to assess the quality of backscatter data currently include visual assessment of artefacts/ system related effects as well as comparison of the backscatter data with ground truth data. The user survey identified videos, photographs, sediment grabs and real-time observations of seafloor geology and biological cover recorded from a towed camera sled as the most commonly used ground truth methods. The seafloor backscatter data provides the geo-acoustical properties of the seafloor and traditional ground truthing data may not provide explanation for the variations in the seafloor backscatter [86]. In-situ ground truthing in terms of sediment acoustic properties have been proposed [97] but so far these ground truthing methods have not gained widespread acceptance mostly due to the fact that users are more interested in the geophysical properties that they can infer from the geo-acoustical observations (i.e., seafloor backscatter). The linkages between the geo-acoustical and geophysical properties is an active field of research and beyond the scope of this paper but it is important to realize that seafloor backscatter is not capable of

providing all the geophysical properties that a user may want to obtain and therefore combination of ground truthing data and seafloor backscatter should be dealt with due caution to avoid over interpretation of the seafloor backscatter data. To appropriately use backscatter data (both for image processing and signal processing), critical information about data collection procedures, data processing steps, lineage of applied corrections, and environmental conditions need to be carried forward to the backscatter products. Currently this remains a challenge but this can be achieved by developing a framework for establishing backscatter metadata standards.

2.5. Conclusions

MBES backscatter users have expanded from traditional users including hydrographers, navigators, engineers, marine geologists and military planners to maritime explorers, archaeologists, fisheries biologists, geomorphologists and ecosystem modelers to name a few. This wide-ranging and ever-growing community of MBES backscatter users are adapting and extending the potential of MBES data to address unique and unforeseen applications. Although this extension of technology is welcome, it has created unique challenges as differences in backscatter acquisition, processing and dissemination amongst different user groups, reflecting diverse user needs, can hamper re-use of backscatter severely. The GeoHab association identified this need to standardize the backscatter data acquisition and processing protocols. The goal of this survey was to understand diversity of backscatter users, their unique requirements in terms of accuracy and resolution of the backscatter, and the intended use of backscatter.

The user survey results consisted of 97 responses and included civilian government agencies (41%), academia (24%), private companies (31%) and government defense agencies (4%). The users were found to use backscatter in a wide range of depth; from near-shore coastal regions to deep waters (Figure 2.2 a), and in various applications with top three being: seafloor type mapping, marine habitat mapping and collecting backscatter opportunistically while conducing hydrographic surveying.

For seafloor type and habitat mapping applications resolution and accuracy were identified as major requirements. About half of the users stated a desire to obtain 1-m resolution which in reality may not be supported by the spatial resolution of backscatter

samples except with the current narrow beam shallow water MBES. The identification of suitable backscatter data is a complex issue and requires technical training that may be missing for some of the users who are trying to use backscatter for their application. Improvements in the multibeam technology are ongoing but unfortunately, currently the accuracy of the backscatter data cannot be fully determined without dedicated efforts to calibrate multibeam sonar. In absence of a uniform methodology to determine the accuracy of backscatter, the users of backscatter have been using backscatter as a discovery tool where comparison among repeat measurements is not critical. The results of the user survey determined that lack in backscatter quality assessment is a hindrance in standardizing the backscatter acquisition and processing as well as use backscatter for monitoring applications where repeat backscatter need to be compared. The users, multibeam manufacturers, multibeam software developers and multibeam vendors have a shared responsibility to respond to the need to improve backscatter accuracy.

For the third major use of backscatter, which is opportunistic acquisition of backscatter while conducting hydrographic surveys, an implementation of methodologies to collect concurrent high-quality backscatter and bathymetric data is needed. Appropriate generation of backscatter that can follow standards will require commitments not only from manufacturers but also from data collectors, software vendors and agencies that support multibeam data acquisition.

Improvements in data acquisition and processing have to be guided by user needs. Almost all the respondents agreed that utility for backscatter data will continue to develop (98%). As most of the multibeam sonars now manufactured have the capability to collect seafloor and water column backscatter, it is only natural that backscatter user group will expand further in the near future. 84.3% of respondents had invested resources to acquire their own backscatter data (either in house or contract) showing an ongoing commitment to improve this data source. Although the Geohab Guidelines and Recommendations [15] was very well received, the community still needs to agree upon a minimum set of appropriate standards. Continuing work to understand user needs will bring the diverse applications to adopt a minimum multibeam backscatter standard that is useful for the broader backscatter user community.

CHAPTER 3

A FRAMEWORK TO QUANTIFY UNCERTAINTIES OF SEAFLOOR BACKSCATTER FROM SWATH MAPPING ECHOSOUNDERS

This chapter is based on a published peer reviewed journal article. My contribution to the article included conceptualization of the study, methodology development, writing the original draft, review and editing of the draft, code development and data interpretation. The article has been formatted to meet UNH dissertation formatting guidelines and reproduced here with permission. Paper citation: Malik, M.; Lurton, X.; Mayer, L. A framework to quantify uncertainties of seafloor backscatter from swath mapping echosounders. *Mar. Geophys. Res.* **2018**, *39*, 151–168. doi.org/10.1007/s11001-018-9346-7

Abstract: Multibeam echosounders (MBES) have become a widely used acoustic remote sensing tool to map and study the seafloor, providing co-located bathymetry and seafloor backscatter. Although the uncertainty associated with MBES-derived bathymetric data has been studied extensively, the question of backscatter uncertainty has been addressed only minimally and hinders the quantitative use of MBES seafloor backscatter. This paper explores approaches to identifying uncertainty sources associated with MBES-derived backscatter measurements. The major sources of uncertainty are catalogued and the magnitudes of their relative contributions to the backscatter uncertainty budget are evaluated. These major uncertainty sources include seafloor insonified area (1-3 dB), absorption coefficient (up to > 6 dB), random fluctuations in echo level (5.5 dB for a Rayleigh distribution), and sonar calibration (device dependent). The magnitudes of these uncertainty sources vary based on how these effects are compensated for during data acquisition and processing. Various cases (no compensation, partial compensation and full compensation) for seafloor insonified area, transmission losses and random fluctuations were modeled to estimate their uncertainties in different scenarios. Uncertainty related to

the seafloor insonified area can be reduced significantly by accounting for seafloor slope during backscatter processing while transmission losses can be constrained by collecting full water column absorption coefficient profiles (temperature and salinity profiles). To reduce random fluctuations to below 1 dB, at least 20 samples are recommended to be used while computing mean values. The estimation of uncertainty in backscatter measurements is constrained by the fact that not all instrumental components are characterized and documented sufficiently for commercially available MBES. Further involvement from manufacturers in providing this essential information is critically required.

3.1. <u>Introduction</u>

Amongst acoustic sensors, multibeam echosounders (MBES) are commonly the tool of choice for most seafloor studies because they concurrently offer high-resolution, co-located bathymetry and backscatter [11,13,98]. Historically the analysis of multibeam sonar data has focused on the bathymetric component and the critical role it plays in nautical charting and in offering insights into geologic and tectonic processes of the seafloor. The rich history of the use of MBES for critical mapping applications has resulted in significant progress over the last two decades in quantifying the sources of uncertainty associated with the bathymetric component of MBES [56,99–102] adding tremendously to the credibility and value of bathymetric data.

More recently, the interpretation of the second component of MBES systems, namely seafloor backscatter, is playing an increasingly important role in many ocean-mapping applications including habitat characterization, environmental monitoring, geological and geotechnical studies, and natural resource prospecting [39]. In support of these applications, efforts have been made to use MBES backscatter to characterize the nature of the seafloor, typically through broad descriptions of seafloor or sediment type (e.g., rock, sand, mud) or in other instances, to further estimate basic parameters like grain size or acoustic properties (Hasan et al. [103] and references therein). Unlike for bathymetry, however, there has been little effort made to understand the uncertainty associated with MBES backscatter measurements and thus methods of seafloor characterization using backscatter are not constrained with respect to associated uncertainty.

41

The interpretation of backscatter data for seafloor characterization is typically done through the analysis of backscatter mosaic texture or seafloor backscatter angular response. The backscatter mosaic is a georeferenced image of the signal intensity scattered back to the sonar. With different seafloor materials showing different intensity levels, mosaics can be used to segment the seafloor into different types either subjectively by an interpreter, or more objectively through image processing approaches (e.g., [84,94,104]. As the echo intensity varies with the angle of incidence of the acoustic signal at the seafloor, the angular variations of backscatter have to be normalized (typically at 45°) for the mosaic to be interpretable. As a result of this normalization process, a key quantitative aspect of the seafloor properties (its angular response) is lost, hence limiting the use of mosaics to qualitative interpretation [64]. Even when viewed qualitatively, the lack of knowledge of the uncertainty associated with the backscatter levels depicted on a mosaic calls into question the meaning of the interpretation. Issues of uncertainty in seafloor backscatter measurements have become apparent when combining and comparing data sets from different MBES surveys (e.g., [42,105]) where surveys from different systems resulted in wildly different backscatter results.

Unlike the backscatter mosaic, the analysis of the backscatter angular response allows for the extraction of quantitative features and algorithm-based seafloor characterization approaches (e.g., [31]). Such approaches can provide useful predictions of seafloor type provided that uncertainties are appropriately constrained [35,103,106] but suffer from the current lack of understanding of uncertainties in the underlying backscatter measurements. With more emphasis on automated and physical model driven characterization techniques, quantification of backscatter data is becoming more important [107] involving efforts in MBES calibration, and in better understanding, modelling, and estimating the associated uncertainty.

The aim of this paper is to identify the major sources of uncertainty for MBES-derived seafloor backscatter values, evaluate (when possible) their causes and estimate their magnitudes. In doing so, we hope to establish a framework for further analyses that may be broadly applied to various systems and situations so that end-users and operators may aspire to a more quantitative understanding of seafloor backscatter. We begin with a

review of the basics of seafloor backscatter measurements. We then seek to identify the significant sources of uncertainty and quantify their respective magnitudes. Finally, suggestions are made that might help mitigate the major sources of uncertainty.

3.1.1. Preliminary notions

3.1.1.1. Elements of backscatter measurement

MBES backscatter data result from the measurements of seafloor target strength (see e.g., Urick [25]), a quantity that relates the incident and scattered pressure fields from a given target - in our case a small patch of the seafloor instantaneously insonified by the sonar signal. The ensemble average of squared scattered pressure $\langle|p_s|^2\rangle$ is proportional to the insonified area A and the squared incident pressure $|p_i|^2$, and inversely proportional to the sonar-target squared distance r_s^2, neglecting absorption and refraction effects:

$$\langle|p_s|^2\rangle = |p_i|^2 A\sigma_b \frac{1}{r_s^2}$$

[Eq. 3.1]

where the proportionality coefficient σ_b is referred to as the "backscattering cross-section" its logarithmic equivalent is the "bottom scattering strength" [25]:

$$S_b = 10\log_{10}\sigma_b .$$

[Eq. 3.2]

The target strength (TS in dB re 1 m^2) of the seafloor area A is then related to the scattering strength by:

$$TS = S_b + 10\log_{10}A.$$

[Eq. 3.3]

$10\log_{10}A$ is used here instead of the correct form $10\log_{10}(A/A_0)$ for notation simplicity where $A_0 = 1$ m^2 is the reference unit surface. In the practical situation where TS is measured by a directional transmitter and receiver, the mean square voltage at the receiver output is expressed in dB as:

$$10\log_{10}\left[\langle|V_{r(t)}|^2\rangle\right] = EL + RS_o = SL_o + D_{TX} - 2TL + 10\log_{10}A + S_b + RS_o + D_{RX}$$

[Eq. 3.4]

where $\langle |V_{r(t)}|^2 \rangle$ is the average squared voltage at receiver, EL the echo level at the receiver, RS_o the sensitivity of the receiver transforming the incident acoustic pressure into an electrical signal along its maximum response axis, SL_o the source level along its maximum response axis, $2TL$ the two-way transmission loss, A the insonified area, D_{TX} and D_{RX} the transmit (Tx) and receive (Rx) directivity function values in the sonar-target propagation direction [19]. The received voltage is then converted to a digital number DN through an Analog-to-Digital Converter (ADC) and recorded; this operation introduces a specific offset G_{AD} so that:

$$DN = 10 \log_{10} \left[\langle |V_{r(t)}|^2 \rangle \right] + G_{AD}. \qquad \text{[Eq. 3.5]}$$

The value of G_{AD} is related to how the digitization process is carried out, including the ADC's technological characteristics [64]. The measured backscatter strength can then be expressed from [Eq. 3.4] and [Eq. 3.5] as:

$$S_b = DN - RS_o - G_{AD} - SL_o + 2TL - D_{TX} - D_{RX} - 10 \log_{10} A. \quad \text{[Eq. 3.6]}$$

For a given seafloor type and frequency, this value of S_b is also related to the seafloor incidence angle θ. The various uncertainty sources contributing to the measured S_b and θ are analyzed in the rest of this paper. In the following the S_b uncertainty expressed in dB relates to the percentage uncertainty in σ_b; for example, a 1 dB uncertainty in S_b relates to a 10% uncertainty in σ_b.

3.1.1.2. <u>Sources of seafloor backscatter measurement uncertainty</u>

The expression [Eq. 3.6] for seafloor backscatter strength can be grouped as:

$$S_b = \{DN - RS_o - G_{AD} - SL_o - D_{TX} - D_{RX}\} + \{2TL\} - \{10 \log_{10} A\}$$

$$\text{[Eq. 3.7]}$$

suggesting three main components of uncertainty:

1. The first component $\{DN - RS_o - G_{AD} - SL_o - D_{TX} - D_{RX}\}$ is the practical output of the target strength measurement, combining the measured echo level (DN), the source level (SL_o), the sonar Rx sensitivity (RS_o and G_{AD}) and directivity (D_{TX} and D_{RX}), but

excluding the transmission losses ($2TL$). In the following it is conventionally designated as the "compensated echo level". Sources of its uncertainty include:

a) the stochastic nature of the physical echo intensity variations. An ensemble average process helps in reducing the variance around the estimated mean, but as the number of available samples is limited, some uncertainty remains in the backscatter estimate;

b) the sonar characteristics including electroacoustic (transducer sensitivity and directivity), and electronic characteristics (Tx power amplification, Rx pre-amplification, various gains, filtering, A/D conversion);

c) the environmental conditions (noise level added to the echo level).

The details of MBES-related uncertainty sources in (b) are not always available to end-users and in the absence of this information the sounder must be considered a "black box", without a real estimate of the uncertainty related to its actual transfer function. This uncertainty may be globally determined from experimental data on a controlled target [15], but this can be an expensive, logistically difficult, and time-consuming process.

Additionally, not all MBES systems provide an estimate of S_b in the recorded data, but rather only the DN values. Even when S_b values are explicitly provided in datagrams, they must still be considered cautiously. Specific gains (either static or time-varying gain TVG) are applied before digitization to keep the signal within the ADC input range; these must be removed in order to retrieve the original physical S_b values. Such system-specific processing steps, if not correctly implemented by the manufacturer, may result in large offsets in the reported S_b. Several studies have highlighted these MBES-design shortcomings [42,108–111].

2. The second component $\{2TL\}$ is the two-way transmission loss between the sonar and the target. It features both the geometrical divergence loss (function of the oblique range) and the absorption loss (depending on both the range and the local absorption coefficient, a function of frequency and water properties). The uncertainty in TL is mainly controlled by both the range estimation accuracy and the knowledge of the seawater characteristics involved in absorption.

3. The third component $\{10 \log_{10} A\}$ is the insonified footprint area instantaneously active in the backscatter process delimited by the sounder beam pattern and/or the pulse duration. This component also depends on the propagation range and the incident angle of the signal on the seafloor (to be considered in a 3-D geometry) (Figure 3.1).
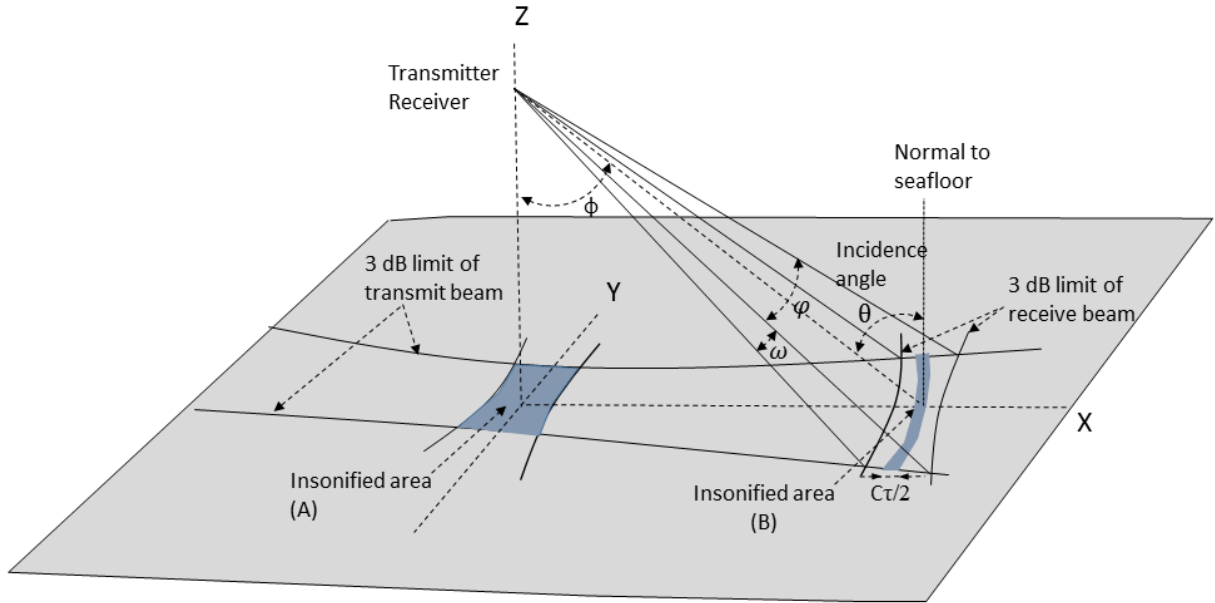
Figure 3.1: Measurement geometry of MBES and area insonified for near nadir (A) and at oblique angle (B).

Additionally to these three sources of radiometric measurement uncertainty, the incidence angle estimation, upon which S_b is dependent, can be another major cause of uncertainty. The S_b dependence on seafloor incidence angle and frequency is a fundamental characteristic of seafloor backscatter data. With the MBES frequency fixed (or slightly varying with different Tx sectors), the mean seafloor angular response (AR) is characterized by its S_b values associated with incidence angles. Given such relationships, many research efforts have used comparisons of measured AR to theoretical models as a basis for seafloor segmentation and characterization (e.g., [31,76,106,112]. The uncertainty of the incidence angle is a function of Tx-Rx angle estimation accuracy, refraction by the sound-speed profile, and seafloor local slope. The position of the backscatter samples, similar to bathymetric samples, is determined through use of MBES geometry and positioning of the vessel. The Total Horizontal Uncertainty (THU) in the position of

soundings, at the 95 percent confidence level, is not expected to exceed 5 meters + 5 percent of the depth [113]. For backscatter samples, the effect of position uncertainty is therefore assumed to be negligible in this paper.

3.2. <u>Elementary analysis of major uncertainty components</u>

As outlined above, the elementary analysis proposed here focuses on the magnitude of the S_b uncertainty broken down into the four parameters controlling the $S_b(\theta)$ estimate: compensated echo level, seafloor incidence angle, transmission loss, and insonified area. In evaluating the sources of uncertainty, two significance thresholds of 1 dB and 1° are adopted here for radiometric and geometric uncertainties respectively. These values are selected based on the observation that in order to differentiate confidently between seafloor types, differences in backscatter levels of approximately 1 dB are needed [39].

3.2.1. <u>Compensated echo level</u>

3.2.1.1. <u>Random fluctuations of the echo level and SNR</u>

The stochastic nature of the backscatter process results in a randomly-fluctuating sonar echo level [25]. A simplified but widely used theoretical model assumes backscatter amplitudes to follow a Rayleigh distribution, implying a standard deviation of 5.57 dB for elementary backscatter samples [26,114]. Physically interpreted, this model assumes an instantaneous insonified area (signal footprint) wide enough to enclose a large number of simultaneously activated scatterers with statistically independent random phases [115]. In order to reduce the resulting uncertainty associated with randomly fluctuating sonar echo levels, the backscatter level can be averaged over an increasing number of signal samples [116], however at the cost of degraded resolution. For MBES measurements, the number of samples available for averaging depends on depth, system parameters, and angular region of the measurement, and ultimately controls the random uncertainty of the mean backscatter [26]. A more detailed discussion of the statistical uncertainty of the echo-level can be found in Appendix 3A.

The echo level measurement uncertainty also depends on the signal-to-noise ratio (*SNR*). Noise sources in ocean are numerous and highly variable [25], including noise caused by sea-surface agitation, biology, and bubbles created by the ship motion and/or

surface wave action. Also, the sonar performance may be limited by reverberation in the water column due to biological, gaseous or inorganic scatterers. Self-noise caused by the sonar and its carrier platform adds to these environment-related causes. A *SNR* better than 10 dB [102] can be taken as a reasonable lower limit for acceptable measurements of bathymetry according to today's standards [113]. A generalized prediction of uncertainty caused by *SNR* is not suggested here as there are too many causes and individual cases may degrade *SNR* up to a level such that backscatter measurements are no longer possible. The S_b uncertainty due to *SNR* can be simply modelled as:

$$\delta S_b = 10 \log_{10} \left(\frac{S+N}{S} \right) = 10 \log_{10} \left(1 + 10^{-\frac{SNR}{10}} \right) \quad \text{[Eq. 3.8]}$$

where *S* and *N* are the intensities of the expected signal and the additive noise respectively, defining *SNR=S/N*. Assuming the worst case of a 10 dB *SNR*, the corresponding uncertainty in backscatter measurements is around 0.4 dB (increase in the resulting average intensity for {signal + noise} compared to signal alone). Therefore, while *SNR* can be a major uncertainty source in some individual measurement scenarios, *SNR* can be practically considered as a minor source of uncertainty for MBES data if currently acceptable quality for bathymetry is achieved. Recommendations for improving the MBES data reliability in relation to *SNR* can be found in [68].

3.2.2. <u>Uncertainty of source level and receiver sensitivity</u>

A detailed characterization of uncertainty in the MBES parameters is still lacking [117]. MBES manufacturers have only offered nominal magnitudes of uncertainty related to backscatter measurements. For example, for Kongsberg systems Hammerstad [118] provided a typical uncertainty of ±1 dB related to MBES transducer sensitivities but cautioned that this uncertainty might be larger for a specific system. Although several studies have attempted to measure sonar sensitivity in calibration tanks and by field comparisons [108,119–121], MBES electronics are complex and there are many causes of instrumental uncertainty that users cannot be expected to measure and estimate, let alone keep track of the various engineering parameters needed to confidently estimate these uncertainties. Involvement of MBES manufacturers is therefore critically needed to model the MBES characteristics essential for calibration.

3.2.3. <u>Relative sonar calibration</u>

In the absence of readily available calibration documentation, users have to rely on empirical data to derive the calibration offsets. Often, while repeating backscatter measurements over the same seafloor using different settings or with different MBES systems, discrepancies in the observed backscatter values are observed. These differences can then be estimated to adjust backscatter values to match in a relative sense. This empirical method to make backscatter data consistent among different settings or MBES systems is called relative calibration. The adjustment protocols for relative calibration operations and the removal of systematic artifacts have been studied extensively [13,42,44,73,108,122–127]. These relative calibration protocols can provide valuable information about the overall health of the MBES including system degradation due to transducer aging or bio-fouling [128] and therefore are also being incorporated into sonar acceptance protocols [120,129,130]. While such relative calibrations provide a means to have the same seafloor appear to have consistent backscatter irrespective of different settings or MBES systems used, it provides no indication of the actual backscatter uncertainty.

3.2.4. <u>Absolute sonar calibration</u>

As individual MBES systems may show differences in calibration from system to system, the only alternative to manufacturer-provided information is to subject MBES to empirical checks in a tank or at sea. The aim of this MBES calibration is to estimate the device-related parameters required for S_b estimation including: transmit and receive beam patterns, pulse length and the quantitative impact of gain changes applied during the data acquisition. Absolute calibration using reference spheres is a well-accepted method developed for fisheries sonars and proposed for application to MBES [119,131,132]: using this method, the combined transmit and receive characteristics of the sonar are measured. The two-way beam pattern thus obtained can be used as a single correction to the measured backscatter. Since accurate placement and controlling motion of a reference sphere inside MBES narrow beam patterns are challenging, a calibration approach using extended targets has also been demonstrated [133]. An alternate method to target calibration (either sphere or extended target) is the use of a reference hydrophone [132]; this method is required if

transmitter and receiver characteristics need to be determined separately [134]. For practical reasons, the use of hydrophones and transducers in a tank is suitable only for high-frequency portable systems with small arrays. Alternately this method has also been used to measure the beam pattern of a large array by fitting a hydrophone on an ROV [135], however, this approach is complex and expensive. Finally, using a reference seafloor patch as a benchmark [136,137] is an attractive option although the seafloor backscatter itself may change depending on a number of factors including temporal changes due to sediment movement and the formation of bedforms and other features that can cause seafloor backscatter to have strong dependence on azimuth [138].

Given that a general model for this class of drifting uncertainty cannot by defined and hence applied to quality control of backscatter data, the reality is that if a reduction in this source of uncertainty is desired, it is currently the user's responsibility to conduct regular calibration operations, either by test tank measurements, surveys on reference seafloor areas, or by comparison with calibrated sonar systems [15].

3.3. Incidence angle

The incidence angle considered in seafloor backscatter computations is the angle between the signal arrival direction at the seafloor and the local perpendicular to the interface (considered as locally flat although possibly tilted). The incidence angle uncertainty depends on three components:

A. The angle measured by the sounder at the receiving array (*Rx*), relative to the vertical. This measurement depends both on the intrinsic performance of the sensor array processing and on the platform motion (normally compensated for, with some instrumental uncertainty). The angles associated with the backscatter signal samples are referenced to the arrival angle at the sounding point (bottom detect) of the beam. Hence this instrumental uncertainty is equivalent to the one considered for the bathymetry uncertainty budget [99]. Considering that most of the bathymetry relative error is given by its angle component [100,102]:

$$\frac{\delta z}{z} = \tan\theta . \delta\theta \qquad \text{[Eq. 3.9]}$$

50

and using typical magnitudes met for acceptable-quality bathymetry data measured by MBES, one finds an angle error around 0.15° for limit values of $\delta z/z = 1\%$ and $\theta = 75°$.

This angular uncertainty is increased by the beam-pointing uncertainty caused by the ship motion but considering the high accuracy of today's motion sensors (typical uncertainty for roll, pitch and heading accuracy is below 0.1°) the quadratically-cumulated angular uncertainty due to both sensor and ship motion can be considered to stay below 0.2° and hence can be neglected.

B. The effect of refraction due to propagation inside the water column. Uncertainties in the estimated sound speed profile impact the accuracy of compensation for the refraction effect. The sound speed profile has a twofold effect on incidence angle estimation: (1) the beam steering angle at the sonar's head; and (2) refraction in the water column. Angular uncertainty introduced in the computation of beam steering by a sound speed uncertainty δc_s at the sonar head is given by [99]:

$$\delta\emptyset_s = \frac{\tan\emptyset_s}{c_s}\delta c_s \qquad\text{[Eq. 3.10]}$$

where $\emptyset_s$ is the beam steering angle from nadir and c_s is the sound speed at the sonar head used for beam steering. In most MBES, the sound speed at the sonar head is continuously measured by a dedicated probe, and therefore the sound speed uncertainty is not expected to be more than ≈ 1 m/s. Considering a pessimistic $\delta c_s/c_s = 0.1\%$ (i.e., δc_s=1.5 m/s), the uncertainty in beam steering will be $\delta\emptyset_s \approx 0.2^o$ at $\emptyset_s = 75°$.

Using the complete sound speed profile to compute an average value c_p the effect of an uncertainty δc_p upon the incidence angle θ (referenced to nadir) can also be estimated as:

$$\delta\theta_p = \frac{\tan\theta}{c_p}\delta c_p \qquad\text{[Eq. 3.11]}$$

51

giving the same magnitude of 0.2° in the pessimistic case of $\delta c_p / c_p = 0.1$ % and $\theta = 75°$. So considering independent errors on c_s and c_p, the incident angle error magnitude should stay within 0.3°.

In summary, the effect of beam steering and refraction on seafloor incidence angle is negligible considering sound speed uncertainties remain smaller than 0.1%.

C. The seafloor local slope. This is best estimated from the Digital Terrain Model (DTM) built from the MBES bathymetry. Three cases can be considered for evaluating the seafloor slope influence on incidence angle uncertainty:

(i)   The slope is completely ignored i.e., the seafloor is assumed to be flat and horizontal. The error in the incidence angle will be equal to the slope of the seafloor. This simplification is still commonly applied at basic levels of backscatter processing but should be avoided in case of requirements of a good quality backscatter level;

(ii)   The seafloor topography is accounted for using a previously-determined DTM. This is normally achievable by most modern seafloor-mapping sonars providing both bathymetry and backscatter data. However, DTM slopes are subject to uncertainties linked to the bathymetry measurement accuracy and to the details of the processing steps applied for their construction;

(iii)   Even for seafloor slopes inferred from a DTM, small-scale slopes in the bathymetry may be unresolved and hence affect the estimate of local incidence angle. Little can be derived from MBES bathymetric data about unresolvable small-scale slopes and thus remains an unquantifiable uncertainty source.

In DTM slope calculations, the random vertical uncertainty in the soundings is considered the most critical uncertainty source. Determining the uncertainty in slope estimation, based on resolution, DTM uncertainty, analysis scale and computation algorithm, is an active area of research in terrain analysis and modeling. Dolan and Lucieer [139] and Zhu et al. [140] have shown uncertainties

52

in slopes to reach up to 5°-6° when using a MBES-derived DTM. Furthermore, assumptions about the macro-relief of the surveyed seafloor at the spatial resolution of the backscatter samples are needed for an *a-priori* estimate of slope uncertainty; for most MBES this cannot be assessed by using only the bathymetry available from the MBES.

Although uncertainty due to the above individual sources (beam pointing angle, refraction and seafloor slope) cannot be differentiated from the beam pointing angle measurement itself, the incidence angle uncertainty affects the S_b measurement in two ways:

- the angle at which measured S_b is reported;
- the footprint area computation that impacts the echo level computation term ($\{10\log_{10}A\}$ in [Eq. 3.6]) as it is related to the incidence angle.

The magnitude of the impact of a wrong angle estimate on the resulting angular backscatter curve can be demonstrated using the derivative (vs. angle) of a canonical angular backscatter model. Using for instance the GSAB model [49] in its simplest form (a Gaussian law for specular regime and Lambert's law at oblique incidences) leads to the results presented in Figure 3.2. The expressions for σ_b, its differential $\frac{\partial \sigma_b}{\partial \theta}$ and the corresponding uncertainty δS_b in dB are given by:

$$\sigma_b = A\exp\left(-\frac{\theta^2}{2B^2}\right) + C\cos^D \theta$$

$$\frac{\partial \sigma_b}{\partial \theta} = -\frac{A\theta}{B^2}\exp\left(-\frac{\theta^2}{2B^2}\right) - CD\cos^{(D-1)}\theta\sin\theta \qquad \text{[Eq. 3.12]}$$

$$\delta S_b = \frac{10}{\ln 10}\frac{\partial \sigma_b}{\partial \theta}\frac{\delta\theta}{\sigma_b}$$

where *A* is the specular maximum amplitude, *B* is the facet slope standard deviation, *C* quantifies the average backscatter level at oblique incidence and *D* is the backscatter angular decrement.
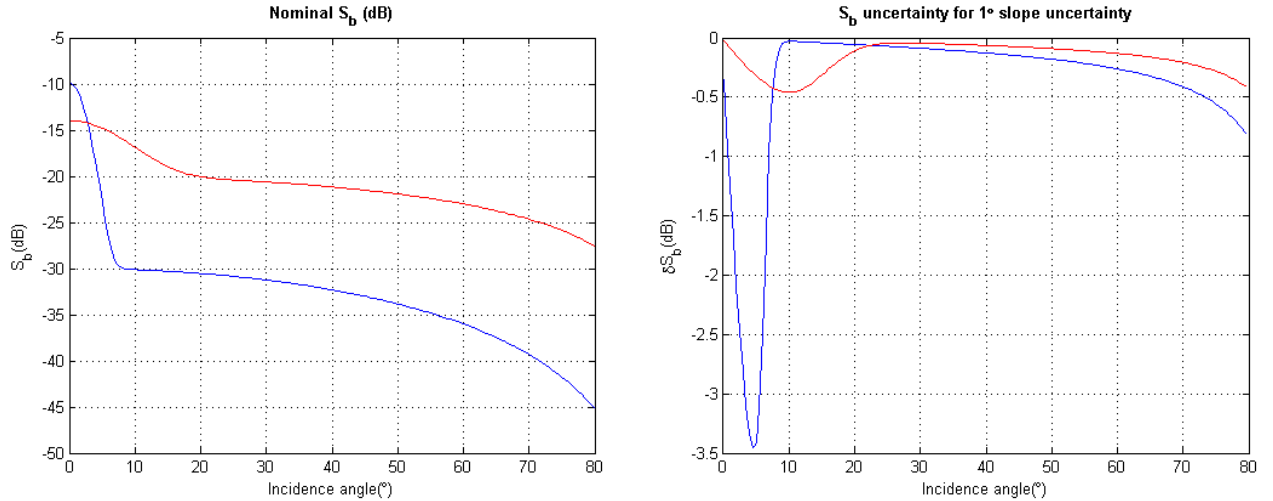
Figure 3.2: Effect of incident angle uncertainty on backscatter. Two nominal angular backscatter curves representing different seafloor types (blue and red, left), and the effect of a 1° slope angle uncertainty on the backscatter values (corresponding colors, right). The impact is maximal in the specular region, where the cut-off effect corresponds to the strongest angular variations (0° to 10° or 0° to 20° according to the case); it is negligible in the "plateau" angle sector (10°-20° to 50°-60°) and increases at high incidence angles.

The two cases illustrated in Figure 3.2 are typical angular backscatter curves for a soft-sediment (*in blue*, high narrow specular backscatter, decreasing in the oblique region with $\cos^2\theta$) and a coarse sediment (*in red*, low and wide specular backscatter, decreasing in the oblique region with $\cos\theta$). For most seafloors the oblique-regime average angle dependence lies between the $\cos\theta$ and $\cos^2\theta$ curves shown here. The model input parameters (*A, B, C, D*) are respectively (0.1; 2°; 0.001; 2) and (0.03; 7°; 0.01; 1). As expected, the impact of incidence angle uncertainty is maximal for the specular regime; in this region its magnitude depends on the specular lobe slope and may reach several dB for a 1° angular change. On the other hand, the sensitivity to incidence angle uncertainty becomes negligible on the "plateau" regime (10°-20° to 50°-60°) where the S_b variation with angle is small. At higher angles (>70° in this example) the angle dependence increases again. In summary the angular dependence at steep angles varies strongly with the specular

lobe, while the oblique regime shows a much more stable behavior regardless of the seafloor type. This stability with angle is one of the major advantages of using the plateau region of incidence for backscatter measurements by MBES and should be preferentially used while comparing one backscatter survey to the other. This approach is also taken by space-borne radars which measure reflectivity only using a subset of the oblique regime [141,142].

3.4. Transmission loss

The transmission loss includes two effects [25]: geometrical divergence (energy spreading along propagation path) and absorption (due to physicochemical properties of seawater). The one-way transmission loss (*TL*) referenced to a 1 m conventional range is classically written:

$$TL = 20 \log_{10} R + \alpha R \qquad \text{[Eq. 3.13]}$$

where R is the range (in m), $20 \log_{10} R$ is the spherical spreading loss ($20\log_{10}R$ is used instead of the correct form $20\log_{10}(R/R_0)$ for notation simplicity, where $R_0 = 1$ m is the reference unit distance), and α is the absorption coefficient. Hence the uncertainty in *TL* will include the combined effects of uncertainties in the measured range (present in both terms) and the absorption coefficient.

3.4.1. Range impact upon spreading loss

The two-way spreading loss considered here is given by $2TL_s = 40 \log_{10} R$. The geometrical range R is determined by measurement of the time-of-flight t and the average sound speed $\bar{c}$ between source and target, through the elementary relation

$$R = \frac{\bar{c}t}{2}. \qquad \text{[Eq. 3.14]}$$

Therefore, the range uncertainty is due to both uncertainties in time measurement and average sound speed ($\delta\bar{c}$); its relative value is the quadratic summation of the values for time and sound speed, assumed to be independent:

$$R = \frac{\bar{c}t}{2} \Rightarrow \frac{\delta R}{R} = \sqrt{\left(\frac{\delta t}{t}\right)^2 + \left(\frac{\delta \bar{c}}{\bar{c}}\right)^2}. \qquad \text{[Eq. 3.15]}$$

The minimum travel-time uncertainty δt is bounded by the sampling step of the digitized time signal, normally smaller than half the pulse duration. For instance, for a high-frequency MBES transmitting 0.2 ms pulses in a 50 m water depth (*z)*, the range uncertainty is bounded by $\delta t = T/2 = 0.1$ ms, compared to a minimum two-way travel time of $2z/c = 66$ ms; so the relative error in this case is $\delta t/t \approx 0.15\%$. Note that an approximate linear scaling exists for the various categories of MBES for pulse duration *vs.* depth range; e.g., a low-frequency MBES typically transmits 20 ms pulses in a 5000 m water depth, hence the same magnitude for $\delta t/t$ is expected for different operational depths.

The $\delta \bar{c}$ magnitude arises from the sound speed measurement uncertainty, which is expected to be better than 0.5 m/s (e.g., [143]), as well as due to spatial and temporal water column variability [144]. The relative uncertainty $\delta \bar{c}/\bar{c}$ integrated over the water depth is not expected to be more than 0.1% ($\delta \bar{c} \sim 1.5$ m/s). With these magnitudes of $\delta \bar{c}/\bar{c} = 0.1\%$ and $\delta t/t = 0.1\%$ the range-relative uncertainty expressed in [Eq. 3.15] is about $\delta R/R = 0.18\% \approx 0.2\%$.

Finally, the associated spreading loss uncertainty is given by:

$$\delta_R(2TL_s) = 40\log_{10}(1 + \frac{\delta R}{R}) \approx 40\log_{10}(1.002) \approx 0.035 \ dB. \qquad \text{[Eq. 3.16]}$$

This result is independent of the range and is valid for all MBES categories and propagation ranges. Moreover, the range term featured in the transmission loss is partly compensated by its role in the footprint area *A* expression, proportional either to *R* or to *R²*. Thus, the actual final dependence of the S_b value upon range will be $20\log_{10}R$ or $30\log_{10}R$, instead of $40\log_{10}R$ and the maximum uncertainty in spreading loss, corresponding to [Eq. 3.16] should be either 0.018 dB (for $20\log_{10}R$) or 0.027 dB (for $30\log_{10}R$). To conclude, the S_b uncertainty caused by the range uncertainty on the

geometrical divergence component of the propagation loss is less than 0.03 dB and can be considered negligible.

3.4.2. Range impact upon absorption loss

The absorption loss is given by $2TL_{abs} = 2\alpha R$. Hence its range-dependent uncertainty for a δR range variation is:

$$\delta_R(2TL_{abs}) = 2\alpha\delta R = 2\alpha R \frac{\delta R}{R} \qquad\qquad \text{[Eq. 3.17]}$$

with the right-hand term containing the product of the absorption loss and the relative uncertainty in range. The relative uncertainty in range is typically 0.2% or less; hence for a numerical estimation of [Eq. 3.17] the magnitude of $2TL_{abs} = 2\alpha R$ has to be specified. Four cases are considered here for different frequencies and maximum oblique ranges typical of various MBES categories (deep, medium, shallow, very shallow) (Table 3.1). The results in Table 3.1 show that the S_b uncertainty due to range in the absorption effect can reach a magnitude of 0.08 dB in the worst cases (extreme oblique range, intermediate frequencies 30-100 kHz with a 0.1% uncertainty in range) – and hence is a negligible effect.

Table 3.1: Uncertainty [Eq. 3.17] in transmission loss due to range uncertainty for four typical categories of multibeam echosounders.

MBES category	Deep	Medium	Shallow	Very Shallow
Frequency (kHz)	12	30	100	300
Approximate absorption coeff.α (dB/km)	1.2	6.7	33.2	72.5
Max depth z (m)	5000	2000	300	50
Max oblique range (m) $R_{max} = z/\cos75° \approx 4z$	20000	8000	1200	200
Max absorption loss (dB) $2\alpha R_{max}$	48.0	107.2	79.7	29.0
Uncertainty [Eq. 3.17] (dB) for $\delta R/R = 0.1\%$	**0.04**	**0.1**	**0.08**	**0.03**

3.4.2.1. Absorption coefficient

The $2TL_{abs}$ uncertainty due to an absorption coefficient uncertainty $\delta\alpha$ is given by:

$$\delta_\alpha(2TL_{abs}) = 2R\delta\alpha = 2\alpha R \frac{\delta\alpha}{\alpha}$$

[Eq. 3.18]

where the relative uncertainty in absorption coefficient $\delta\alpha/\alpha$ has been made explicit. The absorption effect is a combination of the intrinsic absorption coefficient of the seawater (depending both on the absorption model reliability and on the accuracy of the measurements of estimates of local water properties) and the possible additional absorption caused by events in the water column such as bubble clouds (close to the surface or the ship's hull) or suspended sediments (close to the seafloor). The latter effect is more prone to impact high-frequency systems in shallow waters, while surface bubbles can impact systems in any water depth. Unfortunately, it is very difficult to assume *a priori* realistic magnitudes for such causes of uncertainty. The underlying physical phenomena controlling the intrinsic absorption coefficient of seawater are well understood and several models exist, based on fitting datasets of empirical measurements. Although more recent models have been proposed [145], the model by Francois and Garrison [146] is the most commonly used today, with a reported accuracy of 5%. To reduce this uncertainty, more direct observations of absorption coefficients are needed [147]. A rough estimate of uncertainty in transmission loss is proposed in Table 3.2 for an assumed $\delta\alpha/\alpha$ ranging from 1% to 10%.

Table 3.2: Uncertainty in transmission loss due to absorption coefficient uncertainties (1% and 10%) for four typically-used frequencies of MBES.

MBES category	Deep	Medium	Shallow	Very Shallow
Frequency (kHz)	12	30	100	300
Absorption coeff. α (dB/km)	1.2	6.7	33.2	72.5
Max depth z (m)	5000	2000	300	50
Max oblique range (m) $R_{max} = z/\cos75° \approx 4z$	20000	8000	1200	200
Max absorption loss (dB) $2\alpha R_{max}$	48.0	107.2	79.7	29.0
Max. $2TL_{abs}$ uncertainty (dB) for $\delta\alpha/\alpha = 1\%$	**0.48**	**1.0**	**0.8**	**0.3**
Max. $2TL_{abs}$ uncertainty (dB) for $\delta\alpha/\alpha = 10\%$	**4.8**	**10**	**8**	**3**

Therefore in the most probable practical cases of a few percent of relative uncertainty $\delta\alpha/\alpha$ considered at the maximum oblique range of the sounder, the absorption

58

uncertainty may reach several dB (up to 10 dB in the worst case of Table 3.2). These estimates can be refined through a computation as a function of incident angle, for various frequencies and water depths; Figure 3.3 presents such results for a pessimistic $\delta\alpha/\alpha=10\%$. This figure illustrates that uncertainty in seawater absorption coefficient, even at lower levels, can be expected to be a major factor in the final S_b estimation accuracy, especially in the case of medium frequencies (30 and 100 kHz).
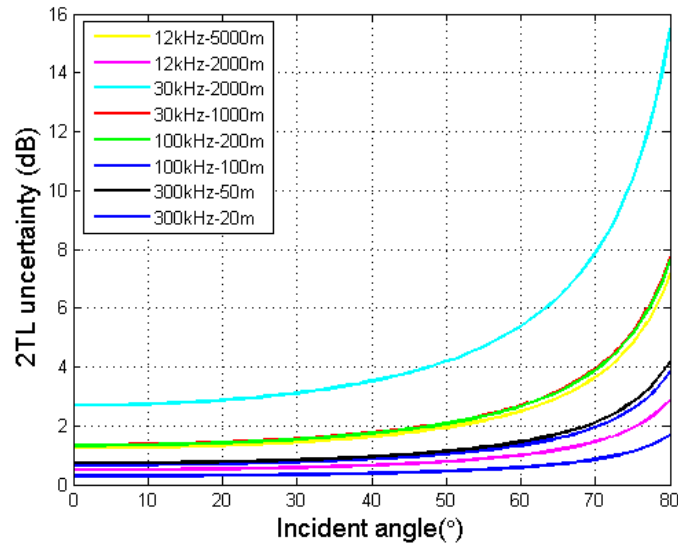
Figure 3.3: Expected uncertainty (on $2TL$, or on S_b) resulting from a 10% uncertainty in absorption coefficient, based on the same parameters (frequency – water depth) as in Table 3.2.

In summary, the main factor to consider for the backscatter uncertainties due to transmission loss is the absorption coefficient which can result in uncertainties in backscatter estimates of several dB (Table 3.2, Figure 3.3). The effects caused by the propagation range uncertainty are negligible in comparison.

3.5. Insonified area

Knowledge of the insonified area A is required to determine the backscatter strength defined per unit area ($10\log_{10}A$ in [Eq. 3.6]). In the classical Mill's cross configuration for MBES arrays, the insonified area extent in the along-track direction is defined by the Tx sector beamwidth [19]. For the oblique incidence region, the across-track extent of the insonified area is bounded by the pulse length projection over the seafloor, while in the

normal incidence region, it is bounded by the receiver beamwidth (Figure 3.1). The detailed accurate computation of the insonified area is complicated if both the full *Tx* and *Rx* beam patterns are considered, however, approximate formulas are commonly used. At oblique incidence (short-pulse regime, see [19]) the insonified area can be approximated as:

$$A \approx \varphi R \frac{cT}{2 \sin \theta \cos \gamma} \qquad \text{[Eq. 3.19]}$$

and around normal incidence (long-pulse regime) as:

$$A \approx \varphi \omega R^2 \frac{1}{\cos \theta \cos \gamma} \qquad \text{[Eq. 3.20]}$$

with R the range; φ and ω the along-track and across-track two way equivalent apertures respectively (Figure 3.1); T the pulse length; c the local sound speed; θ the across-track incidence angle; and γ the along-track slope. The pulse length T considered here is either the length of the physically transmitted pulse in case of continuous waves (CW) or the compressed pulse length after matched filtering in the case of frequency modulated (FM) transmitted signals [19].

These approximations [Eq. 3.19, Eq. 3.20] may lead to biases in the backscattering strength estimates. For narrow beams, this bias can practically be ignored [122]. However, for wide beams, the bias can be significant, as shown for radar [148–150] and sonar backscatter measurements [151]. MBES beamwidths are today usually less than 2° so only a minimal effect on the insonified area is expected. Using a point-scatterer model [152] for a shallow-water MBES (0.15 ms pulse length, 1.5° along- and across-track beamwidths), a numerical simulation is presented here (Figure 3.4) to illustrate the possible bias caused by the approximated formulae used for the insonified area. The area estimated using the simplified equations [Eq. 3.19, Eq. 3.20] matches fairly well with the simulated area defined by the idealized beam-pattern, for a range of depths (Figure 3.4 shows an example in 50 m depth) except for a narrow intermediate angular range at the transition between the near-nadir and the oblique-angle regimes where the computed and simulated areas differ more significantly (up to ~0.5 dB in this example). Thus, the approximations used in footprint area computations can be applied to MBES data without causing significant

60

uncertainty beyond the near-nadir region. The contribution of other terms in [Eq. 3.19, Eq. 3.20] in the insonified area estimation are discussed below.
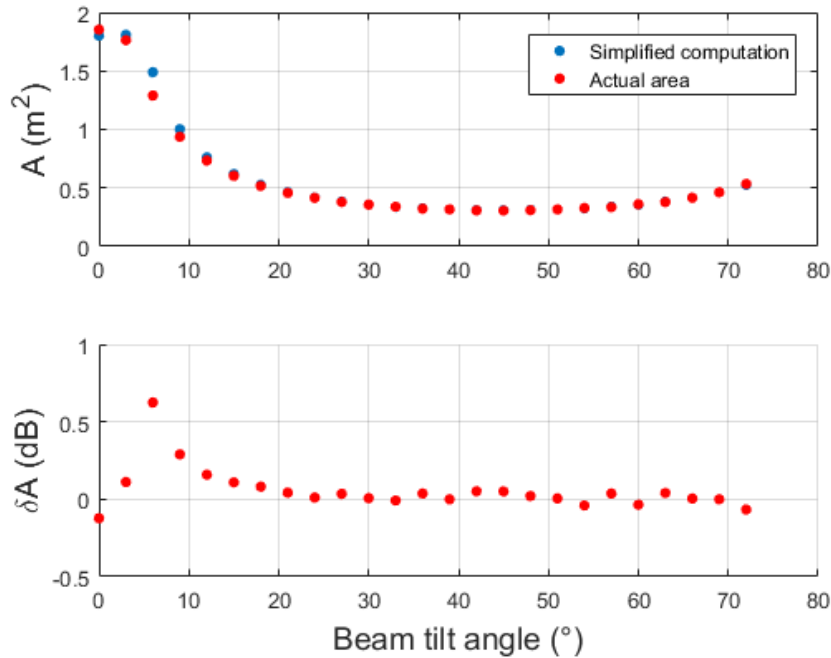
Figure 3.4: Example of comparison of insonified area estimates based on simplified computation [Eq. 3.19, Eq. 3.20] and actual area obtained by numerical simulation. At ~60°, the simplified formula shifts from insonification limited by beam aperture to insonification limited by pulse length, resulting in a slight mismatch with the simulation results. Depth 50 m; pulse duration 0.15 ms; beamwidth 1.5°.

3.5.1. <u>Range dependence</u>

The impact of range uncertainty on footprint area is not considered here. It was considered above in the divergence transmission loss analysis and shown to be a parameter of secondary importance.

3.5.2. <u>Sounder parameters</u>

The sonar system parameters considered here are the beam apertures (φ and ω) and the pulse length T. Uncertainties in these terms can be caused either by shortcomings in the documentation provided by the manufacturer or by unwanted modifications in the MBES characteristics, for example failure of sonar array elements or inappropriate motion compensation [44,153]. In all cases, these uncertainties:

- act as stable biases on the measured/computed backscatter values and can be corrected *a posteriori* provided that their magnitude is identified;

- should not exceed a few percent, whatever their cause.

Table 3.3 gives the S_b uncertainties (in dB) associated with uncertainty of 1% to 20% for the input parameters of footprint A (with the $10\log_{10}$ dependence involved in [Eq. 3.6]). It is expected that the impact of these uncertainties in the footprint extent would remain small (although not negligible, especially if accumulated), considering that the relative uncertainty on the sounder's parameters (beam patterns, pulse length) are likely to stay within a few percent.

Table 3.3: S_b uncertainty caused by a relative uncertainty in individual components of insonified area A (beamwidths or pulse length), from 1% to 20%, expressed in dB (according to the $10\log_{10}A$ dependence in [Eq. 3.6]).

Relative uncertainty (%)	1	2	3	10	20
Uncertainty in dB	**0.04**	**0.09**	**0.21**	**0.41**	**0.79**

3.5.3. Across-track angle

Consider here first the angles in the across-track vertical plane (containing the formed beams). The sources of angle errors are presented in §3.2. If the across-track slope of the seafloor is taken into account when computing the incidence angle θ, an uncertainty $\delta\theta$ causes an uncertainty of A given by (for the short-pulse regime [Eq. 3.19]):

$$A \propto \frac{1}{\sin\theta} \Rightarrow \frac{\delta A}{A} = \frac{\delta\theta}{\tan\theta}. \qquad \text{[Eq. 3.21]}$$

So the S_b uncertainty caused by angle variations in footprint area is given by:

$$\delta_{A,\theta}S_b = 10\log_{10}\left(1 + \frac{\delta A}{A}\right) = 10\log_{10}\left(1 + \frac{\delta\theta}{\tan\theta}\right). \qquad \text{[Eq. 3.22]}$$

Note that normal incidence ($\theta \to 0$) is not considered here; the angle dependence [Eq. 3.18] on $1/\sin\theta$ is not valid in this regime and must be replaced by the long-pulse regime expression [Eq. 3.20]:

$$A \propto \frac{1}{\cos\theta} \Rightarrow \frac{\delta A}{A} = -\tan\theta\delta\theta, \qquad \text{[Eq. 3.23]}$$

$$\delta_{A,\theta}S_b = 10\log_{10}\left(1 + \frac{\delta A}{A}\right) = 10\log_{10}(1 - \tan\theta\delta\theta) \cdot \qquad \text{[Eq. 3.24]}$$

Figure 3.5 shows the S_b uncertainty considering an uncertainty in the across-track incident angle (θ) from -3° to 3°, for the long- (0° to 40° incidence) and short-pulse (15° to 80° incidence) cases. The same slope shows reverse effects on the insonified area uncertainty using short- or long-pulse regimes, thus giving rise to a step change at the incidence angle where the insonified area shifts from the beam limited (long-pulse) to pulse limited (short-pulse) regime. Overall, the S_b uncertainty remains below 0.8 dB for slope-caused angle uncertainties reaching about ±3°.
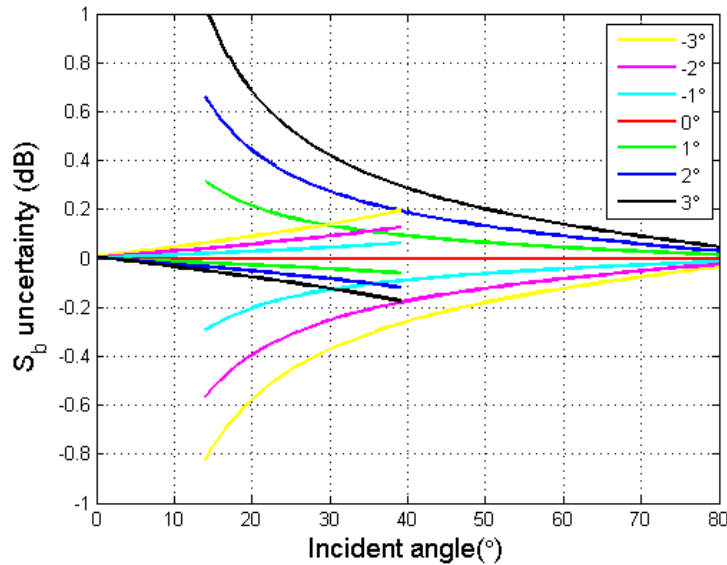
Figure 3.5: Uncertainty in backscatter strength (Sb in dB) caused by variations in footprint area due to across-track incident angle uncertainty ranging from -3° to 3° for the long-pulse (0° to 40°) and the short-pulse cases (15° to 80°).

If no compensation is applied for the seafloor topography (assumed to be flat and horizontal), then the uncertainty of the footprint area estimate is the difference between the angular dependences $A \propto 1/\sin\vartheta$ (where ϑ is the incidence angle for an assumed flat topography) and $A \propto 1/\sin(\vartheta - \beta)$ (accounting for actual terrain slope β). Hence the uncertainty for the short-pulse regime is expressed in dB as:

$$\delta_{A,\beta}S_b = 10\log_{10}|\sin\vartheta/\sin(\vartheta - \beta)| \qquad \text{[Eq. 3.25]}$$

Similarly for the long-pulse regime:

$$\delta_{A,\beta}S_b = 10\log_{10}|\cos\vartheta/\cos(\vartheta - \beta)| \cdot \qquad \text{[Eq. 3.26]}$$

The resulting S_b uncertainty is plotted in Figure 3.6 as a function of incidence angle (0° to 80°) when the seafloor slope β (between -15° and +15°) is not accounted for, for the long- (0° to 40° incidence) and short-pulse (15° to 80° incidence) regimes. For the long-pulse case, the uncertainty is on the order of 1 dB for steeper slopes (15°), however, for the short-pulse region the uncertainty in the seafloor for slopes facing towards the MBES causes large uncertainty in S_b (e.g., > 3 dB for $\vartheta = 15°$ at $\theta < 30°$). Figures 3.5 and 3.6 indicate that the impact of across-track seafloor slope uncertainty is significant and most severe at mid-range incidence angles (20°-50°).
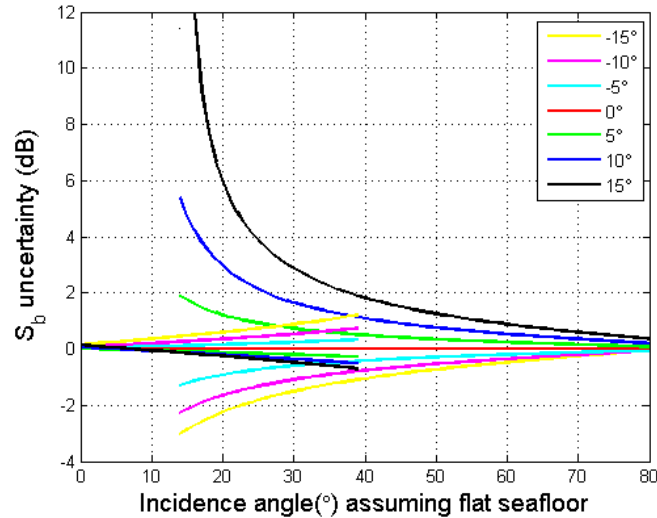
Figure 3.6: Uncertainty in backscatter strength (S_b in dB) if the seafloor across-track slope is not considered for area insonified computation. Unaccounted seafloor slopes from -15° to 15° are considered for the long-pulse (0° to 40°) and short-pulse cases (15° to 80°).

3.5.4. Along-track angle

An uncertainty $\delta\gamma$ in the along-track incidence angle γ causes an uncertainty in the insonified area A given by [Eq. 3.19, 20]:

$$A \propto \frac{1}{\cos\gamma} \Rightarrow \frac{\delta A}{A} = \tan\gamma\,\delta\gamma \cdot \qquad\text{[Eq. 3.27]}$$

The uncertainty in S_b can then be estimated as:

$$\delta_{A,\gamma}S_b = 10\log_{10}\left(1 + \frac{\delta A}{A}\right) = 10\log_{10}(1 + \tan\gamma\,\delta\gamma) \cdot \qquad\text{[Eq. 3.28]}$$

For $\delta\gamma$ ranging from -3° to 3° Figure 3.7 shows that the S_b uncertainty is insignificant for small uncertainties in the incidence angle (1 or 2°) and/or terrains with smooth topography (along-track slope angles up to 10° to 15°); even for steep areas with higher uncertainties in the topography, the S_b uncertainty remains within a few tenths of a dB.
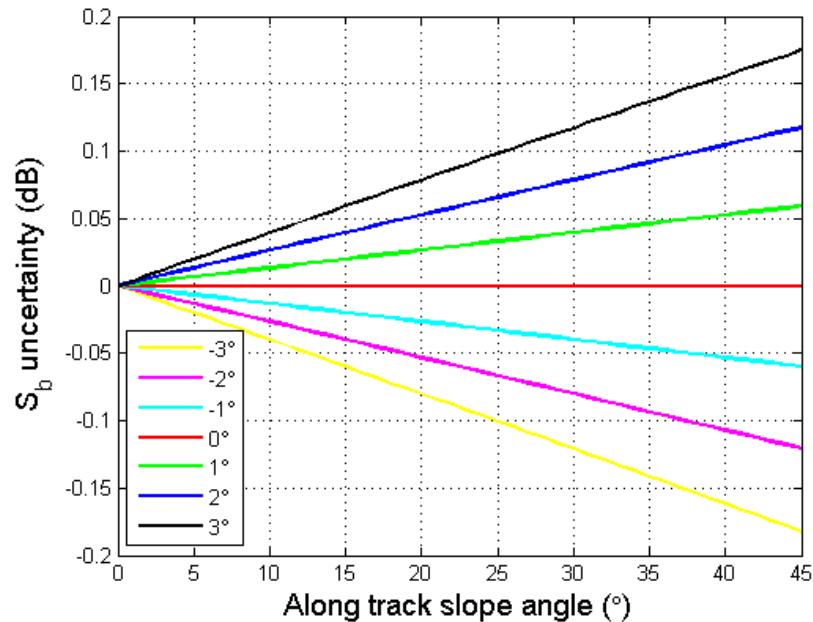
Figure 3.7: Uncertainty in S_b estimation due to uncertainty in along-track slope.

If the along-track slope angle effect is not accounted for (as is often the case), the uncertainty is then directly given by the $1/\cos\gamma$ term (Figure 3.8), where γ represents the slope angle. Here again, the S_b uncertainty may be negligible for smooth terrains (< 0.1 dB for incidence angles up to 15°) but increases significantly for steeper slopes (> 0.5 dB for slopes 30° to 45°). Note these results for along-track angles are valid for short- and long-pulse regimes, since both regimes have the same dependence on $1/\cos\gamma$ (see [Eq. 3.19, Eq. 3.20]).
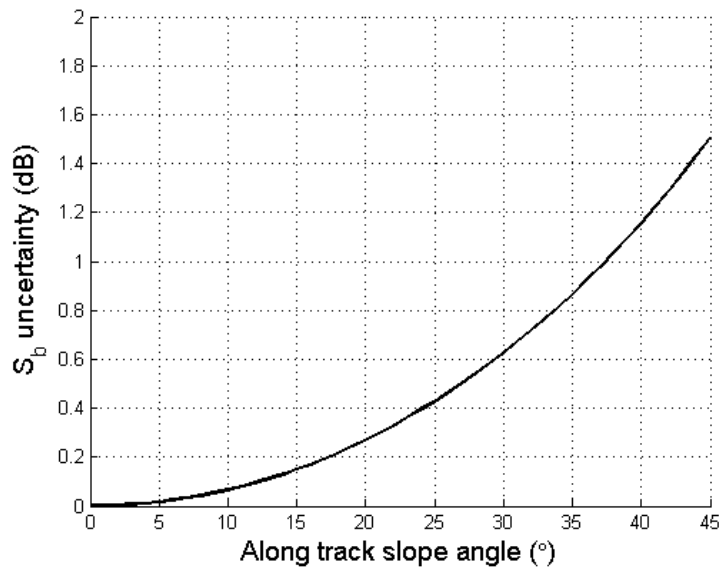
Figure 3.8: Uncertainty in S_b estimation if the along-track slope (0° to 45°) is ignored.

In summary, for the compensation of the insonified area, the impact of inaccuracies in the sounder characteristics remains limited and can reasonably be kept small or negligible. The S_b dependence on incidence angle has a far more significant impact, potentially reaching several dB, depending on the beam angle and local seafloor slope. While computing the insonified area, the across-track slope angle plays the major role, while the along-track angle impact remains limited. Completely ignoring the seafloor slope (both across- and along-track) when estimating the footprint extent, logically leads to the

largest uncertainties. Fortunately, commercially available backscatter processing software tools have started to address such compensations (e.g., [154]). However, even when accounting for the local slopes, uncertainties of a few degrees may remain and the relations provided above can be used to assess their uncertainty contributions.

3.6. <u>Summary of the major uncertainty components</u>

Based on the elementary analysis presented above, the impacts of the main sources of backscatter uncertainty are summarized in Table 3.4. Each of the causes of S_b uncertainty is broken down into "random" or "bias" components. "Random" uncertainties are caused by noise or intrinsic fluctuations (e.g., echo signal instabilities, or small-scale uncertainties in the bathymetry) and can be mitigated through *a posteriori* statistical processing. "Bias" or systematic uncertainties may be caused by variations in the MBES characteristics, by unaccounted changes in environmental conditions, or by insufficiencies in the processing procedures; they may systematically vary as a function of depth, seafloor slope and ship's motion. They can (up to some point) be corrected *a posteriori*, although this implies complementary operations that may prove difficult (e.g., sonar calibration, re-computation of the DTM, improved information about the water column). The bias corrections, once applied, still have some residual uncertainty that must then be included in the uncertainty budget. The following scale is proposed to classify the magnitude of the uncertainty:

- *Negligible* (*N*) : 0.01 to 0.1 dB
- *Small* (*S*): 0.1 to 1 dB
- *Moderate* (*M*) : 1 to 3 dB
- *High* (*H*) : 3 to 6 dB
- *Prohibitive* (*P*) : beyond 6 dB

Table 3.4: Major sources of uncertainty for compensated echo-level, source level (*SL*), transmission losses (*TL*), insonified area (*A*), and seafloor incidence angle. See the code (*N-S-M-H-P*) definition in the text. Uncertainties are categorized as Bias or Random uncertainty based on their effect on the measurement.

Measurement component	First-order uncertainty sources	Bias	Random	Magnitude	Possible quality improvement

Compensated Echo Level	Signal fluctuations		✔	M to H (5.57 dB std.dev. for a Rayleigh distrib.)	Decreased (S) by data averaging (at the expense of resolution)
	Noise Level		✔	S in most cases	Improve sonar performance
	Sonar parameters (without calibration)	✔		Unpredictable – up to P	Calibration
	Sonar parameters (after calibration)		✔	N to S	Calibration accuracy
Incidence angle	Seafloor slope (compensated)	✔	✔	N to M	Bathymetry DTM accuracy
	Seafloor slope (ignored)	✔	✔	N to P according to topography	DTM for slope compensation
Area (A)	Footprint model approximation	✔		N to S	-
	Incidence angle (refraction, seafloor slope)	✔	✔	S to M. Possibly H to P (if seafloor slope ignored)	Improved accuracy in SVP and DTM
	Sonar parameters	✔		S	Constructor's information
	Propagation range		✔	N	-
Transmission Loss (TL)	Absorption coefficient	✔		S to H	Water column absorption profile
	Propagation range		✔	N	-
	Frequency differences (ignored)	✔		N to M	Sector frequency accounted for
	Water column anomalies	✔		N to P	Water column properties

3.7. <u>Conclusions</u>

This work has attempted to identify and model the major causes and magnitudes of backscatter uncertainties from MBES systems. Unraveling the complexities of backscatter measurements is a considerable task, and the approach outlined here is far from complete; however, it is hoped that it offers a framework from which further understanding of the sources and magnitude of backscatter uncertainties can be derived.

The elementary uncertainty analysis proposed here identified the major components of the uncertainty budget (Table 3.4):

- The uncertainty in fluctuating and unreferenced measured echo levels is due to both the random character of the echo intensity (causing noise-like fluctuations to be processed statistically) and the incomplete knowledge of the MBES calibration parameters (leading to biases). The statistical uncertainty can be controlled by averaging a number of samples into a mean echo level with the understanding that increasing this number degrades resolution and thus a trade-off has to be made between resolution and uncertainty. In contrast, the uncertainty stemming from inaccurate values of MBES characteristics can reach unpredictable and unacceptable magnitudes if appropriate calibration operations have not been conducted nor reference data collected. MBES manufacturers should play a key role in addressing this issue by providing the information needed to better document and reduce this fundamental component of uncertainty, which is difficult to detect in the field data and whose accurate evaluation is rarely accessible to users.

- The uncertainty in seafloor incidence angle measurement is mostly affected by seafloor slope uncertainty controlled by the resolution and accuracy of bathymetric data used for DTM production (if used at all). Greater attention must be placed on the incorporation of bi-dimensional slope compensation inside backscatter data processing tools and on the improvement of local slope determination from the bathymetry data. This uncertainty obviously impacts the computation of the backscatter angular response. Moreover, if not accounted for, slope is often the major cause of error in the insonified area computation. The sounder characteristics are normally sufficiently well

69

known for the impact of their uncertainty to remain acceptable; this again falls under the manufacturer's responsibility.

- The transmission loss uncertainty is almost exclusively due to the absorption coefficient estimation, the inaccurate estimation of which can have a significant impact on the backscatter level estimation; however the combination of the measurement of temperature and salinity values over the full water column with appropriate procedures for compensation can keep the impact of the absorption coefficient within acceptable limits. The impact of local perturbations of the water column properties is not well-understood and deserves further investigation, although the use of ocean atlas data or ocean models can help to mitigate this problem. Unexpected phenomena such as bubble clouds sweeping the MBES arrays cause specific issues that are impossible to quantify in advance; however their joint impact on the objective quality of bathymetry data can help detect their presence and justify disregarding corrupted data.

This study was conducted as an initial step in the identification of the fundamental causes and estimation of order-of-magnitude levels of the uncertainties associated with the collection of MBES backscatter data. It has shown that it is difficult to predict broadly applicable numerical values, since many of the major uncertainty sources vary on a case-to-case basis. Future efforts need to be directed towards better provision of sonar characteristics from the manufacturers, improvement of MBES calibration methods, and quantification of their reliability and objective uncertainty. A second area of investigation is the impact of unexpected perturbations of the seawater column properties (e.g., bubble clouds). Both topics suggest the need for new well-designed field experiments and would benefit greatly from collaborative efforts of the concerned communities.

APPENDIX 3A

Statistical uncertainty in measured EL

The statistical fluctuation of the *EL* is an inherent property of backscattered signals and therefore an unavoidable source of random uncertainty. However, confidence in the mean echo level reliability can be improved by increasing the number of samples used in averaging. In MBES data, this is done most often by averaging across-track and along-track samples. However, this should only be done for homogeneous seafloor as the mean

angular response can be corrupted at the transition between two seafloor types. Mosaic segmentation into areas showing similar backscatter can help in selecting regions of the same seafloor type over which the samples can be averaged [106]. The number of samples available for each beam is controlled by the across-track footprint extent, so the largest number of samples is obtained for the outer-most beams. Assuming that the time series is being sampled at a high enough rate compared with the pulse duration, the number of statistically-independent samples N_s inside a beam is computed as the ratio of the length of the receive beam footprint in the across-track direction and the projected pulse duration [23]:

$$N_s(\theta) \approx \left(\frac{z\omega}{\cos^2\theta}\right) / \left(\frac{cT}{2\sin\theta}\right) \qquad \text{[Eq. A1]}$$

where z is the water depth, ω the *Rx* across-track beamwidth, c the sound speed, T the pulse length and θ the incidence angle. Eq. [A1] holds for long-pulse regime, excluding the angles around nadir. Obviously, the benefit of averaging over several samples exists only when $N_s > 1$. Figure A1 presents the number of statistically independent samples for a MBES with $\omega = 0.5°$ and $2°$; and z = 50 m (with $T = 0.05$ ms and 0.15ms) and 1000 m (with $T = 5$ ms and 10 ms). N_s increases with decreasing T and increasing ω.
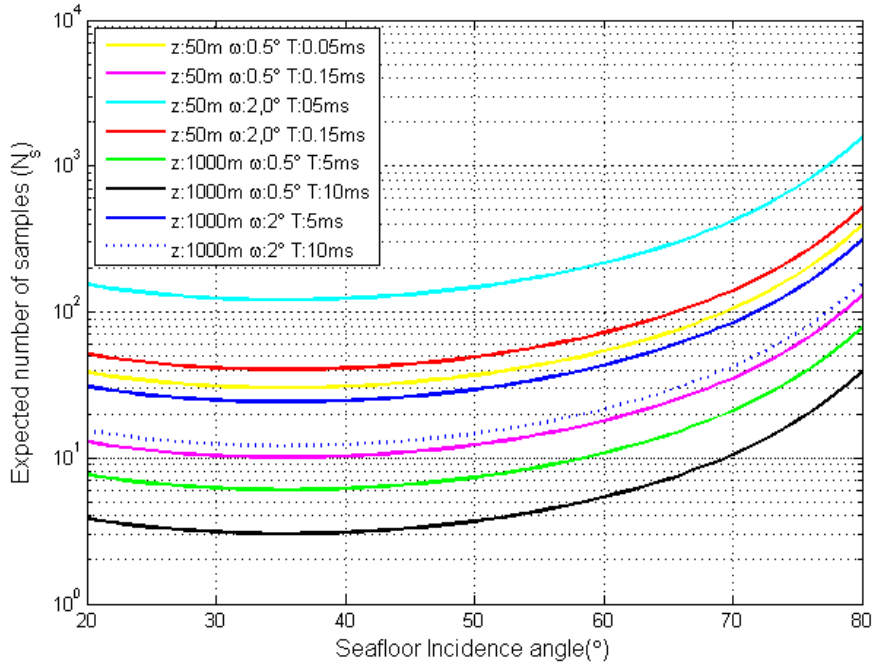
Figure A1: Estimated number [Eq. A1] of statistically independent samples for each beam for a multibeam echosounder at water depths 50 m and 1000 m; beamwidths of 0.5° and 2°; and pulse lengths (0.15; 0.5; 5 and 10 ms).

The standard deviation of *N* averaged independent samples is given as:

$$\sigma_{\bar{x}} = \frac{\sigma_x}{\sqrt{N}}$$

[Eq. A2]

where $\sigma_{\bar{x}}$ and σ_x are the standard deviations of averaged and individual samples respectively. Eq. [A2] is valid provided that the *N* averaged values are statistically independent, are derived from a same population, and have the same variance [155]. Assuming the standard deviation of individual samples is 5.57 dB (Rayleigh distribution) and averaging over the dB values, more than 30 individual samples are required to achieve a 1 dB standard deviation (Figure A2). If the envelope squared amplitudes (i.e., intensity) in natural units is considered for the averaging (which is a preferable way to do it), the dB value of the standard deviation referenced to the mean is $10 \log_{10}(1 + 1/\sqrt{N}) \approx 4.34/\sqrt{N}$ dB [156]. In this case, to reduce the standard deviation to 1 dB, only ~ 20 samples are required (Figure A2). Although the uncertainty is lowered by averaging over larger number

72

of samples, the spatial resolution is adversely affected which may or may not be important depending on the type of application (compare high resolution mapping, with large scale mapping).
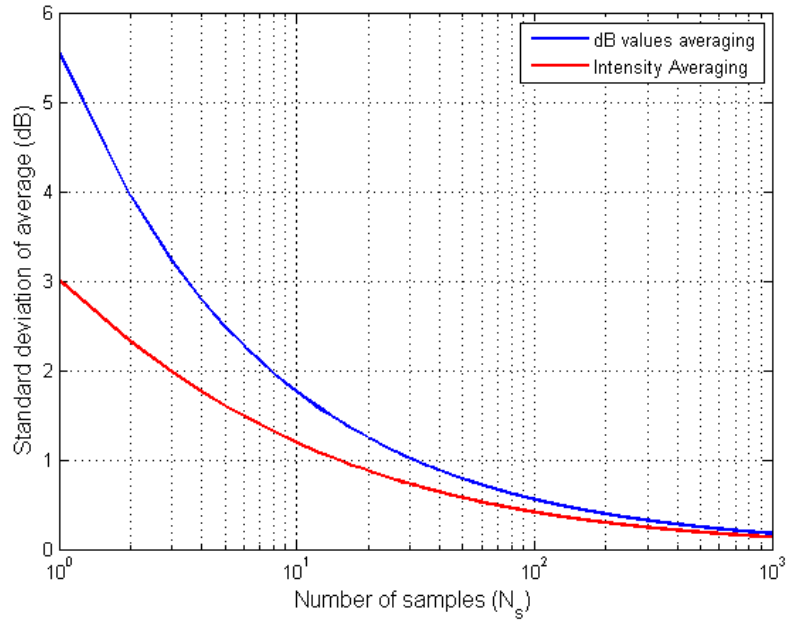
Figure A2: Estimated number of statistically independent samples to be averaged in order to obtain a given standard deviation (in dB). The initial distribution is Rayleigh, with a standard deviation of 5.57 dB.

CHAPTER 4

SOURCES AND IMPACTS OF BOTTOM SLOPE UNCERTAINTY ON ESTIMATION OF SEAFLOOR BACKSCATTER FROM SWATH SONARS

Abstract: Seafloor backscatter data from multibeam echosounders are now widely used in seafloor characterization studies. Accurate and repeatable measurements are essential for advancing the success of these techniques. This paper explores the impact of uncertainty in our knowledge of local seafloor slope on the overall accuracy of the backscatter measurement. Amongst the various sources of slope uncertainty studied, the impact of bathymetric uncertainty and scale were identified as the major sources of slope uncertainty. Bottom slope affects two important corrections needed for estimating seafloor backscatter: (1) the insonified area and; (2) the seafloor incidence angle. The impacts of these slope-related uncertainty sources were quantified for a shallow water multibeam survey. The results show that the most significant uncertainty in backscatter data arises when seafloor slope is not accounted for or when low-resolution bathymetry is used to estimate seafloor slope. This effect is enhanced in rough seafloors. A standard method of seafloor slope correction is proposed to achieve repeatable and accurate backscatter results. Additionally, a standard data package including metadata describing the slope corrections applied, needs to accompany backscatter results and should include details of the slope estimation method and resolution of bathymetry used.

4.1. Introduction

Over the last few decades there have been significant advances in the use of Multibeam Echo Sounders (MBES) to acoustically determine the seafloor properties (e.g., depth, sediment type) that are critical for a host of applications including nautical charting, seabed habitat assessments, and geological interpretations [1,11,13,39]. While the initial premise of MBES studies has been on extracting bathymetric information, more recently there is an increasing shift in focus on seafloor backscatter, particularly with respect to those studies aimed at seafloor characterization. Seafloor backscatter studies fall under the general category of remote sensing. With the growing use of remote sensing data, the topic of uncertainty has been receiving increasing attention, particularly in the terrestrial geographical sciences [157–160]. This focus has led to recommendations that the spatial output of remote sensing data, when compiled into a geographical information system (GIS), should be (at least) twofold: (i) a map of the variable of interest and (ii) some assessment of measurement uncertainty in that map.

Although calls for including uncertainty estimates in remote sensing studies have been numerous, its practical application is challenging. The main reasons for this are: (1) knowledge of uncertainty in the measurements is often not available; (2) the impact of the choice of spatial scale is inherently linked to the variable being mapped (which is essentially the unknown) hence the ambiguity as what should be the ideal spatial scale; (3) data processing tools are often not transparent, i.e., their algorithms can be proprietary, prohibiting the calculation of uncertainty propagation from input to the final outputs; (4) the lack of ground-truthing data to independently verify the remote sensing observations, and; (5) remote sensing data often involves multiple dimensions (at least 3 in most cases: position i.e., *x, y* and variable to be mapped). Representation of uncertainty for each pixel thus becomes an issue. Progress on all five challenges is required to improve the uncertainty estimation of remote sensing data. This study is part of a larger effort aimed at looking at various contributors to uncertainty in seafloor backscatter [161] and addresses the uncertainty introduced by uncertain measurements of seafloor slope and the implications of using seafloor slope at different spatial scales for seafloor backscatter corrections.

Two fundamental properties of the seafloor derived from MBES data are depth and seafloor backscatter strength. A detailed uncertainty model for bathymetry was developed by Hare et al. [99]. Later implementations of uncertainty models, e.g., the Combined Uncertainty and Bathymetry Estimator or CUBE [12] have proven that a better understanding of depth estimation and uncertainty can not only improve data quality but can also simplify data processing. These models identify and capture the bathymetric uncertainty from different sub-components of the sounding measurement, including the echo sounder, the motion sensor, tides, refraction through water, etc. As a result, uncertainty computation methods are now widely adopted across bathymetric data processing tools and end users.

Unlike bathymetric data, which benefits from recognized industry standards used for uncertainty calibration, a "general" uncertainty model for seafloor backscatter has not yet been realized; the sources of uncertainty in backscatter data have only been studied on a case-by-case basis. As techniques to validate backscatter data and treat backscatter quantitatively improve, a need to understand the limitations of backscatter data acquisition and processing has emerged. The major causes of the uncertainty in backscatter data are related to the area correction; incidence angle; transmission loss, and MBES calibration parameters, as well as inherent statistical fluctuations in the measured intensity [117,161]. Two of these corrections (area and incidence angle) depend directly on accurate estimates of seafloor slope. This paper is an extension of an earlier study of the primary factors impacting seafloor backscatter uncertainty [161] and specifically addresses the impact of our ability to measure seafloor slope on the calculation of area and incident angle with respect to determining seafloor backscatter.

Much of the work on seafloor backscatter uncertainty has been focused on the application of image classification algorithms to backscatter mosaics [162]. For the most part, this work has been conducted without particularly considering the accuracy or quality of the input data. While understanding image classification uncertainty is important and certainly deserves attention, evaluation of the components of the measurement that create the image data, including geometric and radiometric corrections, must also be included [117,163]. Understanding these physical/geometrical aspects of backscatter measurements

76

and their uncertainties can help improve the backscatter classification and processing. As a community, we need to ensure that we are identifying the steps in backscatter processing that contribute most to uncertainty and focus our attention accordingly. In this context, this paper explores the uncertainties associated with area correction and incidence angle. Unlike terrestrial studies where photogrammetric techniques can provide very high-resolution determinations of terrain slope, the slope derived from bathymetry does not lend itself to direct validation, hence it is difficult to validate an uncertainty model of seafloor slope. At the same time, it is critical to understand the requirements of seafloor slope for backscatter corrections and how various choices of seafloor slope computation may impact the seafloor backscatter. This paper addresses some of these questions. Specifically, it: (1) presents an overview of insonified area corrections, computation of seafloor incidence angle and in doing so determines that seafloor slope is the most significant source of uncertainty for these corrections; (2) identifies the major sources of uncertainty for seafloor slope computations; and (3) proposes methods to quantify and reduce uncertainty of seafloor slope at appropriate spatial scales in actual real-world surveys.

4.2. **Materials and Methods**

MBES backscatter is derived from the measurements of seafloor target strength (see e.g., [25]). Seafloor target strength is related to the incident and scattered pressure fields from a small patch of the seafloor instantaneously insonified by the sonar signal. The ensemble average ($< >$) of squared scattered pressure $< |p_s|^2 >$ is proportional to the insonified area A and the squared incident pressure $|p_i|^2$, and inversely proportional to the sonar-target squared distance r_s^2, neglecting absorption and refraction effects

$$\langle |p_s|^2 \rangle = |p_i|^2 A \sigma_b \frac{1}{r_s^2}$$
[Eq. 4.1]

where the proportionality coefficient σ_b is referred to as the backscattering cross section [26]. Its logarithmic equivalent is the "bottom scattering strength" [25]

$$S_b = 10 \log_{10} \sigma_b.$$
[Eq. 4.2]

77

The target strength (TS in dB re 1 m^2) of the seafloor active area A is then related to the scattering strength by[1]

$$TS = S_b + 10 \log_{10} A. \qquad \text{[Eq. 4.3]}$$

In practical situations the measurements are made using a directional transmitter and receiver. The relation for S_b can be then derived in dB units as [161]

$$S_b = DN - RS_o - SL_o + 2TL - D_{TX} - D_{RX} - 10 \log_{10} A. \qquad \text{[Eq. 4.4]}$$

Where DN is the received voltage converted and stored as a digital number through an analog-to-digital converter (ADC), RS_o is the sensitivity of the receiver transforming the incident acoustic pressure into an electrical signal along its maximum response axis, SL_o the transmit sourced level, $2TL$ the two-way transmission loss, D_{TX} and D_{RX} the transmit (Tx) and receive (Rx) directivity function values in the sonar-target propagation direction and A the insonified area [19]. For a given seafloor type and frequency, this value of S_b is also related to the seafloor incidence angle θ.

4.2.1. Area Insonified correction

The seafloor patch instantaneously insonified by an MBES signal (defined by the seafloor backscatter sample footprint size) is a function of the transmit and receive beamwidths, as well as the projection of the physical length of the transmitted pulse onto the seafloor. In the classical Mill's Cross configuration for MBES arrays, the extent of the insonified area in the along-track direction is defined by the Tx sector beamwidth [19]. In the across-track direction, the extent of the insonified area is determined by the Rx (receive) beamwidth in the near-nadir region, and by the pulse length at oblique incidence angles (Figure 1). The accurately detailed computation of the instantaneously insonified area is complicated if both the full Tx and Rx beam patterns are considered; however approximate formulae are commonly used. This simplification is based on treating the insonified area as the product of the across-track and along-track extent of the projection of the backscatter sample footprint on the seafloor. This approximation for the instantaneously insonified area has been shown to create negligible uncertainty except in the near-nadir region and for

---

[1] For notation simplicity, $10\log_{10}A$ is used instead of the correct form $10\log_{10}(A/A_0)$ where $A_0 = 1$ m^2 is the reference unit surface.

wide beams [161,163]. With most MBES operating with beamwidths < 1-3°, this approximation is not considered a significant source of uncertainty. At oblique incidence (short-pulse regime, see [19]) the insonified area can be approximated as

$$A \approx \varphi R \frac{cT}{2 \sin \theta \cos \beta_y} \qquad \text{[Eq. 4.5]}$$

and around normal incidence (long-pulse regime) as

$$A \approx \varphi \omega R^2 \frac{1}{\cos \theta \cos \beta_y} \qquad \text{[Eq. 4.6]}$$

with R the range; φ and ω the along-track and across-track two-way equivalent apertures respectively (see Figure 4.1); T the effective pulse length; c the local sound speed; θ the across-track incidence angle; and β_y the along-track seafloor slope. The pulse length T, considered here, is the equivalent length of either the physical pulse duration in case of continuous waves (CW) or the compressed pulse duration after matched filtering in the case of frequency modulated (FM) transmitted signals [19]. It is to be noted that sonar systems currently do not correct for the seafloor slope in real-time. Instead a flat horizontal seafloor is assumed during data acquisition [15]. Therefore, the accurate estimation of the insonified area falls on the end-users either by applying third-party software during the post-processing phase or by developing customized software themselves.
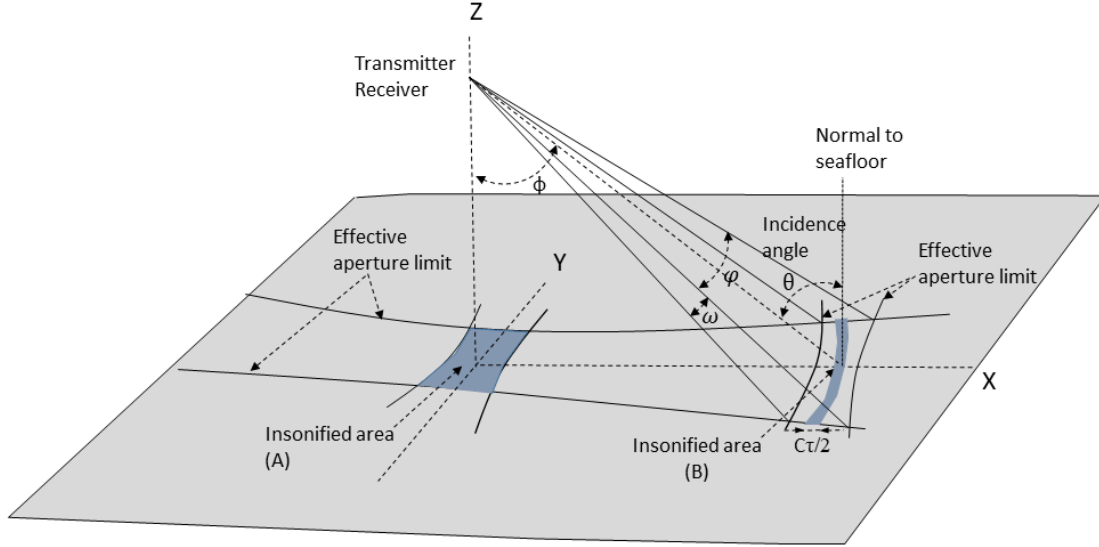
Figure 4.1: Measurement geometry of MBES and insonified area for near-nadir (A) and at oblique angle (B). Figure modified from [161].

4.2.2. <u>Seafloor incidence angle correction</u>

The seafloor incidence angle is defined as the angle between the receiving beam direction and the vector normal to the seafloor insonified patch while the grazing angle is defined as the angle between the beam direction and the vector parallel to the seafloor patch. The normal vector to the surface patch can be defined as [164]

$$\vec{n} = [\tan \beta_x, \tan \beta_y, -1]^T \qquad \text{[Eq. 4.7]}$$

where β_x and β_y represent seafloor slopes in the across-track (x) and along-track (y) directions respectively, and T denotes the transpose operation. The seafloor slope at the beam footprint is computed from the bathymetry in across-track and along-track directions using either the soundings from the individual beams or a gridded data set. Assuming a flat seafloor, the equation for the nominal receiving beam direction is

$$\vec{m} = [0, -\cos \theta_g, \sin \theta_g]^T = [0, -\sin \phi, \cos \phi]^T \qquad \text{[Eq. 4.8]}$$

where $\phi =$ nominal transmission angle, and $\theta_g = \frac{\pi}{2} - \phi$ is the nominal seafloor grazing angle. The true incidence angle is then the angle between the two vectors $\vec{n}$ and $\vec{m}$, and can then be given by

$$\cos\theta_{inc} = \frac{\vec{n}\cdot\vec{m}}{\|\vec{n}\|\|\vec{m}\|} \hspace{3cm} \text{[Eq. 4.9]}$$

where $\cdot$ is the scalar product and $\|\quad\|$ is the norm of the vector. The nominal transmission angle (with respect to the sonar) and seafloor incidence angle (θ_{inc}) are nominally complementary angles unless impacted by refraction through the water column and vessel motion. Hare et al. [99] showed that beam pointing errors at the sonar head depend on uncertainty in ship's motion and estimation of the sound speed at the sonar head. Both of these variables have been well modeled with respect to bathymetric data uncertainty [99] and will not be discussed here as their magnitude as well as their effect on the seafloor incidence angle is usually small.

4.2.3. Estimation of seafloor slope and its uncertainty

The seafloor slope "between points" or "for a patch of seafloor" is defined as the rate of change of depth over distance. Considering z_1 and z_2 as vertical coordinates and x_1 and x_2 as horizontal coordinates the slope (g) can be calculated as

$$g = \tan^{-1}\left(\frac{z_1 - z_2}{x_1 - x_2}\right). \hspace{3cm} \text{[Eq. 4.10]}$$

Applying law of propagation of variance, the variance in slope is given by

$$\sigma_g^2 = \left(\frac{\partial_g}{\partial_{x_1}}\right)^2\sigma_{x_1}^2 + \left(\frac{\partial_g}{\partial_{x_2}}\right)^2\sigma_{x_2}^2 + \left(\frac{\partial_g}{\partial_{z_1}}\right)^2\sigma_{z_1}^2 + \left(\frac{\partial_g}{\partial_{z_2}}\right)^2\sigma_{z_2}^2 \hspace{1cm} \text{[Eq. 4.11]}$$

where σ_X represents the respective error in a quantity X. Hence estimates of vertical sounding uncertainty ($\sigma_{z_1}, \sigma_{z_2}$) and position uncertainty ($\sigma_{x_1}, \sigma_{x_2}$) are required to estimate slope uncertainty.

4.2.3.1. Directional slope (along-track and across-track from reference grid)

For backscatter corrections, the two directional slopes (i.e., along- and across-track) are required. As a preliminary estimation, the depth values obtained within each beam can be used to calculate across-track slopes. This calculation is straightforward to implement in the framework of MBES sounding data processing. A frequently-used option is to take at least two depth measurements on either side of a depth sounding and then fit a plane through the depth values. Unedited individual soundings may have large variance that will

adversely affect the slope estimation. Therefore, it is important to edit the obvious outliers in the bathymetry before attempting the across-track slope calculation.

While using beam depth data is an option for MBES systems that provide co-located bathymetry and backscatter, the common choice for computing slope is to use the gridded bathymetry. To determine the across-track slope, the gradients along two principal axes, *x* and *y* are calculated first. From the values of *dz/dx* and *dz/dy* one can then determine the slope of the plane that approximates the surface at the local depth point (*i, j*) using the formula [165]

$$g_{dir}(\gamma) = \tan^{-1}\left[\frac{dz}{dx}\sin\gamma + \frac{dz}{dy}\cos\gamma\right] \qquad \text{[Eq. 4.12]}$$

where γ represents the across-track orientation of the MBES swath, determined based on the vessel heading, along which the slope was calculated. Directional slopes can be computed by applying a 3 x 3 kernel indexed to each cell (except those at the grid edges). Figure 4.2 illustrates the adopted convention for cell indexing.
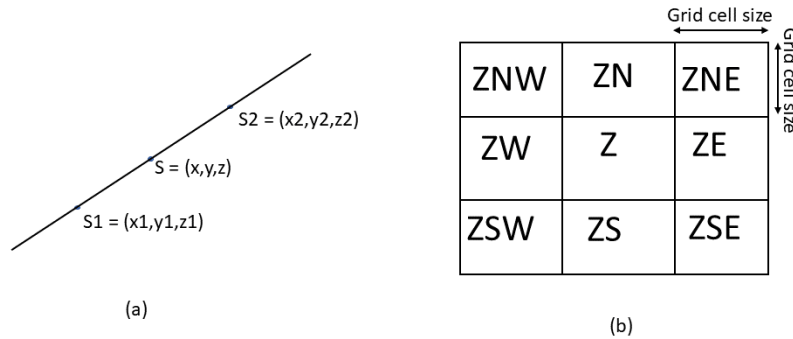
Figure 4.2: (a) Adjacent soundings considered for across-track slope estimation with *x,y* the sounding coordinates and *z* the depth. (b) Neighboring grid cells available for slope estimation. The grid nodes are equally spaced based on the grid cell size.

Various methods are available for the estimation of directional gradients (*dz/dx* and *dz/dy*) from gridded data sets. For a comparison of the performance of these methods see [139]. Two commonly recommended methods are used here: the central difference method [165] and the Horn [166] method. In the case of the central difference method, the values of two neighboring cells are used to compute gradients along the two axes (Figure 4.2)

82

$$\frac{dz}{dx} = [z_E - z_W]/2S$$ [Eq. 4.13]

$$\frac{dz}{dy} = [z_N - z_S]/2S$$

where S defines the grid cell size. In the case of cells at the grid edge, the central cell itself is used to provide the value for the missing data. For the Horn method, values from six neighboring cells are utilized to compute gradients (Figure 4.2). The weight applied to each cell depends on its position relative to the central cell. Formulae for the computation of directional gradients in this case are:

$$\frac{dz}{dx} = \frac{[(z_{NE} + 2z_E + z_{SE}) - (z_{NW} + 2z_W + z_{SW})]}{8S}$$ [Eq. 4.14]

$$\frac{dz}{dy} = \frac{[(z_{NE} + 2z_N + z_{NW}) - (z_{SE} + 2z_S + z_{SW})]}{8S}.$$ [Eq. 4.15]

4.2.3.2. <u>Estimation of slope uncertainty</u>

Studying uncertainty in seafloor slope estimation is relatively difficult as the true value of slope is hard to determine and validate. Dolan and Lucieer [139] and Lucieer et al. [56] recommended using a Monte Carlo simulation to analyze the uncertainty in slope by considering the uncertainty in the bathymetry. Therefore, the uncertainty of bathymetry data estimated using the CUBE algorithm [12] was used to infer uncertainty in estimated slope. Besides the horizontal and vertical uncertainty of the soundings, the slope estimation may also be affected by the method used to compute the seafloor slope. Several different algorithms are available for slope estimation that differ based on the method used to determine the neighboring grid cell sizes [167], resulting in different estimates. Additionally, the scale of the seafloor slope (i.e., at what spatial resolution the seafloor slope is estimated) has been shown as an additional source of uncertainty [168] if the appropriate spatial scale is not chosen for a given application.

Although the uncertainties in the soundings and resulting depth grids can be estimated based on bathymetry uncertainty models, their propagation to the slope values is

not straightforward. Consider a few soundings in Figure 4.3 where an arbitrarily assumed horizontal and vertical uncertainty has been used to plot the error ellipses. The slope between any two points is then the slope of the line joining the two error ellipses. As there can be infinite cases for these lines, uncertainty propagation using the Taylor series expansion method is not feasible and use of Monte Carlo method has been recommended [56]. Therefore, such a simulation was used during this study to estimate effect of bathymetric uncertainty and the slope computation algorithm on slope estimation. For depth grids, the position uncertainty was assumed as 0, as the depth grid node locations are fixed, and only the vertical uncertainty of the grids was considered. For each simulation iteration, a new bathymetric grid was assembled by adding randomly drawn bathymetric uncertainty values to the mean depth values at each grid node.
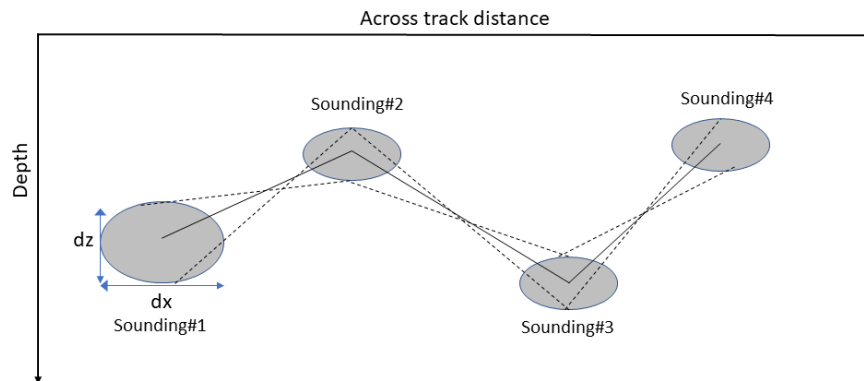
Figure 4.3: Incorporation of horizontal and vertical uncertainties in the slope estimation.

4.2.4. <u>Multibeam sonar test dataset</u>

To illustrate the uncertainty introduced by the processing methodology described above, data from an EM 3002 dual-head MBES collected in water depths of 0.5 – 25 m (in vicinity of Portsmouth, NH) were used. The EM 3002 [169] is a shallow-water multibeam system operating at a nominal frequency of 300 kHz. It transmits a pulse of 150 μs and nominally forms 160 beams. The different methods of seafloor slope estimation were applied to the test data and their differences were noted.

4.2.4.1. <u>MBES bathymetric data processing</u>

The bathymetric data were processed using QIMERA [170]. Tide data were applied based on the Hampton Road, NH tide gauge located ~ 6 km from the survey area. Automated data editing and cleaning were performed using CUBE [12] which provided estimates of horizontal and vertical total propagated uncertainty. The data were successively gridded at 0.5 m, 1 m, 2 m, 5 m, 10 m and 20 m grid resolution. These six bathymetric grids represent the best estimate of depth at the respective grid scales. CUBE also generated an uncertainty layer for the bathymetric grids, at different resolutions, representing one standard deviation of the depth uncertainty at each grid node. An overview of the bathymetry of the study area is shown in Figure 4.4. The survey area consisted of rock outcrops in the northern section of the survey, while the southern section was primarily a flat sandy area. For backscatter data processing the Fledermaus Geocoder Toolbox (FMGT) [171] was used. FMGT was selected for backscatter processing as it can incorporate user defined bathymetric grids for area and incidence angle corrections allowing for studying the impacts of the choice of grid cell size.
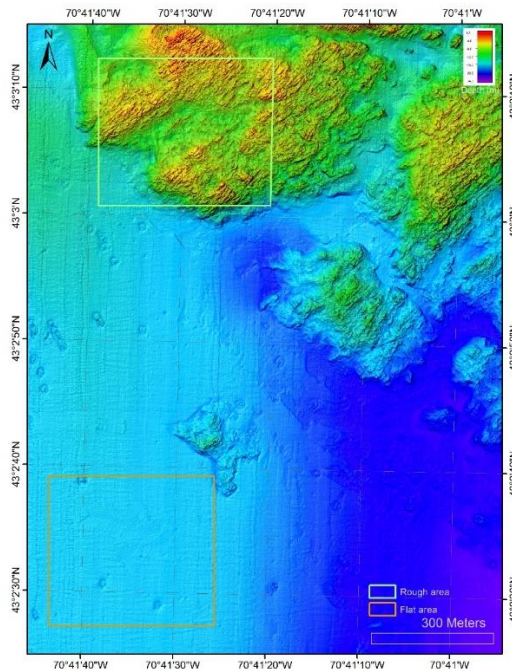
Figure 4.4: Overview showing location of the survey using 1m grid cell sizes. The two boxes delineate the flat area and the rough area that are featured in the discussions.

4.3. Results

Uncertainty of the insonified area and incidence angle caused by seafloor slope uncertainty scale with survey depth and sonar characteristics. To illustrate the uncertainty caused by the seafloor slope and to help quantify the impact of seafloor slope on these corrections, a few examples are presented below based on typical depths where the EM 3002 is operated.

4.3.1. Slope impact on the footprint extent

For a given beam aperture and pulse length, the area correction increases with depth and the resulting area correction can vary in the range [-10 to 15] dB re.1m² (Figure 4.5).
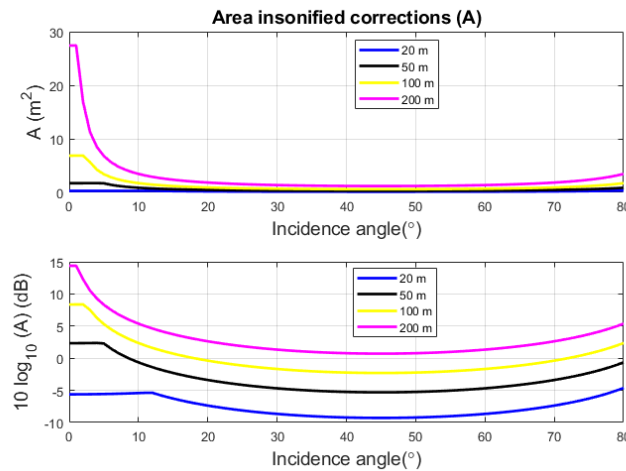
Figure 4.5: Approximated insonified area corrections in m² and dB re. 1 m² at depths varying from 20 to 200 m, with a flat sea floor, pulse length 150 μs and along-track/across-track beamwidths of 1.5°.

The across-track and along-track slopes, if present, can cause significant variations in the above estimation of the insonified area correction and therefore cannot be ignored when computing insonified area. Examples of the expected effects of across-track slope (Figure 4.6) and along-track slope (Figure 4.7) are provided for a depth of 100 m. Both figures show that an across-track slope has the more significant effect on the insonified area extent in comparison with along-track seafloor slope. This could be expected from Eq. [4.5] and [4.6]: the effect of the along-track seafloor slope appears as $\cos\beta_y$, hence causing modest variations (0.62 dB for an extreme slope value of $\beta_y = 30°$).

86
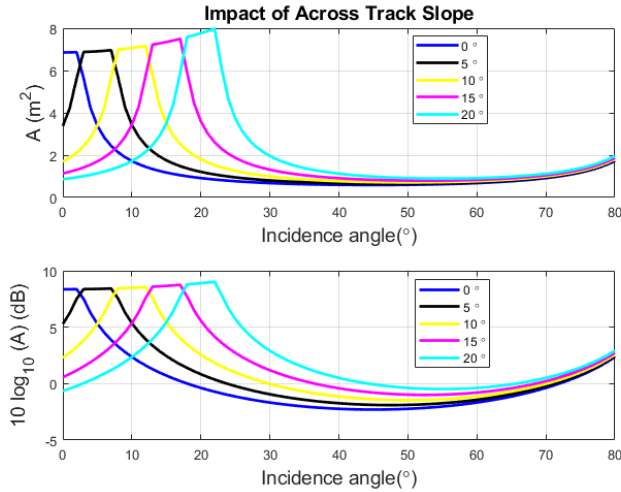
Figure 4.6: Insonified area corrections (*A*) in m² and dB re. 1 m² for various across-track slope values for depth 100 m, pulse length 150 μs and along-track/across-track beamwidths of 1.5°.
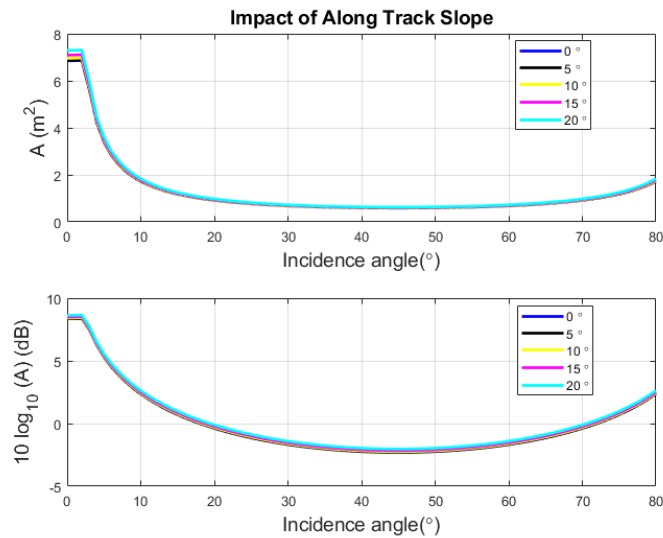
Figure 4.7: Insonified area corrections (*A*) in m² and dB re. 1 m² for various along-track slope values for depth 100 m, pulse length 150 μs, and along-track/across-track beamwidths of 1.5°.

4.3.2. <u>Seafloor slope impact on incidence angle</u>

If not corrected for seafloor slope, the seafloor incidence angles will be subject to errors corresponding to the slope magnitude. Assuming the seafloor slope is ignored in the estimate of the incidence angle, the along-track slope is shown to have a greater effect on

87

the near-nadir beams than on the outer beams (Figure 4.8), while as expected, across-track slope is shown to have a similar effect on all beam angles across the swath (Figure 4.9).
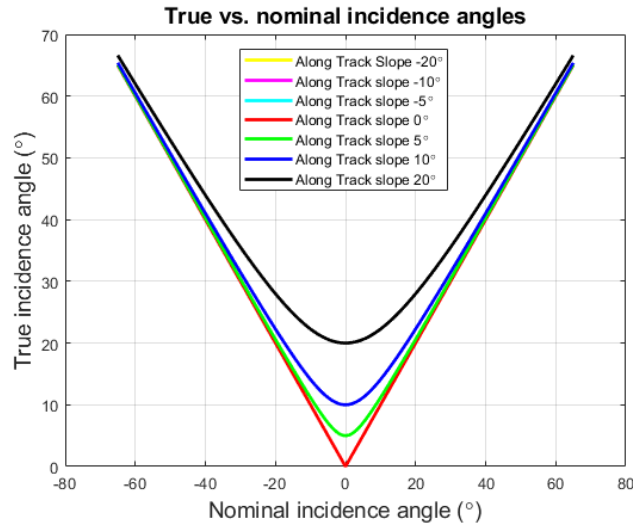
Figure 4.8: Effect of along-track slope on seafloor incidence angle, computed for various across-track *Tx* angles relative to nadir. Across-track slope assumed 0°.
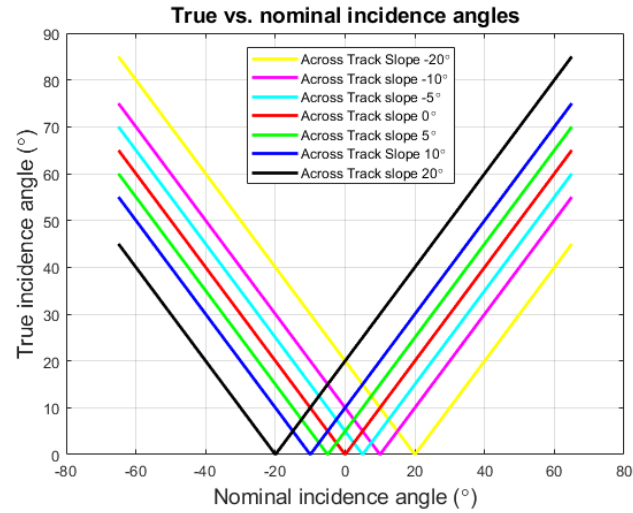
Figure 4.9: Effect of across-track slope on seafloor incidence angle, computed for various angles, relative to nadir. Along-track slope assumed 0°.

The above results clearly illustrate that the seafloor slope is an important factor in the estimation of insonified area as well as of incidence angle. The next sections will focus on results obtained with differences in the scale followed by the uncertainty observed due to the use of different slope estimation methods and vertical uncertainty in soundings.

4.3.3. <u>Scale dependent slope estimation uncertainty</u>

The Horn method [166], as implemented within ARCGIS [172] was used to compute the seafloor slopes for bathymetric grids at various grid cell size resolutions, on the data presented above in Figure 4.4. The differences in the features that can be resolved in the slope layer as a function of resolution are apparent in Figure 4.10, with larger grid cell size smoothing out the detailed seafloor topography. The effect is most prominent in the rough area.
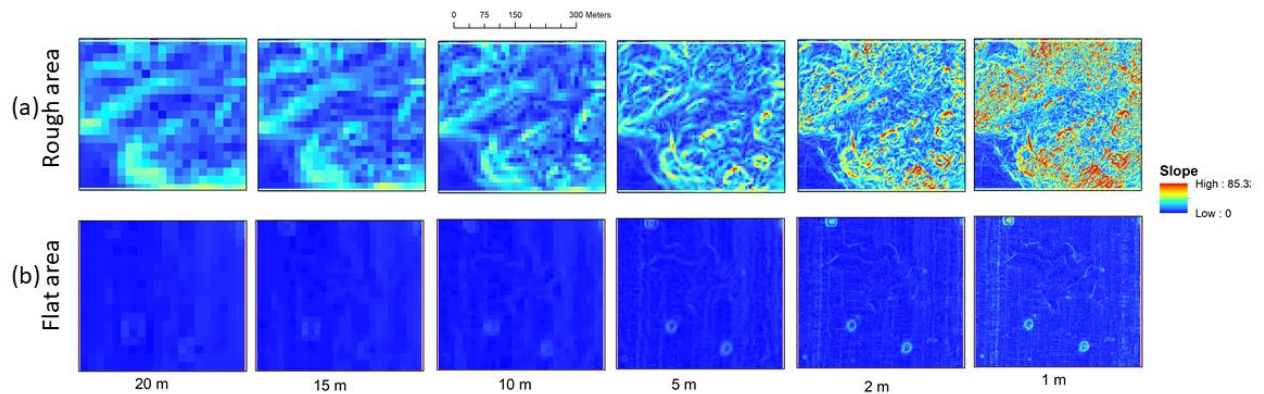
Figure 4.10: Seafloor slopes for the rough (a) and flat (b) area computed using Horn method for cell sizes varying from 1 m (*right*) to 20 m (*left*). Dimensions of each area are ~ 400m x 400m. See Figure 4.4 for location.

Increasing the grid cell size (from 1 m to 20 m) results in a decrease in the spread (range and standard deviation) of the slope values (Table 4.1). This is intuitive since enlarging the grid cell size effectively acts as a low-pass spatial filter on depth; the standard deviation of the slope estimates is hence lowered, but the information content of the slope estimates is also reduced. The uncertainty due to the choice of a cell size therefore cannot be directly estimated from seafloor slope statistics at a single scale. This is an important realization and emphasizes the fact that during the seafloor backscatter processing, the scale of the seafloor slope estimation is a key factor.

Table 4.1: Comparison of seafloor slope statistics obtained for different grid cell sizes (see Figure 4.10). MIN refers to the minimum slope, MAX refers to the maximum slope, RANGE show the differences between MIN and MAX while MEAN is the average and STD is the standard deviation in each cell.

	Grid cell size	MIN	MAX	RANGE	MEAN	STD
Flat area	20	0.02	1.02	0.99	0.24	0.14
Flat area	15	0.00	1.22	1.22	0.26	0.16
Flat area	10	0.01	1.84	1.84	0.28	0.18
Flat area	5	0.00	3.44	3.44	0.35	0.29
Flat area	1	0.00	16.70	16.70	0.78	0.64
Rough area	20	0.06	6.48	6.42	2.10	1.30
Rough area	15	0.05	7.33	7.28	2.24	1.33
Rough area	10	0.02	17.24	17.22	3.32	2.14
Rough area	5	0.03	29.98	29.95	4.51	3.18
Rough area	1	0.00	45.07	45.07	5.74	4.39

Recognizing that the grid cell size has a strong impact on the slope values, the question of an optimal choice of the grid cell size for the computation of seafloor slope arises. This is a fundamental issue which essentially depends on the specific application. Instead, this question can also be approached practically from the perspective of the highest resolution possible from a given data set. In regard to backscatter corrections, the seafloor slope used to determine incidence angle and insonified area should ideally be at a scale comparable to the backscatter sample footprint. Near nadir, the footprint is defined by the combined *Tx-Rx* beamwidth for both across- and along-track extent. Away from nadir, the across-track extent is fixed and depends on the pulse length projection in across-track direction, while the along-track extent is controlled by the receive beamwidth and depth. However, in contrast to backscatter samples, the soundings are usually obtained by considering several adjacent time samples, resulting in bathymetric resolution that is typically less than the resolution of the backscatter. Subsequently, the best bathymetric resolution that can be obtained from the depth data is actually limited by the beam spacing. Moreover, to compute a bathymetric grid, the depth points are averaged together resulting in low noise but also lower resolution. Therefore, the bathymetric data derived either from

individual soundings or from grids (even constructed at the highest possible resolution) may be inadequate for slope correction of the backscatter data. Additionally, the choice of larger grid cell sizes may be necessary to simplify processing and to reduce noise in the bathymetry-derived slopes.

4.3.4. <u>Uncertainty due to the slope estimation method</u>

An assessment is made here of two different methods for estimating slopes using either the bathymetric depths within the measurement swath for each ping, or the gridded bathymetry. For gridded bathymetry with 1-m cell size, the slope was evaluated using two different computing schemas, the central difference method and the Horn method. The beam bathymetry will invariably provide a better resolution as compared to the gridded data set. The expected resolution from beam bathymetry depends on the depth and beam spacing defined by the MBES settings. Commonly used beam-spacing modes include equiangular or equidistant placement of soundings on the seafloor. Typical beam-spacings for various depths for near nadir and outer beams are given in Table 4.2 for a MBES with beamwidth of 1.5° and 160 beams using equiangular and equidistant mode for a swath of $\pm 65°$. As can be seen in Table 4.2, the highest possible resolution of bathymetry obtained from beam bathymetry is insufficient for backscatter corrections.

Table 4.2: Across-track beam spacing and backscatter sample footprint for various depths, transmission angle for MBES with beamwidth of 1.5° and pulse length of 150 μs assuming a sound speed of 1500 ms^{-1}. Across-track backscatter footprint depends on the depth in near nadir region but only depends on pulse length at oblique angles.

	Across-track Beam spacing (m)				Across-track Backscatter footprint	
	Equiangular			Equidistant		
Depth (m) θ_{inc}	0°	45°	60°	All angles	Near Nadir	Oblique Angles
10	0.26	0.53	1.09	0.26	0.26	0.11
20	0.52	1.06	2.19	0.53	0.52	0.11
50	1.30	2.68	5.48	1.34	1.30	0.11
100	2.61	5.37	10.97	2.68	2.61	0.11
200	5.23	10.75	21.94	5.36	5.23	0.11

Using the previously mentioned MBES survey data in water depths of ~10 m, large differences (as much as 15°) are apparent between the slopes estimated from the beam bathymetry *vs.* the slopes derived from gridded bathymetry (Figure 4.11) for a single ping chosen in the rough area. Whereas the differences between the two grid-based methods are comparatively small (Figure 4.12). The differences in the slopes from the beam bathymetry and gridded data set were comparable for the flat areas (not shown). This observation indicates that the bathymetry type (individual soundings vs. gridded bathymetry) has a more prominent effect on slope than the choice of the algorithm used to estimate the gridded slope. Considering that bathymetric detail is lost when using bathymetric grids (especially with larger grid cells), it is recommended that individual soundings be used when computing seafloor slopes for backscatter corrections. It is also to be noted that individual soundings were not edited for outliers for this comparison. This did not result in spikes in the estimated slopes in this case, but this can be a major issue where excessive noise is present in the individual soundings. The large variability in the slopes from individual soundings is not an indication of large uncertainty but it more closely captures seafloor slope changes. When the bathymetric soundings are excessively noisy, the only choice is to use the highest possible resolution of the bathymetric grid.
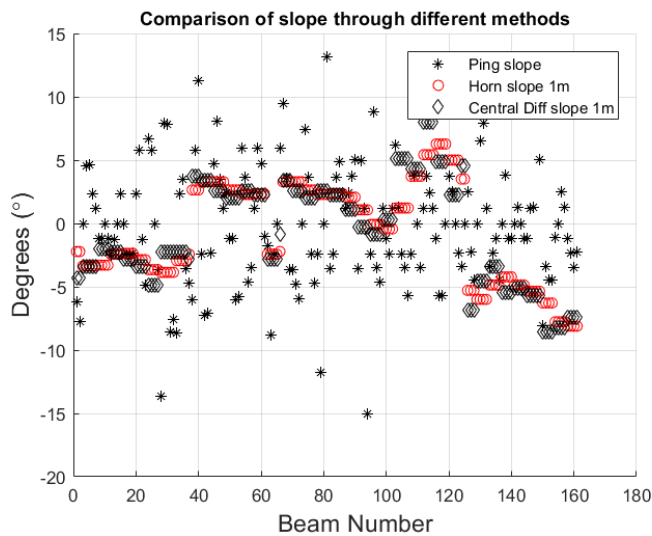
Figure 4.11: Comparison of slopes from three different estimation methods: "Ping" method (black dots) where all the soundings from a ping are used to compute across-track slope show large differences from "Horn" and "Central Difference" methods (plots as

92

black and red diamonds) where 1-m grid cell size bathymetry is used to compute across-track slopes.
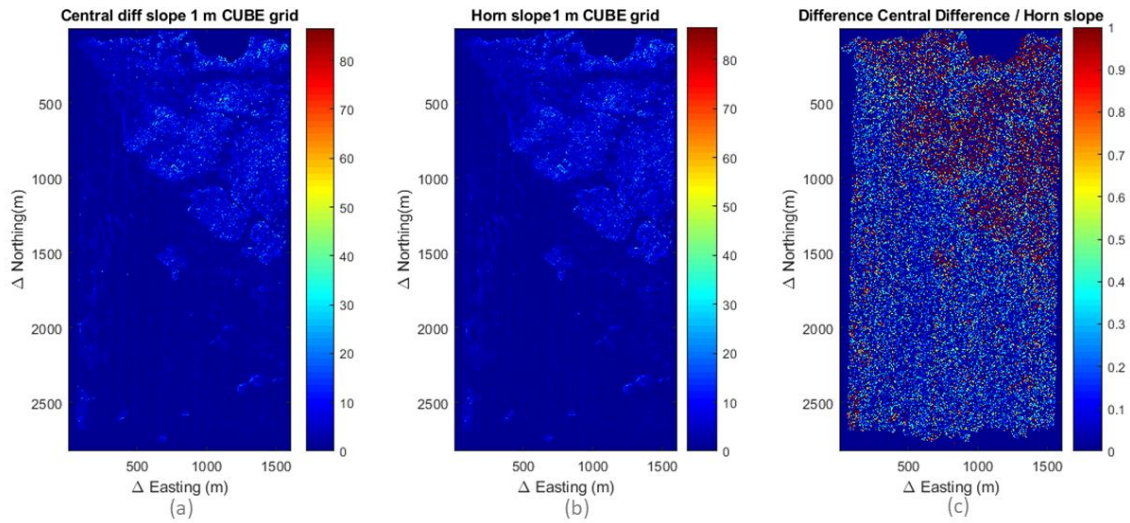
Figure 4.12: Comparison of the estimated magnitude of slopes from entire survey area using the (a) Central Difference and (b) Horn methods applied to data gridded to 1-m cell sizes. (c) Difference in slope computed using the two methods shows that it is $< 0.3°$ in flat areas and $< 1°$ in rough areas.

The difference between slope computation algorithms was minimal in flat areas but reached ~ 1° for rough areas. Therefore, the choice of algorithm is considered a minor source of slope uncertainty but cannot be totally ignored.

4.3.5. <u>Propagation of depth uncertainty to slope uncertainty</u>

Slope values are directly impacted by the horizontal and vertical uncertainty of depth measurements. The Horn method described in the previous section is used here to illustrate the propagation of depth uncertainties to slope values. As the horizontal positions of the grid nodes are fixed at regular intervals, the horizontal component is not included in the uncertainty propagation. The CUBE algorithm implemented in QIMERA was used to derive the vertical uncertainty for each grid node at grid cell size of 1 m (Figure 4.13).
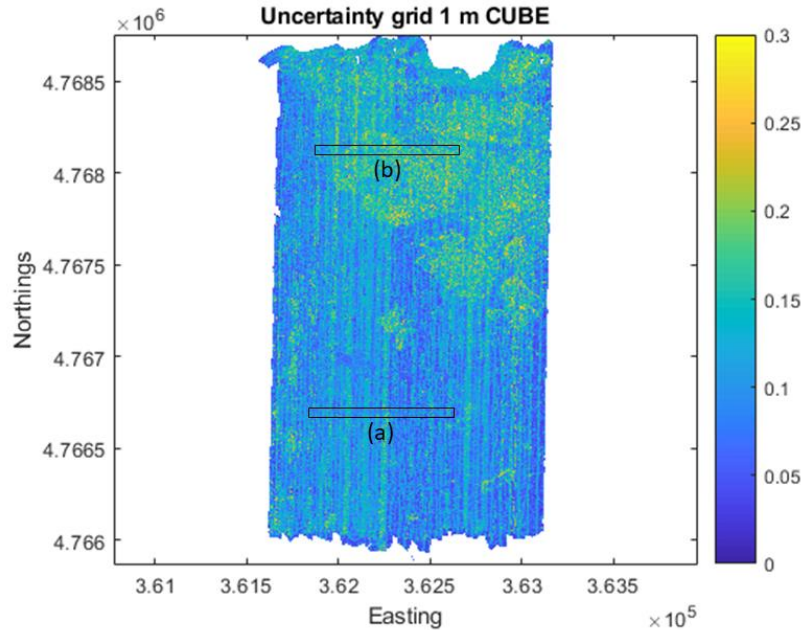
Figure 4.13: CUBE-generated uncertainty for the survey area. The color scale for uncertainty is given in meters. Locations of flat and rough areas displayed in Figure 4.14 are shown as (a) and (b) respectively.

The slope for each grid point was computed over 50 iterations. For each iteration, the vertical uncertainty values were randomly drawn from the range of CUBE-generated uncertainties and a new bathymetric grid was assembled. The resulting grid was then used as input to compute seafloor slope using the Horn method.

For the example provided in Figure 4.14, the slope standard deviation is related to the slope value of the seafloor: for steep seafloors the value of standard deviation is larger (2-3°) and for flat seafloors the slope standard deviation is comparatively small ($< 2°$). It is to be noted that uncertainty due to the bathymetric uncertainty is related to the seafloor slope as well. The areas with rough seafloor are expected to exhibit higher bathymetric uncertainty due to large slope variations. The Monte Carlo simulation has been shown as a potential approach to compute seafloor slope uncertainty due to bathymetric uncertainty [139]. But estimates of slope uncertainty due to bathymetry uncertainty cannot be generalized and for each data set the simulations (e.g., using the Monte Carlo method) will need to be carried out to compute slope uncertainty. This poses a challenge for end users who may not have resources to conduct such simulations.

94
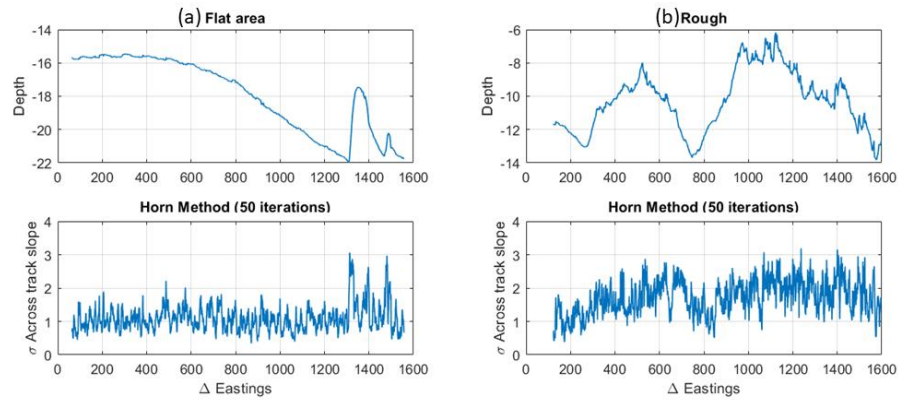
Figure 4.14: Result of iteration of 50 slope estimation runs by perturbing the vertical uncertainty of CUBE grid with grid cell size of 1 m using the Horn method. (a) For flat area; depth (top) and across-track slope standard deviation (bottom). (b) For rough area; depth (top) and across-track slope standard deviation (bottom). Locations of the depth profile shown in Figure 4.13.

4.3.6. <u>Impact of unresolved seafloor slope on backscatter ensemble average</u>

When considering the impact of low-resolution bathymetry on backscatter uncertainty, the effect of the scale of the bathymetry on ensemble averaging of the backscatter must be considered. To avoid bias in backscatter strength, the averaging needs to be at a scale where the individual samples can be assumed to be derived from the same seafloor patch. Currently, a widely accepted standard does not exist to define the bin size for ensemble averaging and a large range of bin sizes are used: ranging from angular bins of 0.5° to 1° with cell sizes much smaller than corresponding bathymetry for the creation of high-resolution mosaics. Slope-related insonified area and incidence angle uncertainties for individual backscatter samples therefore are propagated to the backscatter strength estimate with their magnitude depending on the variance of the unresolved seafloor slope. The variance of unresolved slopes, however, is a function of local topography and cannot be determined using the MBES bathymetry. Despite the inability to demonstrate this empirically, it is expected that the bathymetry (at a particular scale) enables computation of the mean slope reliably and the variations around the mean slope will likely follow a normal distribution. Thus, the spatial scale of the slope should practically provide the lower limit of scale below which ensemble averages should not be carried out. For instance, if

95

one samples the slope values at the scale of the bathymetry grid, one cannot build $S_b(\theta)$ by using backscatter elementary values at a finer scale where the seafloor slope is not resolved.

Although not known, but assuming an arbitrary value of variance in unresolved seafloor slopes, a first-order estimate of the resulting uncertainty in backscatter can be made. To demonstrate this numerically, the values of modeled backscatter have been calculated using the Generic Seafloor Acoustic Backscatter (GSAB) model [49] and used to estimate the effect of angular averaging. In its simplest form (a Gaussian law for specular regime and Lambert's law at oblique incidences) the impact of averaging over $\pm\theta$ is plotted in Figure 4.15. The expression for σ_b for the GSAB model is given by

$$\sigma_b = A\exp\left(-\frac{\theta^2}{2B^2}\right) + C\cos^D\theta \qquad\qquad \text{[Eq. 4.16]}$$

where A is the specular maximum amplitude, B is the facet slope standard deviation, C quantifies the average backscatter level at oblique incidence and D is the backscatter angular decrement [49]. The two cases illustrated in Figure 4.15 are typical angular backscatter curves for (a) a soft-sediment with high narrow specular and oblique decrease in $\cos^2\theta$ and (b) a coarse sediment with low and wide specular and oblique decrease in $\cos\theta$. For most seafloors the oblique-regime average angle dependence lies between the $\cos\theta$ and $\cos^2\theta$ curves shown here. The model input parameters (A, B, C, D) are respectively (0.1; 2°; 0.001; 2) and (0.03; 7°; 0.01; 1). The values of backscatter obtained from GSAB model were first computed for each incidence angle, then binned (at various angular bins 1° to 10° corresponding to the assumed variance of the unresolved slope) and reported at the central angle of the bin. As expected, the resulting uncertainty is maximum for the specular regime where its magnitude depends on the gradient of the specular lobe. On the other hand, the sensitivity to unresolved seafloor slopes becomes negligible in the "plateau" regime (> 15° in this example) and at larger incidence angles. This implies that averaging backscatter at a scale larger than the backscatter sample footprint (e.g., at the scale of gridded bathymetry cells) does not cause a detectable bias even if the small-scale relief causes significant slopes variations (as high as 10°) inside the grid cells around the average slopes determined from bathymetry.

96

On the other hand, the exact impact of unresolved slopes on the insonified area correction cannot be predictively modeled using GSAB. But if the highest possible resolution of bathymetry is used (i.e., the individual soundings), the variations in the slope are expected to result in negligible bias in the computed ensemble average over random variations in the insonified area. Hence averaging backscatter at the scale of the gridded bathymetry is feasible except for the specular region (Figure 4.15a), as it provides bias-free smoothed backscatter at a resolution consistent with the bathymetry.
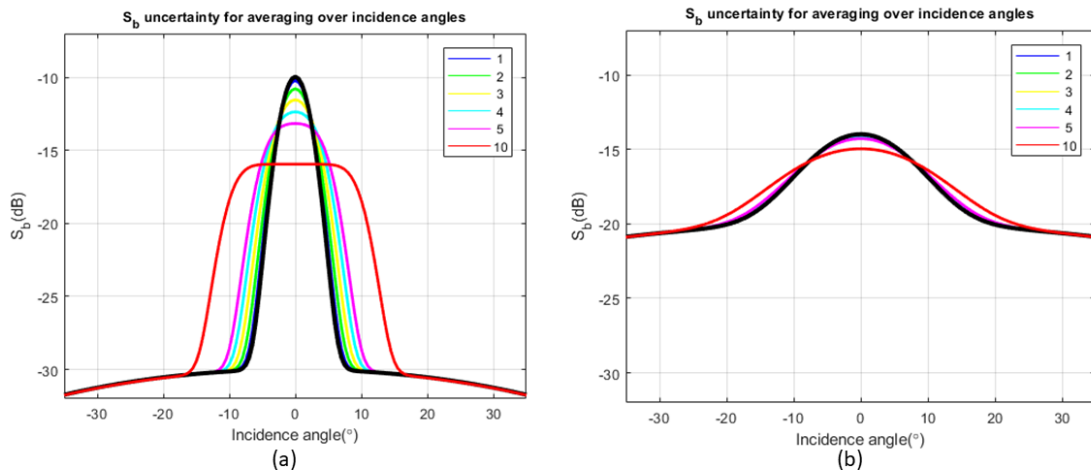
Figure 4.15: Effect of incident angle binning on averaged backscatter values. Two nominal angular backscatter curves representing seafloor types (*a: high narrow specular* and *b: low and wide specular*) showing the effect of angular binning over 1°-10° corresponding to the incidence angle standard deviation due to slope uncertainty. The impact is maximal in the specular region, where the angular binning effect corresponds to the strongest angular variations (0° to 15° incidence angles); it is then negligible in the "plateau" angle sector (> 15° incidence angles).

4.3.7. <u>Practical impact of slope scale on incidence angle and processed backscatter</u>

<u>results</u>

The MBES survey data processed using different spatial scales for the seafloor slope correction showed that the incidence angle could vary up to tens of degrees depending on the spatial scale of the seafloor used to estimate incidence angle. To look at the impact of slope scale on incidence angle QPS FMGT was used as it enables the use of a reference grid to calculate incidence angles. For comparison, the results were exported

as text files using the built-in export functionality of QPS FMGT ('ASCII ARA beam detail'). The exported data included the true incidence angle as well as corrected backscatter data after applying corrections for seafloor slope (based on whether a reference grid was used) and insonified area. For both incidence angles and backscatter levels, the largest differences were observed between no-slope corrections and slopes computed at a 1-m grid resolution (Figure 4.16). The backscatter values showed variations of up to 3 dB around the specular area, decreasing at oblique angles (Figure 4.16). As QPS FMGT currently does not provide details of area corrections separately, these differences show the cumulative effect of the backscatter corrections including the insonified area. However, as the only difference in processing was the change in the reference grid resolution, the differences in the backscatter results imply that these are related to insonified area corrections.
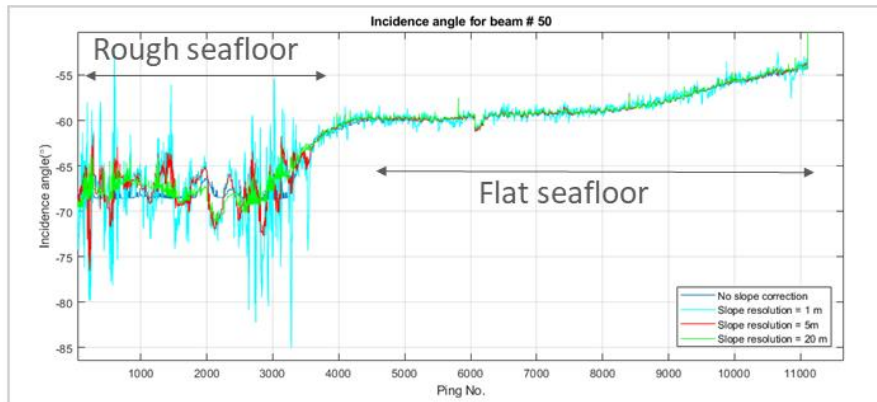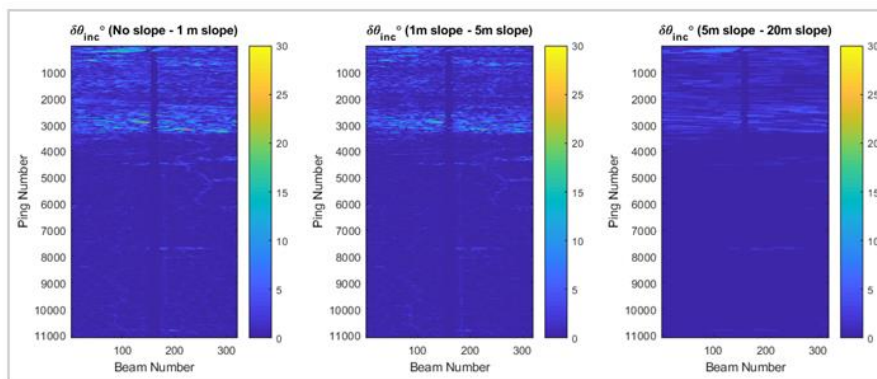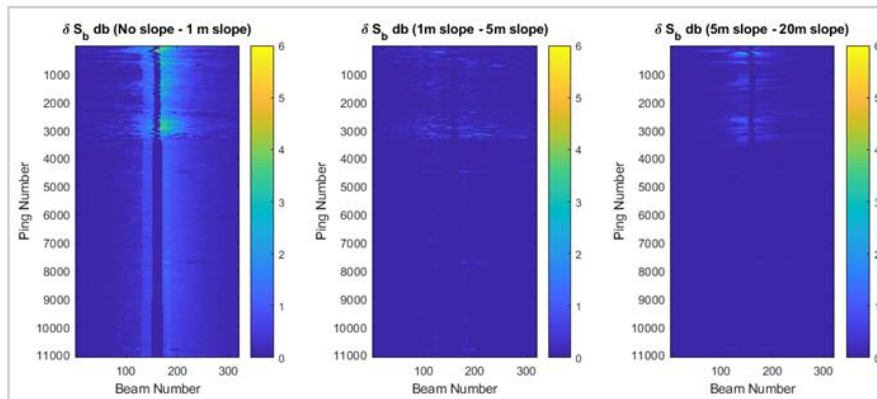
Figure 4.16: (a) Comparison of incidence angle from one beam (#50) showing results with no slope correction compared to slope corrections using bathymetric grid of 1m, 5m and 20m spatial resolution. (b) Differences (absolute) in the incidence angle as computed with no slope correction and using 1m spatial resolution grid; 1m and 5m grid resolution; and 5m and 20 m grid resolution. (c) Differences (absolute) in processed backscatter results computed with no slope correction and using 1m spatial resolution grid; 1m and 5m grid resolution; and 5m and 20 m grid resolution.

4.4. <u>Discussion</u>

The focus of this research has been understanding sources of slope uncertainty while correcting seafloor backscatter data for insonified area and incidence angle. This cannot be separated from the issues of analysis scale and choice of methodology for creating underlying bathymetry that is used to correct the backscatter data for slope and incident angle. As multibeam survey acquisition becomes prevalent, the use of multiple backscatter data sets from different sources is also becoming more widespread. The compilation of backscatter data from various sources, collected using multiple MBES systems, and processed with different tools, highlights a need to understand and quantify uncertainty in the backscatter data. The results presented here have demonstrated that the slopes estimated for correcting seafloor backscatter vary depending on the computational algorithm and uncertainty of the bathymetry. The greatest uncertainty is introduced if the seafloor slope is not resolved at an appropriate scale. Unfortunately, documentation accompanying backscatter results often lacks a description of how the seafloor slope was corrected for, making it difficult for end-users to determine uncertainty due to slope corrections. Information about computation algorithm, bathymetric data used, and scale of analysis should accompany seafloor backscatter data so that users can interpret the backscatter data and their intrinsic uncertainty.

4.4.1. <u>Summary of uncertainty components of seafloor backscatter measurements related to seafloor slope</u>

The impact scale adapted from [161] is used to classify the magnitude of the uncertainty related to area correction (in dB) and incidence angle (in °) (Table 4.3). The impacts of the main uncertainty sources in seafloor slope computation are summarized in Table 4.4.

Table 4.3: Scale adapted from [161] to classify the magnitude of uncertainty in area correction and incidence angle.

	Negligible (N)	Small (S)	Moderate (M)	High (H)	Prohibitive (P)
Area correction (dB)	0.01 to 0.1	0.1 to 1	1 to 3	3 to 6	Beyond 6
Incidence angle (°)	0.01 to 0.1	0.1 to 1	1 to 3	3 to 6	Beyond 6

Table 4.4: Major sources of uncertainty for seafloor slope required for area insonified and seafloor incidence angle. See the code (N-S-M-H-P) definition in Table 4.3.

Seafloor slope uncertainty source	Magnitude of uncertainty in area insonified and incidence angle	Possible quality improvement
Flat seafloor assumption (seafloor slope completely ignored)	N to P depending on topography	Use bathymetry in slope compensation
Inappropriate scale of seafloor slope computation (beam bathymetry vs. grid at lower resolution)	M to H depending on large scale topography	Use of highest available resolution bathymetry
Unresolved seafloor slope	N to M depending on small scale topography	Average backscatter values inside angular bins
Bathymetry uncertainty	S to M depending on bathymetric uncertainty and magnitude of seafloor slope	-
Seafloor slope algorithm based on bathymetry grid	N to S	-

4.4.2. <u>Approaches to using bathymetry for slope estimation</u>

As is evident from the discussion above, the largest uncertainty levels are obtained when the seafloor slope is ignored while processing backscatter data. Several works have highlighted this issue (e.g., [164]). This uncertainty directly depends on the slope magnitude (i.e., on the local topography); therefore, its prediction cannot be accomplished *a priori*. However, as the collection of concurrent bathymetry is conducted during MBES backscatter surveys, this uncertainty source can be reduced if the bathymetry data are used to compute the seafloor slopes. At this point, the issue of the bathymetry spatial scale must be carefully considered. Terrestrial studies of slope accuracy support the conclusion that

spatial scale is an important factor for accurately estimating the terrain slope [168,173] which has also been shown to be critical for seafloor slope [139]. Several options, with varying resolutions, are available for end-users to compute the slope from the available bathymetric data. An important question is whether to use across-track beam bathymetry (pros: optimal resolution; cons: noise unfiltered; does not give the across/along-track slope at consistent spacing) or gridded bathymetry (pros: gives along and across-track slopes with a consistent sampling spacing, and well filtered; cons: the gridding is often too coarse to provide detailed slopes). The results from Figure 4.7 indicate that along-track slope effects are relatively small (0.1 – 1dB) for area insonified and affects only the near-nadir beam adversely. In contrast, the results from Figure 4.11 indicate that estimated slope values vary significantly depending on whether beam bathymetry or a bathymetric grid is chosen for the slope estimation, especially for seafloors with large topographic variations. The uncertainty in the area insonified and incidence angle can be prohibitively high (> 6 dB; $> 6°$) as indicated in Figure 4.16 for complex terrains with rough topography. Therefore, for the across-track slopes, beam bathymetry is the preferred choice. For along-track slope, the gridded bathymetry at highest resolution can offer a reasonable solution. Hybrid processing of bathymetry (using beam bathymetry for across-track slope and using gridded bathymetry for along-track) could also provide an optimal solution.

4.4.3. <u>Impact of spatial scale</u>

For the insonified area computation required for backscatter processing, the spatial scale at which the slope needs to be resolved should be ideally the backscatter sample footprint extent. The interplay between calculable uncertainties *vs.* lack of information caused by using larger grid cell size will remain an unanswered question as generalized terrain characteristics cannot be reliably assumed for a surveyed area. However, it is reasonable and useful to estimate upper bounds for this cause of uncertainty. Although not predictable, if the variations of slopes within spatial scale of soundings are large ($> \pm 5°$), the angular shape of the specular region of the backscatter will be distorted (Figure 4.16). For a given beam, the incidence angle is provided by the best available bathymetry. However, the variations in the local slope can introduce uncertainty in the incidence angle and therefore while binning backscatter values, the backscatter values from other incidence

angles will be averaged together introducing the uncertainty shown in Figure 4.16. Even if the highest possible resolution of bathymetry is used to compute the seafloor slope, there will still remain some level of unresolved seafloor slope. However, it is concluded that based on the requirement of taking averages over an angular bin, these unresolved seafloor slopes are problematic only in some cases of specular region of backscatter. Binning backscatter data to a resolution similar to the bathymetry grid offers a solution to reduce the impacts of variations in local seafloor slopes. Also, this can provide a practical guideline for applications where selecting a spatial scale of backscatter strength is required. For example, Buscombe et al. [174] recently suggested spectral filtering to remove high frequency noise from the backscatter data. The low-pass filtered backscatter data was suggested to be representative of the underlying sediment. The selection of spectral filtering parameters can, however, be subjective. Using the bathymetry resolution scale as a guide to binning size can provide a quantitative and practical means to select a low-pass filter for the backscatter data.

4.4.4. Impact of bathymetric uncertainty

Bathymetric uncertainty was shown to cause moderate uncertainty ($< 3°$) in the seafloor slope (Figure 4.14). This was based on the empirical uncertainty derived for one case-study from CUBE and using a Monte Carlo simulation to run 50 iterations of slope estimation for the bathymetric grid at 1 m grid cell size. The bathymetric uncertainty, however, will vary for different depths as well as within the swath extent. Multibeam surveys are usually run to comply with bathymetric uncertainty guidelines from the International Hydrographic Office (IHO) [113]; however modern multibeam systems often surpass these guidelines by far. The total vertical uncertainty (TVU) of soundings is required to be better than IHO Special Order for shallow water surveys (< 40 m) and better than IHO Order 1 (< 100 m) or IHO Order 2 (> 100 m) for deep water surveys. The vertical uncertainty σ_z (at 95 % confidence) is depth-dependent and defined by IHO as [113]

$$\sigma_z = \pm\sqrt{a^2 + (b \times d)^2} \qquad \text{[Eq. 4.17]}$$

where a is the portion of uncertainty that does not vary with depth, b is a coefficient that represents the portion of uncertainty that varies with depth d. For local slope calculations the soundings are not expected to be affected by non-random (stable) errors (such as biases

103

caused by the system installation or by the sound velocity profile), therefore only random relative vertical uncertainties should be considered. Values of a and b for IHO Special Order, Order 2 and Order 1 are provided in Table 4.5 and can be used to estimate worst case vertical uncertainty.

Table 4.5: Parameters used to estimate vertical uncertainty using IHO [113] uncertainty guidelines for various depths.

	Water depth (d)	a	b (% d)	σ_z
Special Order	20 m	0.25	0.0075 (0.75)	0.29
Order 1	50 m	0.5	0.013 (1.3)	0.82
Order 2	100 m	1	0.023 (2.3)	2.50

Using the vertical uncertainties provided in Table 4.5 to perturb the soundings, Monte Carlo iterations applied to Eq. [4.10] can provide slope perturbation estimates as a function of the horizontal spacing of the soundings. The resulting standard deviation of the slope estimates shows that bathymetric data (even complying with IHO Special Order standards) provide very high standard deviations in estimated slopes (Figure 4.17). For example, for 0.5 m sounding spacing, the Special-Order survey shows a local slope uncertainty exceeding 35°. The dependence of slope uncertainty on sounding spacing as observed in Figure 4.17 is due to the fact that the same vertical uncertainty will result in higher errors in computed slope from smaller sounding spacing due to the reduction in the denominator in the slope estimation Eq. [4.10]. However, for modern MBES the depth uncertainty is well controlled, and several studies have suggested that the vertical random uncertainty will surpass Special Order requirements. For example Marks and Smith [175] found that 95% of multibeam sonar surveys archived at the NOAA national archives show a repeatable depth within 0.47 % of water depth (to be compared to the Special Order parameter b = 0.75%). Similarly, performance testing of several new systems (e.g., [176,177]) have shown that depth uncertainty is constrained well below the IHO standards. Estimates of slope uncertainties with TVUs of 0.1% and 0.47 % of water depth are plotted in Figure 4.17 for comparison and show that slope uncertainty can be reduced to manageable levels if vertical uncertainty is constrained well.
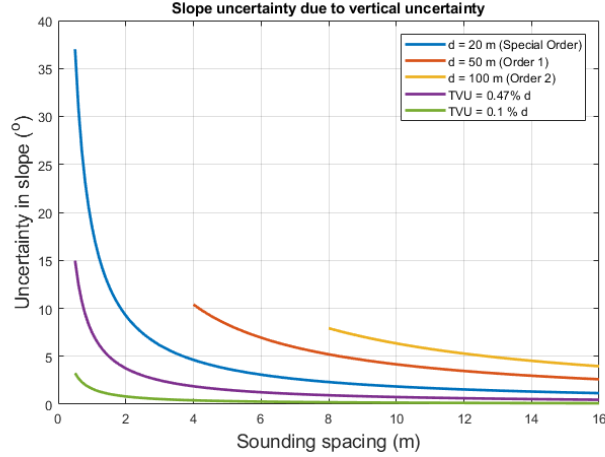
Figure 4.17: Uncertainty in slope (standard deviation) computed through Monte-Carlo iterations of Eq. [4.10] while considering different vertical uncertainty (Special Order: 0.29m, Order 1: 0.82m, Order 2: 2.5m; 0.47 % of depth and 0.1 % of depth), with sounding spacing from 0.5m-16m for Special Order uncertainty; 4m-16m for Order 1 uncertainty and 8m-16m for Order 2 uncertainty. Horizontal uncertainty (HorU) is ignored in this simulation.

The TVU for multibeam soundings strongly depends on the angle with respect to vertical (tilt angle). For the demonstration, one may adopt a model to approximate depth dependent TVU of the form

$$\frac{\delta z}{d} = \sqrt{\alpha^2 + \beta^2 \tan^2 \theta}.$$ [Eq. 4.18]

Using typical values of 0.001 for α and 0.003 for β provide TVU estimates that replicate approximately the uncertainty observed with respect to the tilt angle [176] (0.1%d near nadir to $\sim$ 1%d at outer beams). To estimate slope uncertainty using the above TVU estimate, the across-track sounding spacing is assumed based on equidistant beams spread over the angular swath. The across-track distance between the soundings as a function of depth (d) can then be approximated as

$$\Delta x/d = 2\tan\theta_M/N_b$$ [Eq. 4.19]

where θ_M is the maximum tilt angle and N_b is the total number of beams. Using θ_M as 75° and N_b as 160 the depth-dependent sounding spacing can be computed (Eq. [4.19]). Considering the vertical uncertainty (Eq. [4.18]) and sounding spacing (Eq. [4.19]) are both linearly dependent on depth d, the slope uncertainty is finally depth-independent and can be estimated by computing standard deviation of Monte-Carlo iterations of the slope

105

computation (Eq. [4.10]). The standard deviation of slope using the likely TVU and beam spacing (with 0.1m position uncertainty) shows the resulting dependence on the tilt angle (Figure 4.18). For this configuration, the slope uncertainty varies from 3° at nadir to 8° at the swath end. Note that the slope uncertainty can be further reduced by computing slope over larger across-track intervals, at the expense of spatial resolution (§3.3); Figure 4.18 illustrates the reduction in slope uncertainty when increasing Δx by a factor 2 and 4. In conclusion, bathymetric surveys strictly complying with IHO standards can still result in prohibitive uncertainty in local seafloor slopes usable for backscatter computation; however, modern MBES can outperform IHO bathymetric standards by many orders and having an optimal TVU will enable slope to be computed with high ($< 6°$) uncertainty that can be further reduced to moderate levels ($< 3°$ as defined in Table 4.3) if slope is computed over multiple soundings.
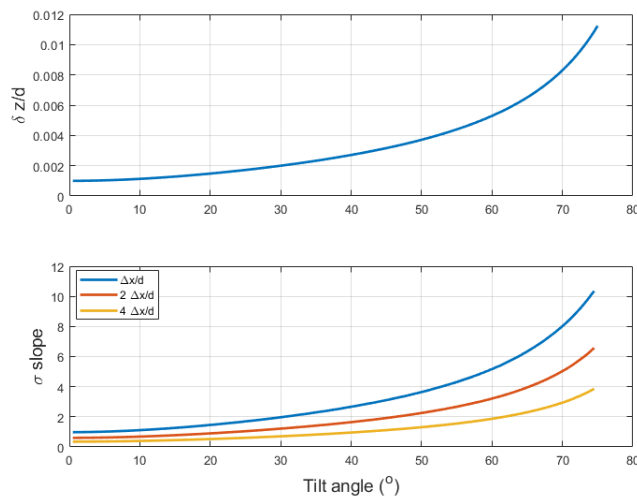
Figure 4.18: Typical angle-dependent depth uncertainty (*top*) for a modern shallow water MBES, and uncertainty in slope (*bottom*) using (10) with sounding spacing (Δx) defined by equidistant beams (160 beams) spread over 75° angular swath. Horizontal uncertainty (HorU) is assumed to be 0.1m in this simulation.

4.4.5. <u>Slope uncertainty vs. grid resolution and computation approach</u>

The choice of seafloor slope computation algorithm does not contribute significantly to the seafloor slope uncertainty. Two computation algorithms were tested during this study. The differences between the results of these two algorithms were

observed to be small ($< 1°$). Other studies have assessed impacts of the choice of slope algorithms and have determined that this effect is not as pronounced as the choice of the spatial scale [178,179]. In conclusion, considering that robust computational algorithms are available, choice of computation algorithm has limited impact on the seafloor slope uncertainty.

The practical question of assessing uncertainty of seafloor slope by end-users for seafloor backscatter correction still requires development of tools accounting for computation algorithm, scale and bathymetric uncertainty. An important realization is that the standard deviation of slope (computed at a single scale) does not represent the actual practical uncertainty in the slope estimation. For example, while considering smaller grid sizes (or small sounding spacing as in case of beam bathymetry), large values of slope uncertainty are realized. Using coarser grid cell sizes (or large distances between beam soundings) the computed standard deviation of slope is reduced significantly. This falsely implies that coarser grid resolution results in lower slope uncertainty. An alternate approach to quantify uncertainty is to estimate seafloor slope at various (possible) resolutions then compare these to estimate uncertainty of the insonified area and incidence angle. The majority of end-users rely on the commercial software packages to process MBES backscatter data [39]. Therefore, they have limited choices of which method to choose and too often these choices are not transparent. In commercially-available backscatter processing tools, no uncertainty in the seafloor slope (either from sounding uncertainty or from the choice of grid-cell size and methodology) is explicitly defined in the final results. Therefore, validation of backscatter results without the availability of their uncertainties becomes a challenge for end-users. Software developers are hence urged to provide more details about their data processing algorithms and ideally to incorporate uncertainty estimators. Comparing and validating processed backscatter results and providing detailed data processing steps (including insonified area and incidence angles) have been recommended by the ad hoc Backscatter Working Group [15]; this approach will help end-users in comparing and contrasting effects of the processing options, and hence in optimizing the methodology and the spatial scale of slope correction.

4.5. <u>Conclusions</u>

Uncertainty quantification is a complex and important part of seafloor acoustic remote sensing that is integral to the repeatability of the processing and interpretation of backscatter data. The issues highlighted in this study relate to the computation of seafloor slopes and their impact on incident angle and insonified area calculations. The magnitude of seafloor slope uncertainty is impacted by the uncertainty in the measurement of seafloor topography, the methods used to model the topography and the spatial scale of bathymetry used to compute seafloor slopes. The order of magnitude of uncertainty expected from each source has been identified (Table 4.4) showing that the flat-seafloor assumption often used during data acquisition is justified only by the real-time computation constraints and should be avoided in post-processing. Fortunately, software processing tools now enable end-users to correct for the seafloor slope. However, the corrections still can suffer from large uncertainties if the highest possible resolution of the seafloor slope is not used. The spatial scale of the bathymetric data dictates the scale at which backscatter data can be accurately estimated; consequently, the backscatter values should be averaged at the scale of the bathymetry used for slope estimation. It is hoped that by making the issues of slope, incidence angle and insonified area more explicit in post-processing operations, future studies of seafloor backscatter will incorporate uncertainty in their analyses of seafloor backscatter strength, end-users will pay more attention to these issues during data processing and interpretation, and software developers will provide processing tools with more accurate compensations of the slope effects.

CHAPTER 5

RESULTS FROM THE FIRST PHASE OF THE BACKSCATTER SOFTWARE INTER-COMPARISON PROJECT (BSIP)

This chapter is based on a draft submitted for publication in a peer reviewed journal. My contribution to the article included conceptualization of the study, project management, methodology development, writing original draft, review and editing of draft, code development and data interpretation. The article has been formatted to meet UNH dissertation formatting guidelines. Paper citation: Malik, M.; Schimel, A.; Masetti, G.; Roche, M.; Deunf, J.L.; Dolan, M.; Beaudoin, J.; Augustin, J.M.; Hamilton, T.; Parnum, I. Results from the first phase of the Backscatter Software Inter-comparison Project. *Appl. Acoust.* ***Submitted***.

Abstract: Seafloor backscatter mosaics are now routinely produced from multibeam echosounder data and used in a wide range of marine applications, such as benthic habitat mapping and geomorphic studies. However, large differences (> 5 dB) can often be observed between the levels of mosaics produced by different software packages processing the same dataset. This is because the backscatter data processing pipeline is a sequence of complex steps, the order and the implementation of which have not been standardized to date. The resulting lack of consistency between backscatter data products is a major limitation for a number of possible uses of backscatter mosaics, including quantitative analysis, monitoring seafloor change over time, and combining mosaics from different surveys.

In order to recognize the source(s) of inconsistency between software, it is necessary to understand at which stage(s) of the data processing chain the differences become substantial. In May 2018, the Backscatter Software Inter-comparison Project (BSIP) was initiated – under the auspices of the GeoHab's Backscatter Working Group – to better understand such differences. To this end, willing commercial and academic software developers were invited to generate intermediate processed backscatter results

from a common dataset, for cross comparison. The first phase of the BSIP requested intermediate processed results consisting of two stages of the processing sequence: the one-value-per-beam level obtained after reading the raw data and the level obtained after radiometric corrections but before compensation of the angular dependence. Both of these intermediate results showed large differences between software solutions. This study explores the possible reasons for these differences and highlights the need for collaborative efforts between software developers and their users to improve the consistency and transparency of the backscatter data processing sequence.

5.1. <u>Introduction</u>

Commercial multibeam echosounders (MBES) were designed in the 1970's [180] for the purpose of bathymetry data acquisition, but it is only in the past two decades that software packages became generally available to process seafloor backscatter data (henceforth, *backscatter*). The earliest software packages were developed and privately used by academics [9,13]. As backscatter started proving important in seafloor characterization studies [1,11,19,26], the user base expanded, and several commercial, proprietary software packages became available. Today, backscatter is collected by a broad range of users for a variety of applications, including by scientists and resource managers to assess and quantify seafloor resources (sediment, geology, habitats, etc.), by hydrographic and military agencies to determine seafloor type, and by coastal zone managers for infrastructure planning. Most of these end-users rely on commercial software for data processing [39]. Due to their commercial nature, these software packages are often closed source and very limited information is available about their proprietary data processing routines and algorithms.

Processing backscatter data involves applying various and complex environmental and sensor-specific corrections to the raw level recorded by the system [41]. Those corrections have been well studied [15,19,26,41], but neither the details of each correction, nor the order in which they are applied have ever been standardized [15,41,181]. This lack of standards for data processing and metadata, combined with the need for commercial software manufacturers to protect their intellectual property, resulted in software being developed mostly independently. Recent comparisons of the backscatter products obtained

110

from processing the same datasets with different software highlighted differences in the results [39,182–184]. The approach adopted during these comparisons included comparing the backscatter end-results in the form of mosaics as obtained from various software packages. Having recognized that different software likely process backscatter differently, the challenge remains for the end-users to assess which, if any, of the processing methodology is most accurate. This challenge is further compounded by the lack of standards for backscatter data acquisition [15,161]. The uncertainty in backscatter results due to the hardware and environment have only recently begun to be recognized [161,185], and uncertainty standards still need to be developed in the manner that they were developed for multibeam bathymetry data over a decade ago [99]. With the goal to improve consistency among backscatter data acquisition and processing methodologies, the Backscatter Working Group (BSWG) was established in 2013 under the auspices of the GeoHab (Marine Geological and Biological Habitat Mapping) association. The BSWG compiled its guidelines in a report published in 2015 [181]. Among other recommendations, the BSWG encouraged comparative tests of processing software packages using common data sets [15]. As an outcome of this recommendation, the Backscatter Software Inter-Comparison Project (BSIP) was launched during the GeoHab 2019 conference.

The long-term objective of the Backscatter Inter-comparison Project is to understand the reasons for the differences between the end-results obtained from a common dataset by various backscatter processing tools. The results in this paper represent the first phase of this project. Since comparing the end-results of the processing solutions does not allow for understanding the root causes of the discrepancies, the developers of commonly-used software were invited to provide a set of intermediate stages from the processing of a common dataset. This approach allows comparison of intermediate corrections without requiring software developers to disclose the details of their proprietary algorithms.

A recent survey of backscatter end-users [39] identified the most-commonly used backscatter data processing software packages to date: HIPS and SIPS by Teledyne CARIS, Fledermaus Geocoder Toolbox (FMGT) by QPS, Geocoder by the University of New Hampshire (UNH), Hypack by Xylem, MB-System by the Monterey Bay Aquarium

Research Institute, and Sonarscope by IFREMER. The developers of FMGT [171], HIPS and SIPS [186], SonarScope [187] and MB-Process (a data processing research tool by Curtin University) agreed to participate in this study. This paper describes the results of the first phase of the project and the lessons learned.

5.2. Data and Methods

5.2.1. Selection of test backscatter data

Five datasets were selected for this study (Table 5.1), representing a range of shallow- and deep-water MBES: Kongsberg EM 2040, EM 3002, EM 710, EM 302 and Teledyne Reson SeaBat 7125. These datasets do not represent an exhaustive list of commercially available MBES but were opportunistically chosen because data from these surveys were publicly available. The test data sets were collected by different agencies (Table 5.1). List of individual data files used during this study are provided as Appendix 5A.

Table 5.1: Datasets used during the study

Sonar model (Nominal Frequency)	Vessel	Data acquisition software	Agency	Location	Weather	Date	Depth range
EM 2040 (300 kHz)	RV Simon Stevin	SIS	FPS Economy	Kwinte reference area (Belgium)	Calm	12 April 2016	23-26 m
EM 3002 (300 kHz)	HSL Guillemot	SIS	SHOM	Carre Renard area, Brest Bay, France	Calm	13 Jan 2010	18-22 m
EM 710 (70-100 kHz)	BH2 Borda	SIS	SHOM	Carre Renard area, Brest Bay, France	Calm	14 Feb 2013	18-22 m
EM 302 (30 kHz)	Okeanos Explorer	SIS	NOAA	Johnston Atoll near Hawaii, USA	Rough	17 July 2017	~3000 m
SeaBat 7125 (400 kHz)	HMSMB Owen	PDS2000	Shallow survey common dataset 2015	Plymouth, UK	Calm	29 July 2014	< 10 m

5.2.2. <u>Selection of intermediate processed backscatter level</u>

A template backscatter data processing pipeline and nomenclature were recently proposed for adoption to assist standardizing backscatter data processing [41]. In this theoretical pipeline, the various stages of radiometric and geometric corrections are chronologically ordered, and the intermediate backscatter levels obtained between each stage are named (BL_0 through to BL_4), providing a sequence of intermediate results (Figure 5.1). However, since each software package applies these corrections in different orders, most of these specific outputs cannot be produced without significantly modifying the data processing code. For the current study, after discussion and agreement with software developers, it was concluded that a phased approach would be most effective. In this first phase, only the intermediate levels that can be provided without significantly altering the code were considered (BL_0 and BL_3).
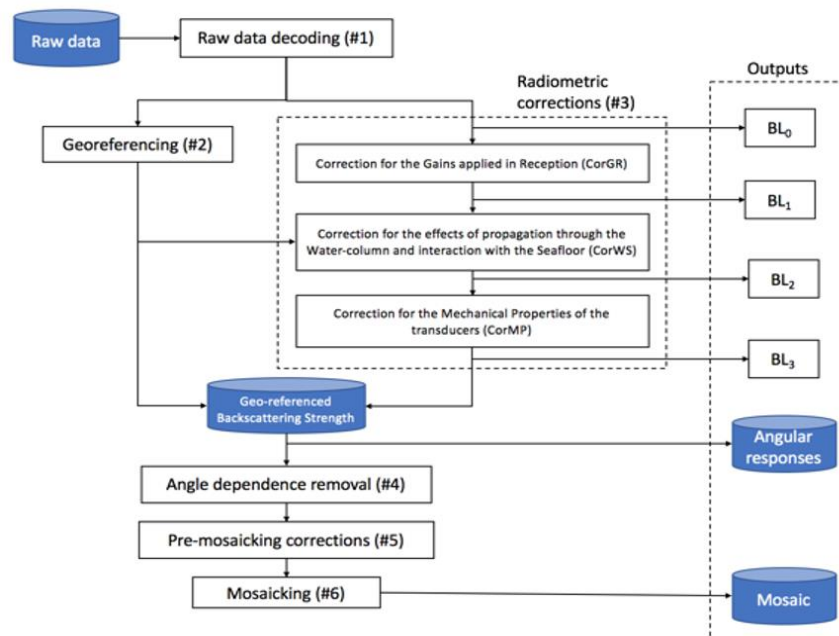
Figure 5.1: Visual workflow of the backscatter data processing pipeline (adapted from Figure 1 in [41]), resulting in the two common backscatter products: angular response curves and mosaic. Only the BL_0 and BL_3 intermediate outputs were requested from software developers during the current study.

5.2.2.1. BL_0: the backscatter level as read in the raw files

The first stage of backscatter processing consists of reading the raw backscatter data recorded in the MBES raw data files. For both Kongsberg and Teledyne Reson systems, the raw data format organizes the collected information into several types of data units, known as datagrams, and the structure of each datagram type is described in format specifications made publicly available by the manufacturers [188,189]. Not only are backscatter data typically available in different datagrams, but the formats, the intermediate calculations applied, and the output resolution may have changed over the years. For example, in Kongsberg systems, backscatter data are available in both the "one-value-per-beam" and "several-samples-per-beam" formats in two different datagrams ("Depth" datagram for the former and "Seabed Image" datagram for the later). In November 2005, the "Depth" datagram was superseded by the "XYZ 88" datagram, and the "Seabed Image" datagram was superseded by the "Seabed Image 89" datagram, with both newer datagrams upgrading the data resolution from 0.5 dB to 0.1 dB [188]. For Reson system, datagrams with multiple samples per beam data are referred to as "snippets". With the aim of using the same raw data, software developers were requested to start the processing with the Seabed Image / Snippets data as the original level (BL_0).

5.2.2.2. BL_3: the backscatter level after radiometric corrections but before compensation for angular dependence

Typically, several radiometric corrections are applied to the raw data (BL_0) after they are extracted from the file. According to Schimel et al. [41], they can be classified in three types: (i) **Cor**rections for **G**ains applied during **R**eception (CorGR), (ii) **Cor**rections for propagation through **W**ater column and interaction with **S**eafloor and (CorWS) and (iii) **Cor**rections for **M**echanical **P**roperties of the transducer (CorMP). This is not the approach that has been historically taken in different software implementations; some software may apply all corrections in bulk, others may combine several, or apply only partial corrections, or apply corrections in different orders. Therefore, we could only request the levels before and after all radiometric corrections (BL_0 and BL_3, see Figure 5.1). BL_3, the backscatter level corrected for radiometric corrections, as a function of the incident angle, is the

"angular response curve", that is one of the two backscatter outputs commonly produced. Further corrections would need to be applied to BL_3 to obtain a backscatter mosaic, including the flattening of the backscatter angular dependence.

5.2.3. <u>Data processing by software developers</u>

Software developers provided the results as an ASCII text file in the format requested (Table 5.2). One of the software packages already had some variations of ASCII export built into their processing routine, while for others the ASCII export was developed as a result of this request.

Table 5.2: Requested variables to be included in ASCII export files for this study.

Column #	1	2	3	4	5	6	7	8
Value reported	Ping #	Beam #	Ping Time (Unix time)	Latitude	Longitude	BL_0	Seafloor Incidence angle (BL_3)	BL_3

Software developers were given option to include additional columns as desired. The details of the data processing as implemented by software developers for this project are outlined in the following sections.

5.2.3.1. <u>HIPS & SIPS backscatter processing workflow</u>

The backscatter processing implementation in CARIS SIPS is a continuation of its bathymetric processing workflow and is aimed towards creating a backscatter mosaic. SIPS supports data sources from Reson and Kongsberg systems in their three record modes: Sidescan (only applicable to Reson systems), beam average intensities and snippets. Two separate backscatter processing engines are available within SIPS: Geocoder and SIPS backscatter processing engine. As the existing SIPS workflow did not allow end-users to extract BL_0 and BL_3, these data were extracted by the SIPS software developers themselves (Pers. comm. Travis Hamilton). The following corrections and settings were selected: Processing Engine: SIPS, Source Data Type: Time series; Slant Range Correction, Beam Pattern Correction; Angular Variation Gains, Adaptive; AVG size filter, 200 samples. As of release of CARIS SIPS 11.1.3 (released March 2019) end-users will have the ability to

export the intermediate processing stages accessed through 'Advanced Settings' and by designating a 'Corrections Text Folder' where an ASCII file is stored that contains results of intermediate processing stages (Figure 5.2, this newly implemented workflow has not been validated by authors as yet).
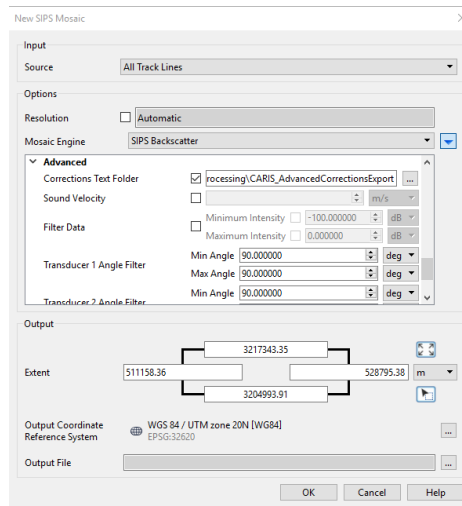
Figure 5.2: CARIS SIPS mosaic creation tool showing the advanced settings where a folder can be set for export of text file that contains intermediate backscatter processed levels. CARIS HIPS & SIPS ver. 11.1.3 (Released March 2019).

5.2.3.2. FMGT backscatter processing workflow

The backscatter data processing in the QPS software suite is a separate toolbox: Fledermaus Geocoder ToolBox (FMGT). A notable factor in this implementation is that all the survey parameters are read directly from the survey line files, while the processing parameters are divided in two categories. Under the "Backscatter" category, the following options were selected: "Tx/Rx Power Gain Correction", "Apply Beam Pattern Correction", and "Keep data for ARA analysis", Backscatter Range was selected based on the minimum and maximum value of backscatter from "calibrated" backscatter with beam angle cut off between 0° and 90°. Export of BL_0 and BL_3 data are available through ASCII export 'ARA beam detail' (Figure 5.3).
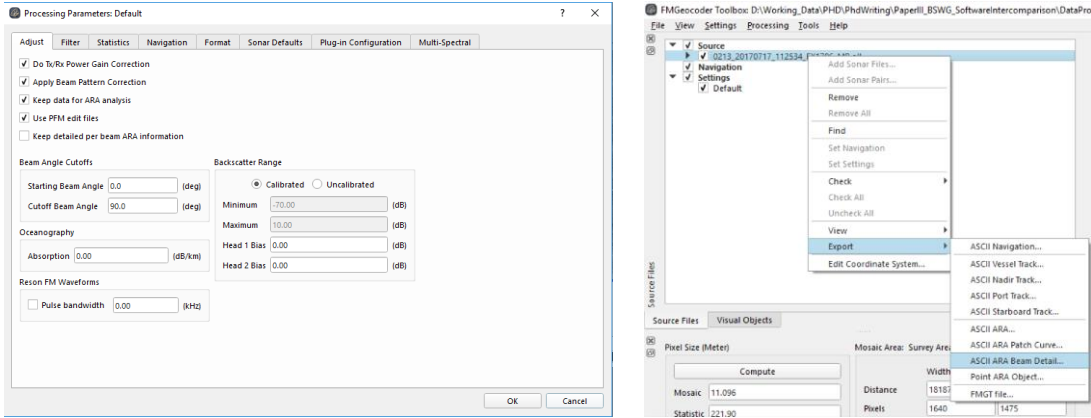
Figure 5.3: QPS FMGT tool settings showing version 7.8.0 (released December 2016). To enable export of ARA Beam detail, enable 'Keep data for ARA analysis' in processing parameters. The 'ASCII ARA Beam Detail' export is available through the contextual display on the main window.

5.2.3.3. <u>**SonarScope data processing workflow**</u>

SonarScope is a research tool developed by the "Acoustics & Seismics" department of IFREMER. SonarScope is available for free under an academic non-commercial use license. This tool is developed in Matlab as a laboratory tool aimed at research and development, rather than production. SonarScope can handle a variety of MBES formats. SonarScope implemented a new backscatter data processing methodology concurrently with this study (Pers. comm. Jean Marie Augustin). A detailed analysis of various processing stages based on the sonar equation [19] are provided in this updated workflow, and exported as an HTML summary file with graphical displays of the various corrections. An ASCII output file is also produced that contain several fields describing the corrections (Figure 5.4).
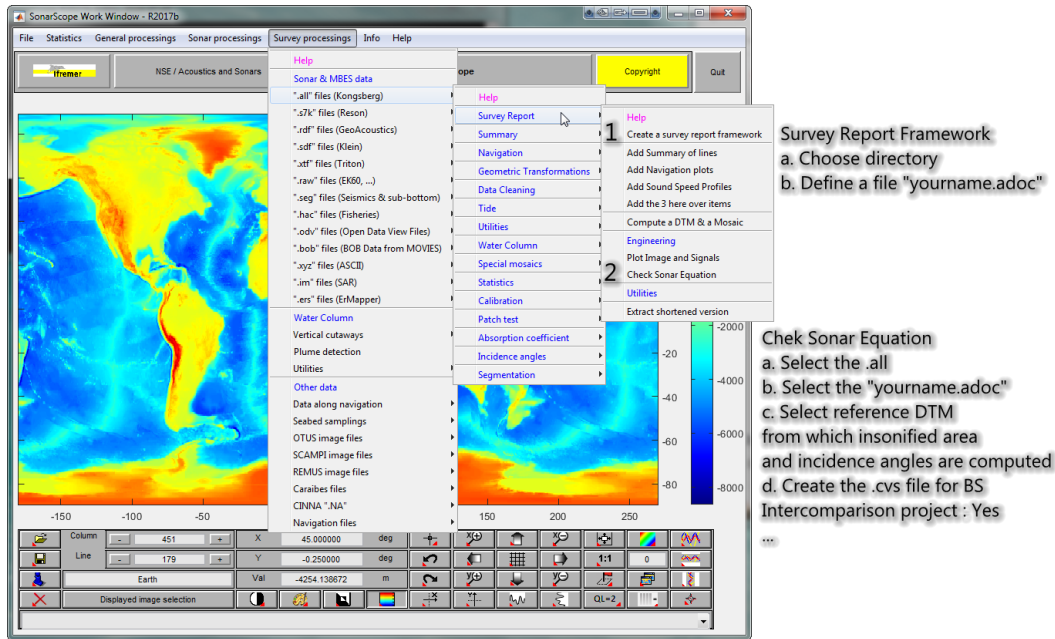
Figure 5.4: The interface in SonarScope to select the export of csv and html file that provides details of the various corrections applied to the produce processed backscatter results. SonarScope ver. 20190702_R2017b (released 2 July 2019).

5.2.3.4. Curtin CMST- GA MB Process data processing and SONAR2MAT data conversion

The CMST-GA MB Process is a proprietary backscatter data processing tool coded in Matlab and developed and used by Curtin University and Geoscience Australia researchers to process Kongsberg (.all) files and Reson MBES (files saved as XTF) [190]. It is available to download for free from: https://cmst.curtin.edu.au/products/multibeam-software/ (last accessed Sept 2019). As this study used Reson (.s7k) files, the converter SONAR2MAT [191] was used to convert the (.s7k) data first to MATLAB (.mat) data files. SONAR2MAT converter supports a variety of MBES data formats and is available to download for free from: https://cmst.curtin.edu.au/products/sonar2mat-software/ (last accessed Sept 2019). The script was used to calculate the mean for each beam (, i.e., BL_0) from the converted snippets data packet (7028) using the samples that fall within +/-5 dB around the bottom detect echo level. The corrections applied followed Parnum and Gavrilov [126], and required other converted data packets, including: settings (7000),

bathymetry (7027) and beam geometry (7004), to produce BL_3 data. Data were then exported in to the ASCII format specified in Table 2 except for beam depth.

5.3. Results

The ASCII files obtained for each software differed in both format and contents. A summary of the contents of the ASCII files is provided in Appendix 5B. The availability of results on ping/beam basis made it convenient to compare data from each software. Data inter-comparison was conducted based on the beam number, BL_0, BL_3 and incidence angle.

5.3.1. Flagged invalid beams

The number of beams flagged as "invalid" by each software were different (Figure 5.5). For the Kongsberg EM 302 data, FMGT showed almost no flagged beams while both SIPS and SonarScope showed a large number of beams flagged. These differences were found to be related to each software's different choice of dealing with soundings with invalid bottom detection. Kongsberg's "XYZ 88" datagram provides information about 'detection information' that specifies among other things whether the beam had a valid bottom detection or not (see note 4 p.44 [188]). FMGT by default allows the use of the beams with invalid bottom detection, while SIPS and SonarScope utilize only the beams that have a valid bottom detection information available. For the purposes of comparison, only the beams that were considered valid by all software packages were used.
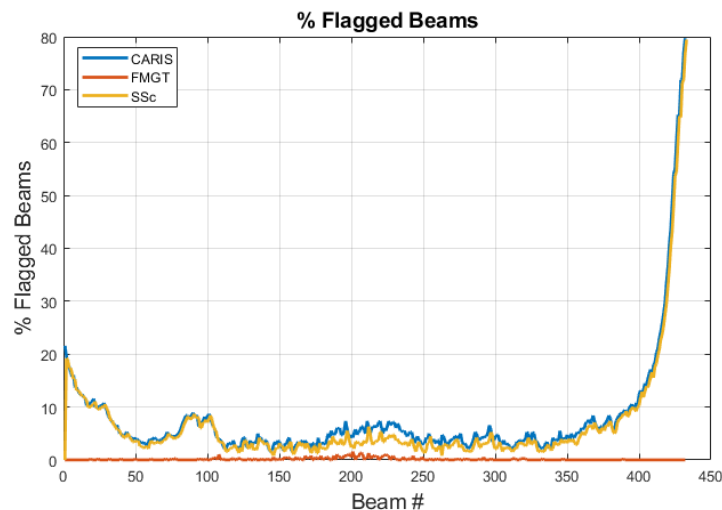
Figure 5.5: Number (%) of flagged beams for three software: CARIS, SonarScope and FMGT for EM 302 data. Number of flagged beams reached to 80 % for CARIS and

SonarScope for the outer beams while the beams flagged as invalid remain < 1 % for FMGT.

5.3.2. Comparison of BL_0 and BL_3

The software provided results whose patterns were qualitatively comparable but whose relative levels were often very different (BL_0 in Figure 5.6 and BL_3 in Figure 5.7). The mean values of BL_0 and BL_3 were computed for each beam and ping and showed that the differences between the tools can be larger than 5 dB (Figure 5.8). It was also evident these differences are not uniform across the swath. A pair-wise comparison revealed that the differences were more pronounced for the outer beams compared to near-nadir beams (Figure 5.9).
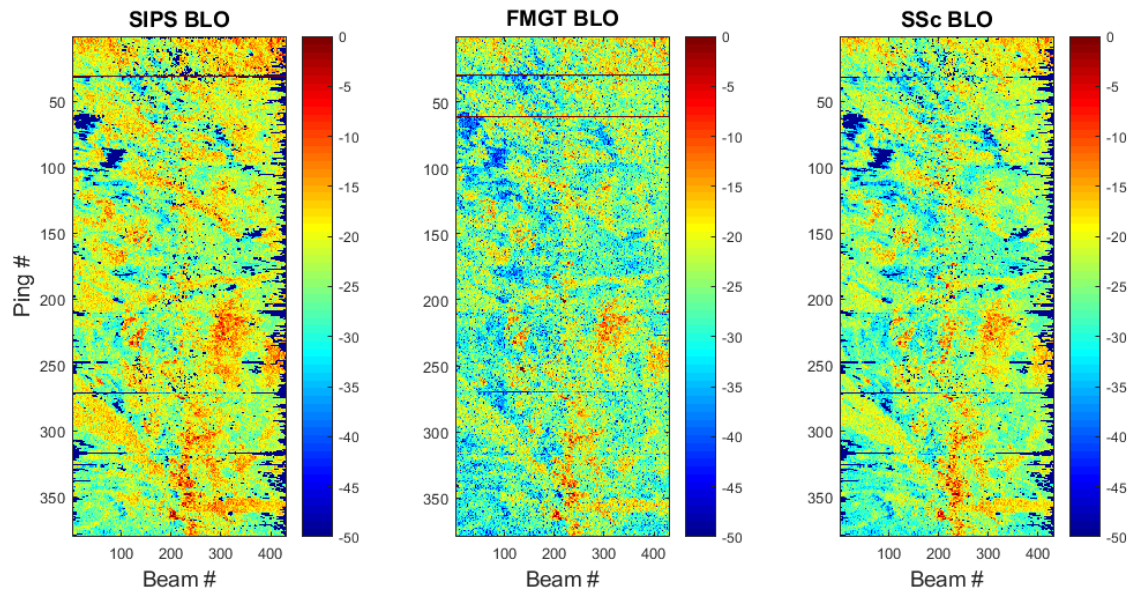
Figure 5.6: Plots showing BL_0 results from CARIS, FMGT and Sonar Scope for EM 302 data.
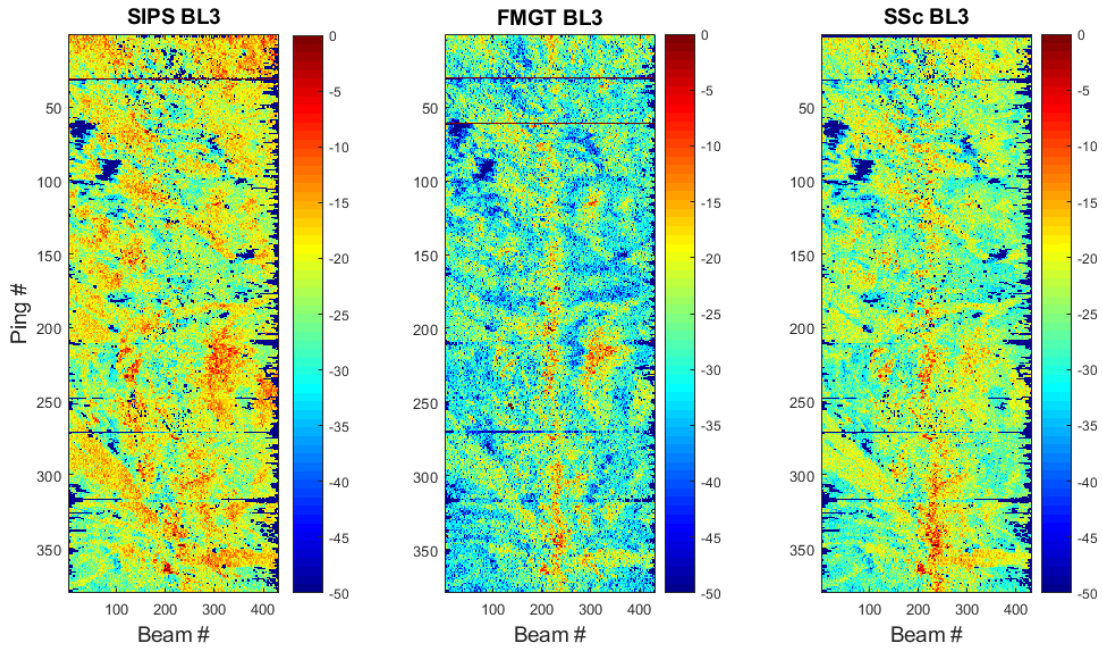
Figure 5.7: Plots showing BL$_3$ results from CARIS, FMGT and Sonar Scope for EM 302 data.
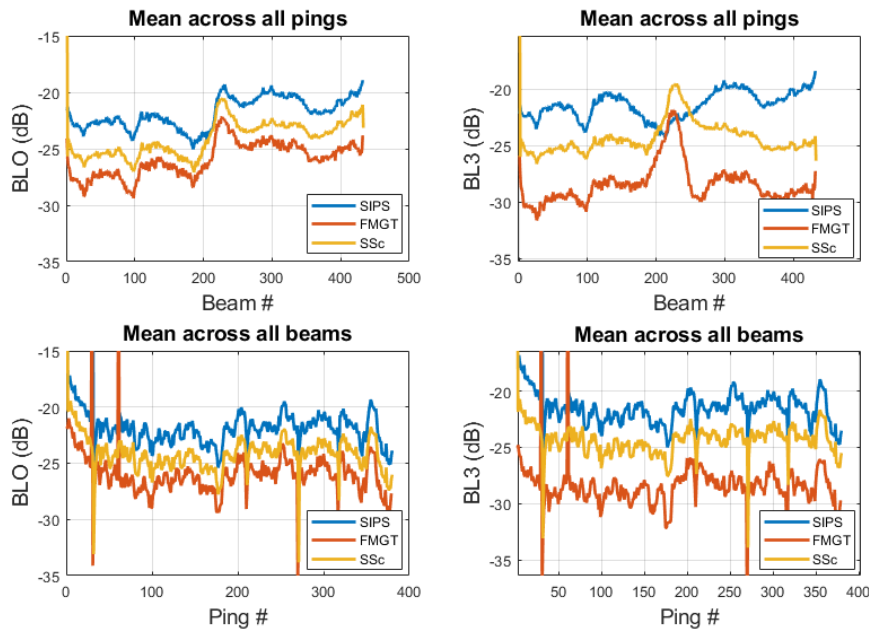
Figure 5.8: Plots showing the BL$_0$ (left panels) and BL$_3$ (right panels) results from CARIS, FMGT and SonarScope for EM 302 data. The plots on top show the average over the entire survey line for all pings reported at each beam. The lower plots show the average of all beam for each ping.
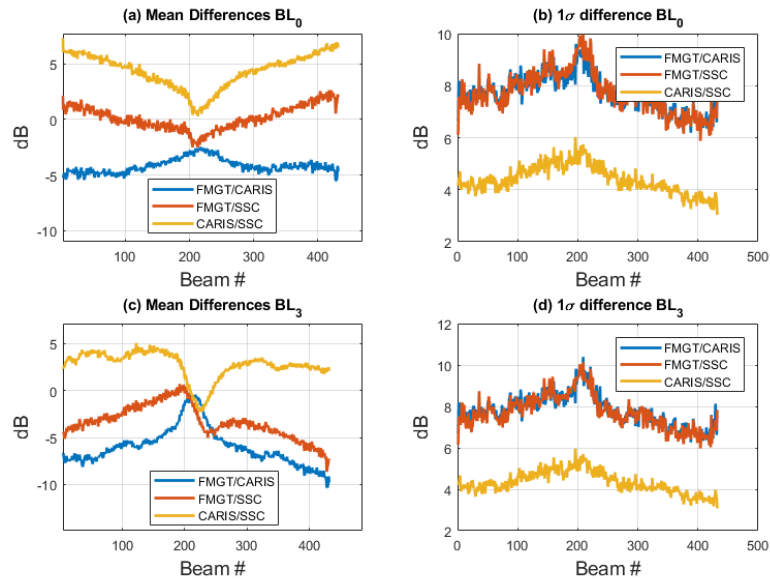
Figure 5.9: Mean and standard deviation of pair-wise differences between BL_0 and BL_3 for each beam computed by software solutions for EM 302 data. (a) Mean differences BL_0 (b) Standard deviation of differences BL_0 (c) Mean differences BL_3 (d) Standard deviation of differences BL_3

5.3.3. <u>Comparison of reported incidence angles</u>

CARIS SIPS reported incidence angles were positive and ranged from 0° to 80° while FMGT and SonarScope reported the incidence angle with range from −80° to 80° with port swath incidence angles reported as negative numbers (Figure 10,11). Topographically-related variations in incidence angles are clearly visible in the output of SIPS, FMGT and SonarScope, suggesting that seafloor slope was considered while computing seafloor incidence angle. However slight variations in the incidence angle are noticeable that may be related to the differences in the cleaning or smoothing of the DTM used to correct for seafloor slope.
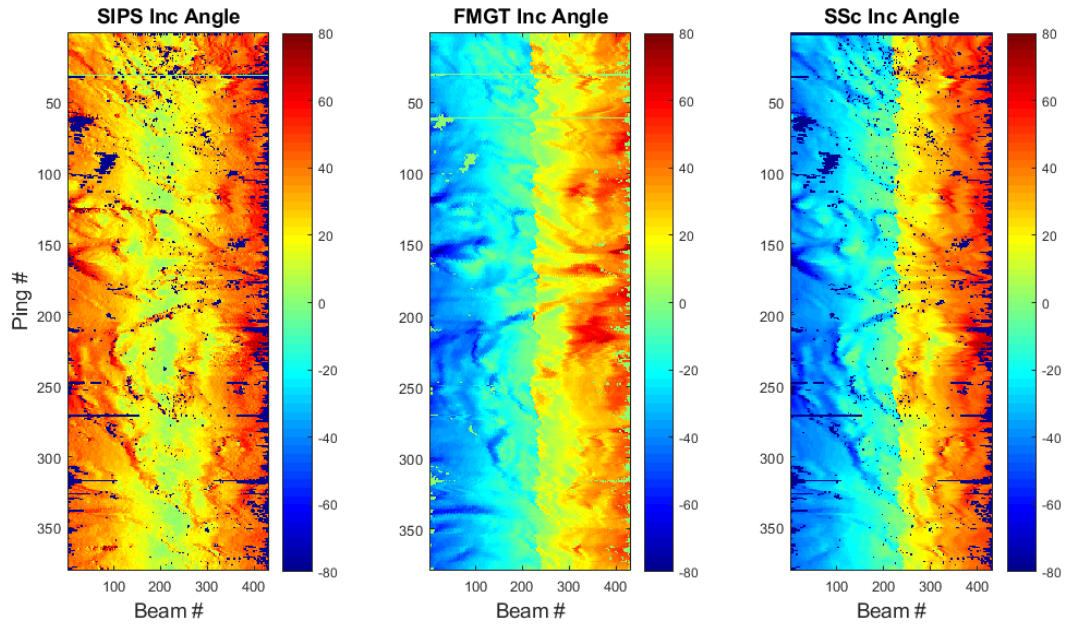
Figure 5.10: Plot showing incidence angle reported for each beam for one file from EM 302 MBES.
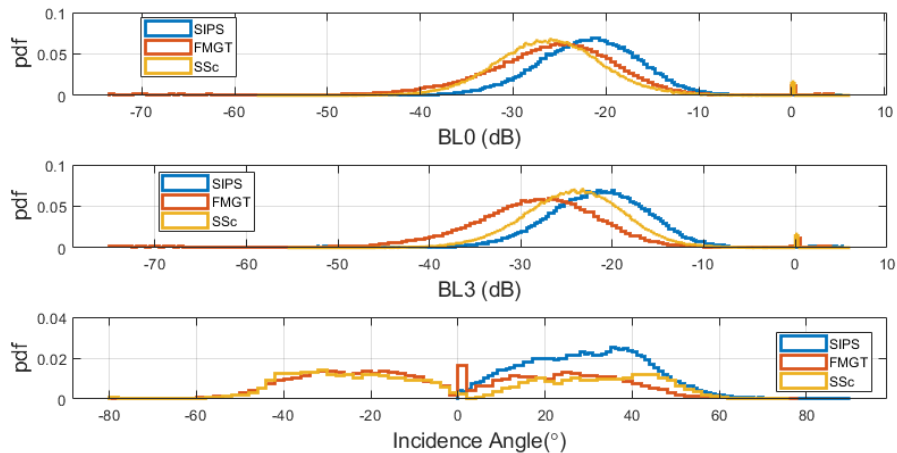
Figure 5.11: Comparison of empirical pdf of BL_0 (top), BL_3 (middle) and Incidence angle (bottom) for the three software tools for one data line collected using EM 302.

5.3.4. Comparison of corrections applied for BL_3 processing

The difference between BL_3 and BL_0 were computed for each software solution in order to obtain the total correction factor applied in the radiometric correction stage (Figure 5.12, 5.13). These show that each software applies very different processing corrections at

this stage. In the case of SIPS, the correction appears as an along-track stripes pattern, which would implicate beam pattern correction (§ 2.3.1). In the case of FMGT, the correction is reminiscent of incidence angle. In the case of SonarScope, the correction increases somewhat regularly away from nadir. Without the knowledge of the intermediate stages between BL_0 and BL_3 (BL_{2A} and BL_{2B} – See Figure 5.1), these interpretations are speculative.
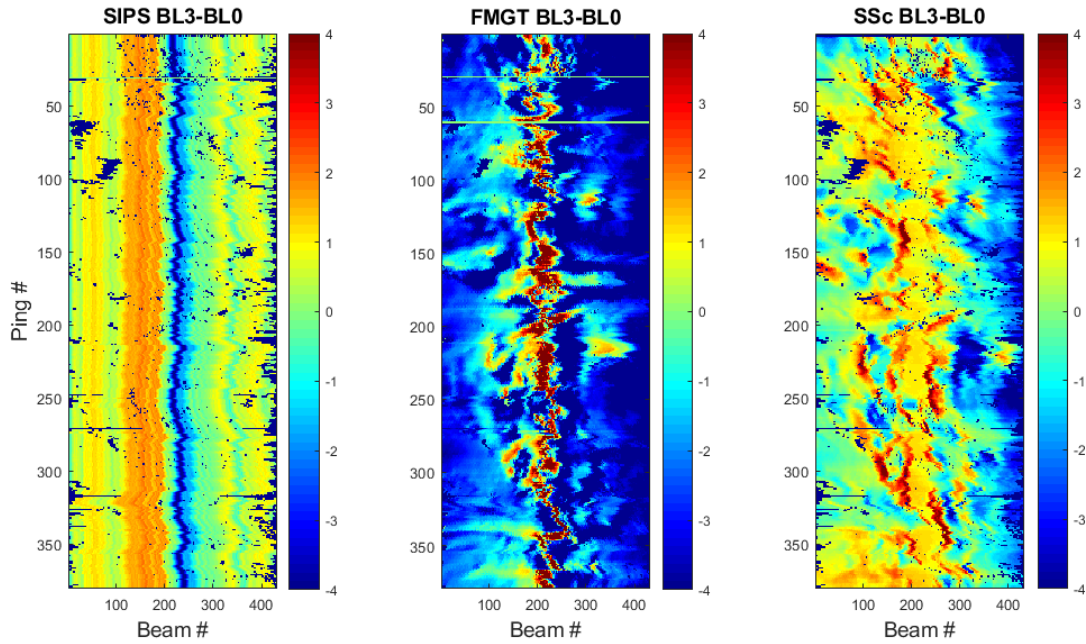
Figure 5.12: Plots showing the total radiometric corrective factor (BL_3-BL_0) for each software package.
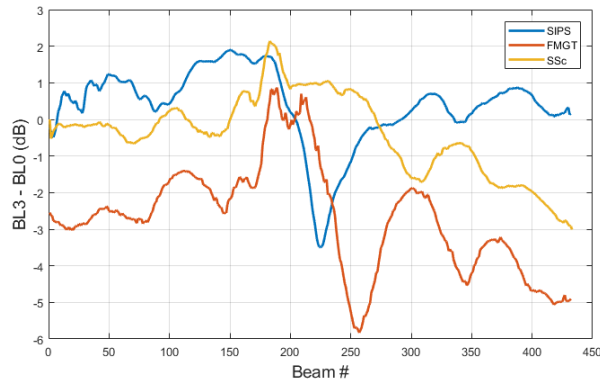
Figure 5.13: Plot showing average of BL_3 - BL_0 over 50 pings (ping # 100 - 150).

5.3.5. Summary of differences between software for different sonar types

In the previous sections, we explored in detail the differences between SIPS, FMGT and SonarScope processing an EM302 data file. In this section the results of BL_0, BL_3 and incidence angle for other sonar types are summarized. The results show that EM 710 (Figure 5.14,15), EM 3002 (Figure 5.16, 5.17), EM 2040 (Figure 5.18, 5.19) and SeaBat 7125 (Figure 5.20, 5.21) also present large differences.
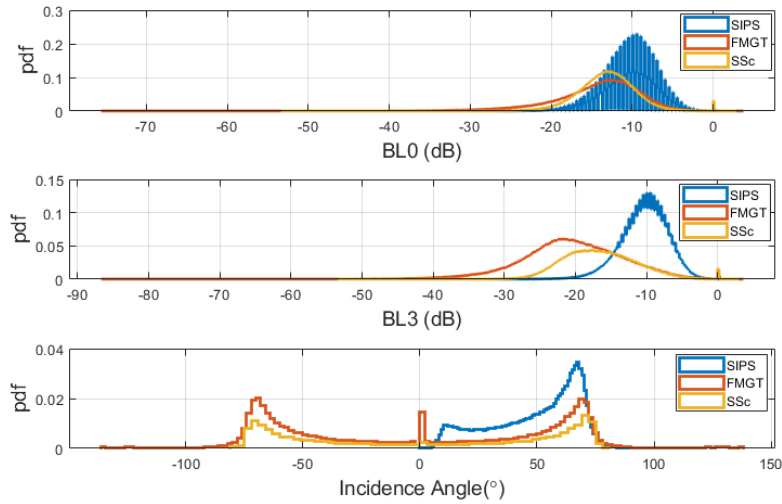
Figure 5.14: PDF of BL_0, BL_3 and incidence angle results from FMGT, CARIS and Sonar Scope for EM 710.
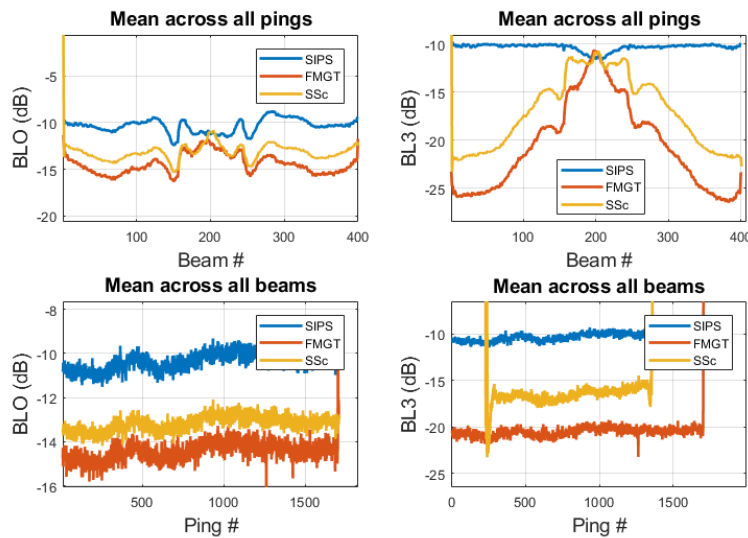
Figure 5.15: Plots showing BL_0 (left panels) and BL_3 (right panels) from CARIS SIPS, FMGT and SonarScope for the EM 710 data. The plots on top show the average over the

entire survey line for all pings reported at each beam. The lower plots show the average of all beams for each ping. SonarScope BL_3 results were clipped for the pings where there was no reference DTM available.
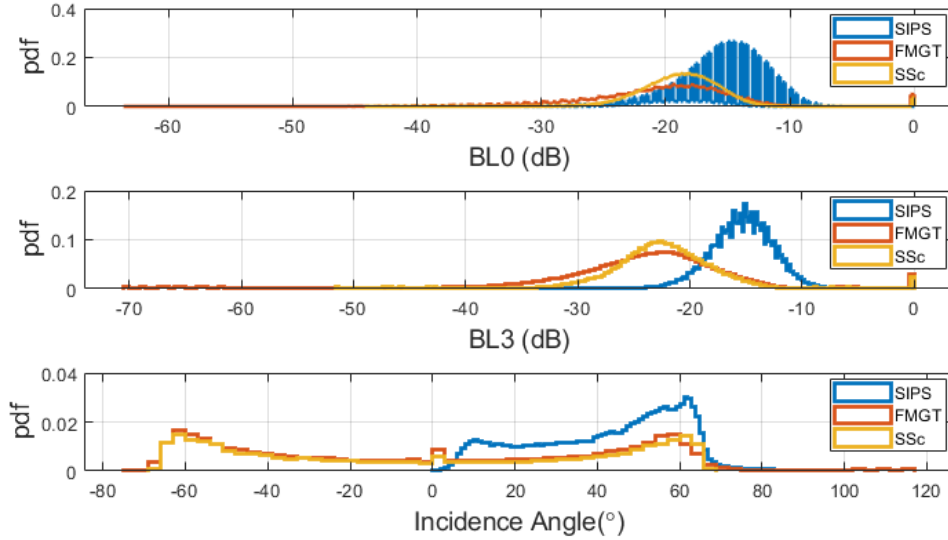
Figure 5.16: PDF of BL_0, BL_3 and incidence angle results from CARIS and Sonar Scope for EM 3002.
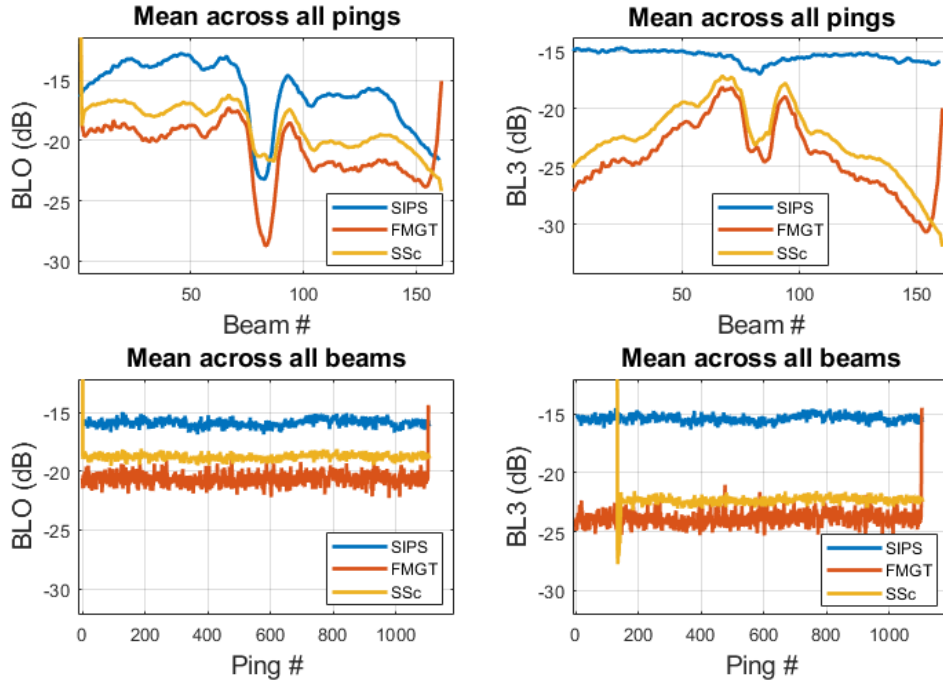
Figure 5.17: Plots showing BL_0 (left panels) and BL_3 (right panels) from CARIS SIPS, FMGT and SonarScope for the EM 3002 data. The plots on top show the average over the

entire survey line for all pings reported at each beam. The lower plots show the average of all beams for each ping.
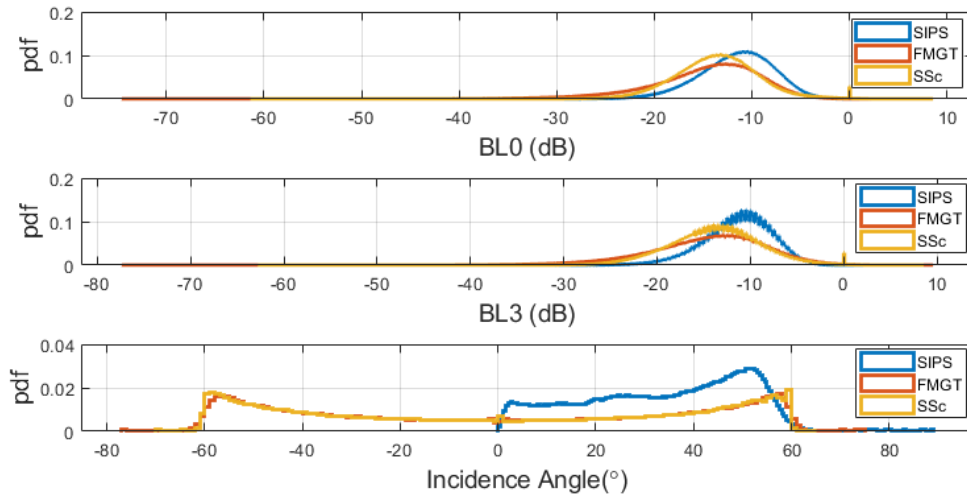
Figure 5.18: PDF of BL_0, BL_3 and incidence angle results from FMGT, CARIS and Sonar Scope for EM 2040.
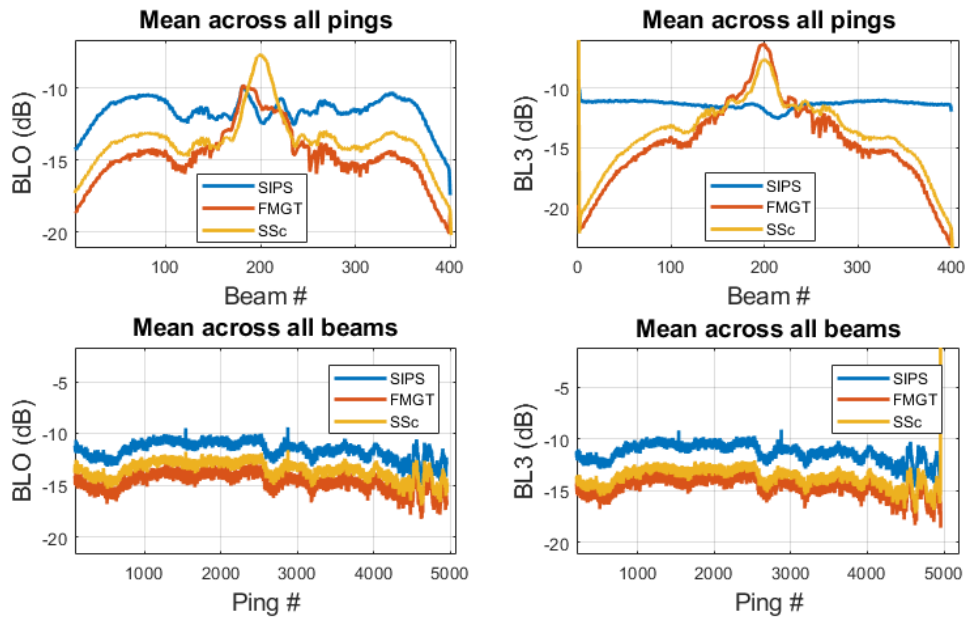
Figure 5.19: Plots showing BL_0 (left panels) and BL_3 (right panels) from CARIS SIPS, FMGT and SonarScope for the EM 2040 data. The plots on top show the average over the entire survey line for all pings reported at each beam. The lower plots show the average of all beams for each ping.
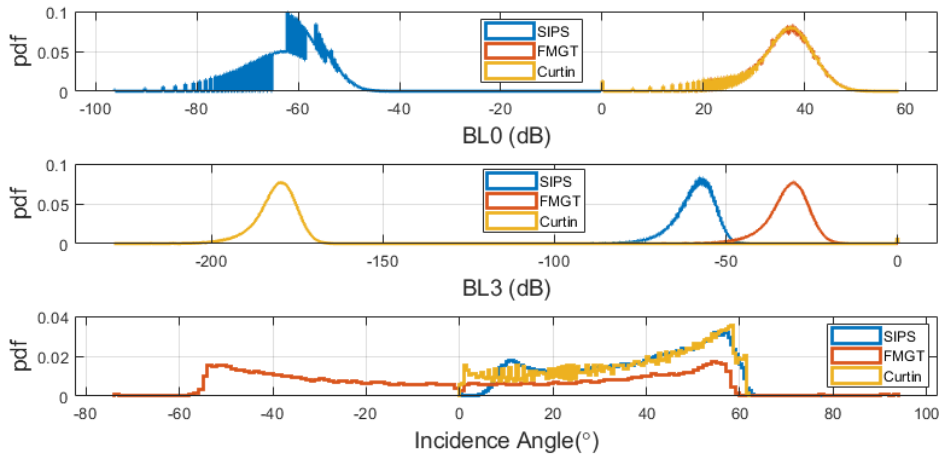
Figure 5.20: PDF of BL_0, BL_3 and incidence angle results from FMGT, CARIS and Curtin MB Process Reson 7125.
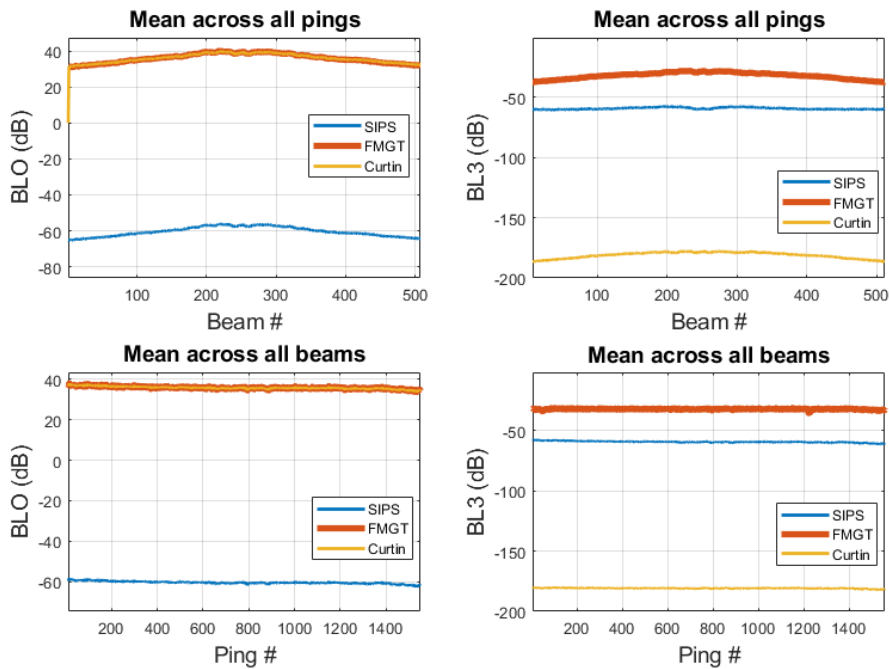
Figure 5.21: Plots showing BL_0 (left panels) and BL_3 (right panels) from CARIS SIPS, FMGT and Curtin University MB Process for the SeaBat 7125 data. The plots on top show the average over the entire survey line for all pings reported at each beam. The lower plots show the average of all beams for each ping.

The pairwise differences show that both BL_0 and BL_3 results differ considerably among processing solutions for the example files from all sonar models. The mean

128

differences (except for the SeaBat 7125 data file) ranged from ~2 dB to ~10 dB with standard deviations of up to 8 dB. For the Seabat 7125 data file, the mean of the difference between FMGT and MB Process results was < 1 dB, but the difference was ~ 100 dB for comparisons involving SIPS. The large discrepancy observed in SIPS results for the SeaBat 7125 data file indicate application of large (yet unexplained) offset while reading the snippets.

5.3.6. <u>Reasons for differences in BL_3 for different sonar types</u>

The results presented above showed that software solutions provided levels that differ both at the initial raw data reading stage (BL_0) and after the radiometric correction have been applied. The differences at BL_0 are concerning as this initial stage consisted of reading the data and these differences indicates that software solutions are reading the raw data in ways that leads to different results. We do not have the details as how each software solution is computing the BL_0, but few possible reasons for differences in BL_0 will be discussed in § 5.4.2.

The differences in BL_3 between software can be either the result of differences in BL_0, or differences in the radiometric corrections (BL_3 - BL_0), or more likely the combination of both. To assess which of the two sources of differences contributes the most to the difference in BL_3, we calculated the absolute value of the ratio between the difference in radiometric correction and the difference in raw data reading (Eq. [5.1]), considering two software solutions A and B):

$$\gamma = \left| \frac{[BL_3^A - BL_0^A] - [BL_3^B - BL_0^B]}{[BL_0^A - BL_0^B]} \right| \qquad \text{[Eq. 5.1]}$$

If the differences in radiometric corrections between two software are large while the differences in data reading are small, γ will tend to be larger than 1. If on the contrary, the two software packages read the data very differently but applied equivalent radiometric corrections, γ would tend towards zero. A value of approximately 1 indicates that the difference in data reading are equivalent in effect to the difference in radiometric corrections. This ratio was computed for each beam of each ping and illustrated for the EM302 data file in Figure 5.22.
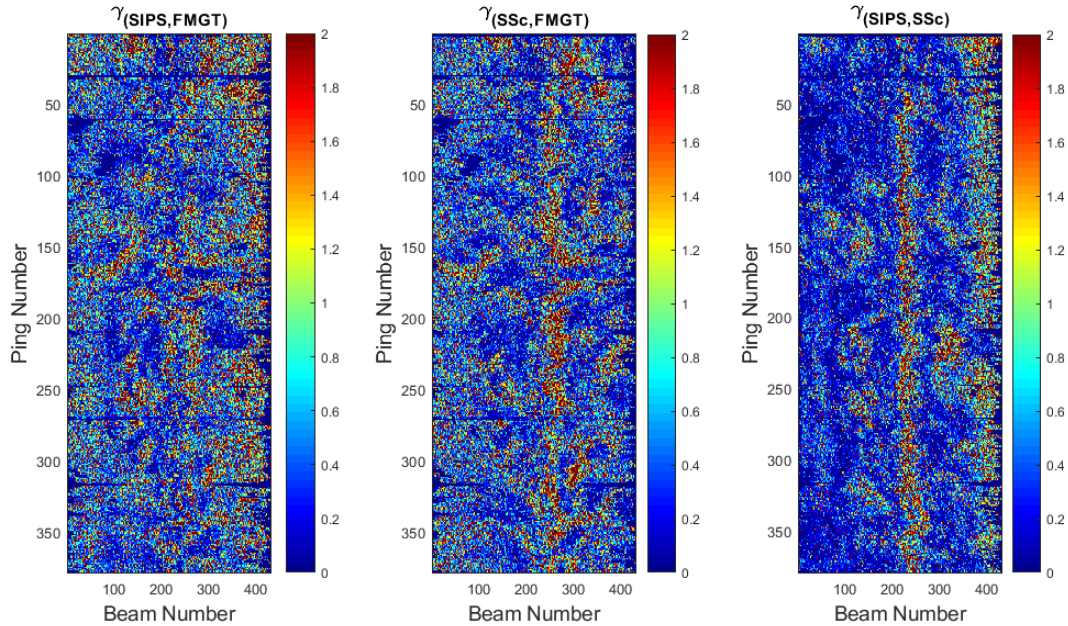
Figure 5.22: The absolute ratio of the difference in processing to the difference in starting value for (left) CARIS SIPS and FMGT, (middle) FMGT and SonarScope, (right) SonarScope and CARIS SIPS for the EM 302 data.

The proportion of soundings for which γ fall below 1 for various systems is shown in Table 4. In the case of Kongsberg systems, the proportion of soundings with $\gamma < 1$ was always in the mid-range, from a minimum of 30.2% (SonarScope/SIPS comparison of EM710 data) to a maximum of 92.9% (FMGT/SonarScope comparison of EM2040 data), indicating that the raw data reading and the radiometric correction have equivalent effect on the difference in the results. However, the fact that $\gamma < 1$ occurred always more than 50% of the time (except for EM 710) implies that the difference in how the software computes the starting value from raw data is at least as often as important, if not more, than the difference in radiometric corrections. This implies that a very significant part of the difference in results between software packages is simply due to the original choice of the starting value (BL$_0$). The same analysis applied on the SeaBat 7125 data produced much different results. The difference in BL$_0$ read by SIPS and FMGT is very large compared to the radiometric corrections implemented by the two software packages (with over 99 % of soundings showing $\gamma < 1$) while the comparison between MB Process and the FMGT

show that most of the differences in the observed BL_3 were due to the differences in radiometric corrections applied.

Table 5.3: Proportion of beams (%) with ratio < 1 computed between various processing tools.

	SIPS / FMGT	FMGT / SonarScope	SonarScope / SIPS	MB Process / FMGT	MB Process / SIPS
EM 302	57.9	61.6	67.8	-	-
EM 710	40.2	37.2	30.2	-	-
EM 3002	61.6	81.3	44.6	-	-
EM 2040	76.7	92.9	77.3	-	-
SeaBat 7125	99.4	-	-	10^{-10}	0.2

5.4. <u>Discussion</u>

MBES backscatter data are increasingly used to provide information about the nature of the seabed, in resource management projects, to assess the potential environmental impacts of human activities on the seabed, and for monitoring and managing marine habitats [15,39]. In many of such projects, it is often required to merge backscatter data from several sources, which often use different data processing and analysis software packages (e.g., EU national monitoring programs in relation with the EU Marine Strategic Framework Directive [192], Seamap Australia – a national seafloor habitat classification scheme [193] and Marine AREA database for Norwegian waters: MAREANO [194]). In this context, the quality control of the data and final products have important regulatory and legal implications. It is incumbent upon government agencies and scientific institutions to recognize that software packages used to process the raw data into useable products impact the interpretation of these products and thus should be accredited for quality level [195]. There is a lot to gain for all the parties involved, to develop quality control approaches for the algorithms and reach a level of standardization sufficient to merge the products from different software packages. The comparative analysis of software intermediate results, as developed in this paper, is a first step in the direction of processing standardization.

5.4.1. Importance of accurate, transparent and consistent software solutions in science

The software solutions provide critical functionality to support data acquisition, processing, analysis and visualization for nearly all the scientific disciplines including benthic studies [196,197]. The choice of the processing software is a critical decision. Software solution(s) may be chosen based on several criteria including accuracy, transparency, consistency, ease of use, price, fit for the specific processing needs, computing resources requirements and compatibility with other tools being used by an organization and project partners. The determination of accuracy, transparency and consistency of software solutions requires detailed testing that is beyond the scope of a single study such as the present one [198]. However, the unexplained differences between the backscatter mosaics processed by the tools that are widely used by scientists is a concern shared by end-users of backscatter data, agencies funding data acquisition and processing; and software solution providers [199,200]. Hook and Kelley [198] identified lack of quality control and means of comparing software output to expected and correct results as a critical challenge to assess a software package. The current study compares some of the intermediate processing results of non-transparent processing chains in an attempt to highlight which parts of these processing chains differ the most. Only four software solution providers participated in this study but it is expected that future efforts will include other software packages. One very positive development has been that through this study and the cooperation of the software manufacturers, each of the three commercial software packages we studied (QPS, CARIS and SonarScope) now have functionality to export intermediate results that will enable future end-users to be able to assess the processing chain themselves.

5.4.2. Why do different approaches to reading raw data exists and which one is correct

The results indicate that the raw data in the form of seabed image / snippets is read differently by various software to create what is termed as 'beam averaged backscatter' and was referred to during this study as BL_0. The impetus to compute beam averaged

backscatter value stems from the need to reduce the statistical uncertainty of seafloor backscatter [26,161]. Through the commercial development of MBES, different approaches have been taken for the collection and provision of backscatter data and these differences may offer some explanation for the discrepancies found. For instance, historically the approaches taken to compute a single representative value per beam from recorded snippets have differed based on:

(a) Choice of central tendency i.e., mean, median or some other measure;

(b) Choice of how the backscatter samples are selected to compute a measure of central tendency e.g., use all the samples within a beam *vs.* using some threshold around the bottom detect to obtain a subset of samples *vs.* some other variations to choose samples;

(c) Choice of calculation method. MBES samples provided by sonar manufacturers represent backscatter strength in dB. These samples can be directly used to compute their central tendency or they can be first converted into linear domain before calculating averages and then the computed average converted back to a logarithmic scale.

For the purposes of this study, the software vendors were not required to disclose the details of their processing steps. The discussions over the course of this study with software developers indicated that this information may not be readily disclosed as the software developers are limited by non-disclosure agreements with hardware manufacturers from openly disclosing the internal processing of hardware. The information about computation of BL_0 for various software that could be obtained during the study are summarized in Table 5.4. The impact of these various choices will result in differences in the reported results depending on the specific data set and range of the recorded backscatter values. These differences are the most likely reasons the BL_0 values reported for various tools were different. A recommendation to use one or the other approach based on rigorous analysis is beyond the scope of the current study but further investigation into this issue should be prioritized in close collaboration with hardware manufacturers as well as software developers.

Table 5.4: Disclosed information by software packages to compute BL_0. The information is produced here with permission from the software packages.

CARIS SIPS	FMGT	Sonar Scope	Curtin Univ. MB process
Reson Systems: Use the snippet sample associated with the bottom detection. Divide the stored value by 65536 (to convert from 2 byte to floating point) before applying the 20log10. *Kongsberg systems:* Fit a curve to snippet samples using a moving window (size 11 samples). Report the max value of the fit curve.	*Reson and Kongsberg systems:* Identify all the samples that fall within +/-5 dB around the bottom detect echo level and compute an average of these qualifying samples using the amplitude values in dB as reported in the datagram.	*Kongsberg systems:* Use all of full time series samples recorded within a beam to compute average value. By default samples are first converted to energy (linear domain) before computing average and returned in dB. The new release (2019) provides the option to compute this value in dB, energy, median, or amplitude. The new default method is now in amplitude.	*Reson systems:* Calculate the mean of samples that fall within +/-5 dB around the bottom detect echo level.

.

5.4.3. <u>Need for adoption of metadata standards</u>

While MBES bathymetry data has long been subject to standards of accuracy [99], quantified uncertainties [101], and validated processing sequences, MBES backscatter mosaics are often considered qualitative products. The long-standing obstacle here is the complexity of the logistics of calibrating MBES backscatter data, and this situation has delayed the development and applications of the usage of this data-type [181]. The shift from a qualitative treatment of seafloor backscatter products such as backscatter mosaics to that of quantitative repeatable measurements may not be complete until feasible calibration procedures are developed, agreed upon, and routinely implemented. In the meantime, however, additional tools needs to be made available to end-users to analyze the impact of their choices of parameters and algorithms in their backscatter data processing routine. Compilation of results from multisource multibeam echosounders (e.g., [201]) and for multi-frequency systems (e.g., [202]) indicate the growing demand for consistent processing methodology. The ability to identify the reason(s) of differences in the

processed results is therefore an essential component to understand if the differences in repeat or adjacent surveys are due to the seafloor changes, acquisition differences or merely due to post processing differences. This study reinforces the need for comprehensive metadata to accompany processed results [181]. In the absence of estimates of the accuracy or uncertainty of a data product (as is the case with MBES bathymetry), metadata provides the backscatter users with the minimum sufficient information to replicate the final product if necessary, and correct issues that may be discovered. Metadata also has an essential role in providing information to end-users (e.g., a geologist interpreting seabed sediment type) who may not be actively involved in, or have an in- depth knowledge of, backscatter processing yet whose perception of the data is influenced by the data provenance from acquisition through processing. The development and implementation of a standard metadata format for backscatter data products by the community (involving sonar manufacturers, software developers, and the users of these hardware and software across industry, academia and government organizations) should therefore be a priority.

5.4.4. Collaboration between backscatter stakeholders

This study has been conducted under the umbrella of the GEOHAB Backscatter Working Group (BSWG) which has been organized to provide a platform for academic, commercial and government entities to collaborate to address a challenge in backscatter processing. Although the calls for such collaborations have been numerous [203–205], collaborations focused on a specific data type (MBES backscatter) are rare. The lessons learned from this collaboration include:

    a) The collaboration works well if all the stakeholders can communicate. The BSWG provided an effective communication platform which facilitated the discussion.

    b) Different entities may have different end goals in mind while collaborating on such projects. The framework of a successful collaboration depends on finding common goals. For example, in this case, the common goal was improvement in the consistency of backscatter results which motivated all stakeholders to agree to work closely. For other similar efforts, e.g., efforts to standardize seafloor backscatter segmentation and characterization, the

identification of a common goal may not be very clear due to multiple divergent needs of end-users or desire to protect commercial interests.

c) The challenges of navigating proprietary restrictions of both multibeam echosounder software and hardware manufactures are very real and may hamper successful collaboration between stakeholders [206].

5.5. Conclusions and future work

The applications of seafloor backscatter data are expanding. To support such an expansion, there is a critical need for an increased consistency of output among various software packages or, at least, a clear explanation for differences among software solutions. The progress made in this study was due to the cooperation of the software providers. For instance, during this study, significant differences were encountered between the outputs of several popular backscatter software packages, but through collaboration, a better understanding of where these differences were introduced in the processing pipeline was achieved. This study adapted the standard processing pipeline and nomenclature proposed by Schimel et al. [41] to produce the results from backscatter intermediate processing stages. However, the data from these intermediate processing stages are currently not produced consistently by all the software developers, and therefore, active participation of software developers was critical during the study to make appropriate changes in the software to enable export of results from intermediate processing stages.

Two intermediate processing levels were assessed during this study: the level read from the raw data files (BL_0) and the level after radiometric corrections but before removal of angular dependence (BL_3). Software developers applied the required changes in their processing methodologies and provided data in Beam – Ping configuration with BL_0 and BL_3 reported for each beam along with incidence angle. Both BL_0 and BL_3 showed differences as high as >10 dB between the software packages. The differences in BL_0 indicate that closed source software have adopted different approaches to read and reduce the raw data. These differences suggest this stage as one of the major causes of the observed differences in the final products. The observed discrepancy between BL_0 calls for standardization of processing at this early stage of backscatter processing as well as more transparency from software providers to describe their computation choices. Critical

choices of BL_0 computation that should be targeted for developing a standard includes: (a) the choice of computation method for central tendency i.e., mean or median; (b) the selection of samples used to compute BL_0, and; (c) the choice of linear or logarithmic domain for computation.

This study has shown the applicability and usefulness of the availability of intermediate processing stages for the inter-comparison of proprietary software without requiring the software vendors to disclose their proprietary algorithms. Hence, although the scope of this study has been limited to understand the differences between the specific software package results, it adds weight to the argument of why it is critical for various sonar manufacturers, commercial and academic software developers, and end-users from diverse domains to work together to develop methods that can improve the consistency of backscatter processing. It is evident from this and several previous studies that accepted protocols to test and compare software processing results is desired. This study offers a first step towards the implementation of previously proposed processing protocols. As software developers start to offer the results from other intermediate processing stages, it can be envisioned that data test benches can be developed to aid end-users in evaluating various processing options currently available in processing tools [207].

Appendix 5A: List of data files used during this study

Sonar Type	Data file
EM 302	0213_20170717_112534_EX1706_MB.all
EM 710	0002_20130214_091514_borda.all
EM 3002	0009_20100113_121654_guillemot.all
EM 2040	0005_20160412_104116_SimonStevin.all
SeaBat 7125	20140729_082527_SMB Owen.s7k

Appendix 5B: Number of columns, and relevant column names in the ASCII files exported from each software

Software	SonarScope	FMGT	CARIS SIPS	MB Process
# columns	31	12	17	11
Time stamp (Unix Time)	Time UTC	Ping Time	Timestamp	Ping Time
Ping #	Ping	Ping Number	Ping	Ping Number
Beam #	Beam	Beam Number	Beam	Beam Number
Beam location (Lat/Long)	Latitude/Longitude	Latitude /Longitude	Longitude /Latitude	Longitude / Latitude
Beam location (E / N)	GeoX / GeoY	Easting / Northing	Easting / Northing	Easting / Northing
Beam depth	BathyRT	Depth	Depth	
Incidence angle	IncidenceAngles	True Angle	IncidentAngle	Incidence Angle
BS as read from data files (BL_0)	ReflecSSc	Backscatter Value	BL_0	Backscatter value
BS processed angular response (BL_3)	SSc_Step1	Corrected Backscatter Value	BL_3	Corr Backscatter Value
Data processed	All except SeaBat 7125	All	All	Only SeaBat 7125

CHAPTER 6

CONCLUSIONS AND PROSPECTIVE FUTURE WORK

Uncertainty quantification is an important but complex part of any measurement. Although quantitative bathymetric and fisheries water column backscatter applications have been developed during the last three decades, seafloor backscatter has been mostly used in a qualitative manner. Still, seafloor backscatter data are now routinely collected in support of a growing range of applications increasing the importance of its quantitative interpretation. With the growing demand for automated and objective interpretation and a desire to combine multiple data sets together, assessment of the quality of quantitative backscatter data has become increasingly important. Uncertainty analysis and quantification is critical to meet this objective, not only to understand the fundamental quality of the data, but also to ensure the repeatability and consistency of the backscatter products. This dissertation attempted to establish a framework for approaching this issue. This dissertation focused on approaches for estimating the uncertainty *of hydrographic multibeam sonar derived seafloor backscatter through the identification and quantified analysis of the key uncertainty parameters and processes.* Where possible the remediation of these uncertainty sources was highlighted.

The four studies constituting this dissertation address various facets of the MBES backscatter uncertainty puzzle and develop and draw from one another. Two of these studies (Chapter 2 and Chapter 5) were conducted under the auspices of the Backscatter Working Group (BSWG). This group was established in 2013 by an international association of researchers loosely organized under an entity called "Geological and Biological Habitat Mapping" (GeoHab) and provided a platform to bring together backscatter stake-holders that consists of backscatter researchers, end-user representatives from diverse applications, and software and hardware manufacturers. The first study (Chapter 2) described the challenges of using MBES backscatter data from various end-

user perspectives and identified accuracy as a major requirement for end-users. The second study (Chapter 3) identified the major sources of uncertainty in MBES backscatter data acquisition and processing. It identified statistical random fluctuations, calibration, seafloor slope, and transmission loss as the major components of uncertainty budget. A key outcome of this study was the realization that along with the uncertainty introduced at data acquisition, the choice of backscatter processing methods used can also lead to a high degree of variability in the final products. The third study (Chapter 4) described the sources and impacts of the seafloor slope while processing the seafloor backscatter data. The uncertainty introduced due to the choices applied during the processing phase should be avoidable or minimal in magnitude. Unfortunately, this is not the case currently for seafloor backscatter processing software packages. Recognizing that commercial and academic software developers play a crucial role and are relied upon by end users for their processing needs, the fourth study (Chapter 5) examined the discrepancies resulting from the processing of the same data set using different processing software and with the cooperation of the software manufacturers, sought to understand the source of these discrepancies. Combined, the four studies provide a synopsis of major challenges being faced by the backscatter end users. Ideally, this dissertation will facilitate the adoption of an improved and widely accepted approach to uncertainty quantification, and increased recognition of the importance of uncertainty in seafloor backscatter studies by all the stakeholders, including sonar manufacturers, processing software developers, and end users.

6.1. <u>User expectations for multibeam echo sounders backscatter strength data</u>

Chapter 2 synthesizes the requirements and challenges faced by end users of seafloor backscatter. This was accomplished through a user survey conducted under the guidance of BSWG. The survey showed that the MBES backscatter users now encompass a large variety of experts in various disciplines. Although this extension of the community is welcome, it has created unique challenges as differences in backscatter acquisition, processing and dissemination among different user groups, reflecting diverse user needs, can hamper re-use of backscatter severely. The GeoHab association sponsored this survey

with the goals to better understand diversity of backscatter users, their unique requirements in terms of accuracy and resolution of the backscatter, and the intended use of backscatter.

The user survey results [39] consisted of 97 responses and included civilian government agencies (41%), academia (24%), private companies (31%) and government defense agencies (4%). The users were found to use backscatter in various applications with the top three being: seafloor type mapping; marine habitat mapping; and collecting backscatter opportunistically while conducting hydrographic surveys. For seafloor type and habitat mapping applications resolution and accuracy were identified as major requirements. About half of the users stated a desire to obtain a 1-m resolution which in reality may not be supported by the spatial resolution of backscatter samples except with the current narrow-beam shallow-water MBES. The use of higher resolution backscatter to detect as small features as possible in seafloor backscatter, should be considered with caution as the physical resolution possible with the MBES depends on the system parameters and environmental conditions that control the backscatter sample footprint (depth, beamwidth, pulse length etc.). As a result the backscatter sample footprint varies across the swath width and / or within a survey area, due to changes in the depth. In addition in order to reduce the stochastic uncertainty, multiple independent backscatter samples need to be averaged together reducing the effective resolution from the backscatter sample footprint. The spatial scale may not be an issue for qualitative products (e.g., a backscatter mosaic) but the spatial scale has to be carefully considered for quantitative products from seafloor backscatter (e.g., backscatter angular response curves). The spatial scale of the backscatter product, therefore, needs to be considered carefully by considering the device and environmental parameters as well as the required accuracy.

The identification of suitable backscatter data is a complex issue and requires technical training that may be missing for many users who are trying to use backscatter for their applications. In the absence of a uniform methodology ensuring a controlled uncertainty in quantified measurements of backscatter, the backscatter data have mainly been used as a discovery tool, where comparison among repeat measurements is not critical. The results of the user survey determined that lack of backscatter quality assessment is a hindrance in standardizing the backscatter acquisition and processing as

well as use for monitoring applications where repeat backscatter need to be compared. For the third major use of backscatter, which is opportunistic acquisition of backscatter while conducting hydrographic surveys, an implementation of methodologies to collect concurrent high-quality backscatter and bathymetric data is needed. Appropriate generation of backscatter that can follow standards will require commitments not only from manufacturers but also from data collectors, software vendors and agencies that support multibeam data acquisition.

Future improvements in data acquisition and processing have to be guided by user needs. Almost all the respondents agreed that utility of backscatter data will continue to develop (98%). As most of the multibeam sonars now manufactured have the capability to collect seafloor and water-column backscatter, it is only natural that the backscatter user group will expand further in the near future. 84.3% of respondents had invested resources to acquire their own backscatter data (either in house or contract) showing an ongoing commitment to develop and improve this data source. Although the Geohab Guidelines and Recommendations [15] were very well received, the community still needs to agree upon a minimum set of appropriate standards. The survey, however, did not explore the various challenges faced by backscatter end users while working with manufacturers and processors towards adopting these standards. Continued involvement of various stakeholders after the completion of the survey encouraged the study reported in Chapter 5 that attempted to develop a collaborative working model between software developers and end users. Continuing work to understand user needs will bring the diverse applications to adopt a minimum multibeam backscatter standard that is useful for the broader backscatter user community.

6.2. <u>A framework to quantify uncertainties of seafloor backscatter from swath mapping echosounders</u>

In order to improve backscatter measurement accuracy, Chapter 3 [161] identified and described the major causes and magnitudes of backscatter uncertainties from MBES systems. Unraveling the complexities of backscatter measurements is a significant task. This chapter offers a framework from which further understanding of the sources and

magnitude of backscatter uncertainties can be derived. The elementary uncertainty analysis proposed here identified the major components of the uncertainty budget as:

- The uncertainty in fluctuating and unreferenced measured echo levels is due to both the intrinsically random character of the echo intensity (causing noise-like fluctuations to be processed statistically) and the incomplete knowledge of the MBES calibration parameters (leading to biases). The statistical uncertainty can be minimized by averaging a number of samples into a mean echo level with the understanding that increasing this number degrades resolution and thus a trade-off has to be made between resolution and uncertainty. In contrast, the uncertainty stemming from inaccurate values of MBES characteristics can reach unpredictable and unacceptable magnitudes if appropriate calibration operations have not been conducted. MBES manufacturers (and to a lesser degree processing software developers) should play a key role in addressing this issue by providing the information needed to better document and reduce this fundamental component of uncertainty, which is difficult to detect in field data and whose accurate evaluation is rarely accessible to users.

- The uncertainty in seafloor incidence angle measurement is mostly affected by seafloor slope uncertainty that is in turn controlled by the resolution and accuracy of bathymetric data used for DTM production (if used at all). Greater attention must be placed on the incorporation of bi-dimensional slope compensation inside the backscatter data processing tools, and on the improvement of local slope determination from the bathymetry data. This uncertainty obviously impacts the computation of the backscatter angular response. Moreover, if not accounted for, slope is often the major cause of error in the insonified area computation. The sounder characteristics are normally sufficiently well known for the impact of their uncertainty to remain acceptable. This again falls under the manufacturer's responsibility. Further involvement from sonar manufacturers is critically needed to estimate and reduce the uncertainty in sonar parameters.

- The transmission loss uncertainty is almost exclusively due to the absorption coefficient estimation, the inaccurate estimation of which can have a significant impact on the backscatter level estimation. However, the combination of the measurement of temperature and salinity values over the full water column with appropriate procedures for compensation can keep the impact of the absorption coefficient within acceptable limits. The potential impact of local and uncontrolled perturbations of the water column properties is not well-understood and deserves further investigation, although the use of ocean atlas data or ocean models can help to mitigate this problem. Unexpected and occasional phenomena such as bubble clouds sweeping the MBES arrays cause specific issues that are impossible to quantify in advance. However, their joint impact on the objective quality of bathymetry data can help detect their presence and justify disregarding corrupted data.

This study was conducted as an initial step in identifying the fundamental causes and estimation of order-of-magnitude levels of the uncertainties associated with the collection of MBES backscatter data. It was shown that it is difficult to predict broadly applicable numerical values, since many of the major uncertainty sources vary on a case-by-case basis. Future efforts need to be directed towards better provision of sonar characteristics from the manufacturers, improvement of MBES calibration methods, and quantification of their reliability and objective uncertainty. A second area of investigation identified was the impact of unexpected perturbations of the seawater column properties (e.g., bubble clouds). Both topics suggest the need for new well-designed field experiments and would benefit greatly from collaborative efforts of the concerned communities.

6.3. <u>Sources and impacts of bottom slope uncertainty on estimation of seafloor backscatter from swath sonars</u>

The study documented in Chapter 4 [185] highlighted the issues related to the computation of seafloor slopes, and their impact on incident angle and insonified area calculations. The magnitude of seafloor slope uncertainty is impacted by the uncertainty in the measurement of seafloor topography, the methods used to model the topography, and

the spatial scale of the bathymetry used to compute seafloor slopes. The impacts of seafloor slope uncertainty on incidence angle and area insonified computation were empirically studied on a small survey conducted using an EM 3002 in the vicinity of Portsmouth, NH. The order of the magnitude of uncertainty expected from each source was identified, showing that the flat-seafloor assumption often used during data acquisition is justified only by the real-time computation constraints and should be avoided in post-processing. Fortunately, software processing tools now enable end-users to correct for the seafloor slope. However, these corrections can still suffer from large uncertainties if the highest possible resolution of the seafloor slope is not used. The spatial scale of the bathymetric data dictates the scale at which backscatter data can be accurately estimated. Consequently, the backscatter values should be averaged at the scale of the bathymetry used for slope estimation. The uncertainty introduced due to the use of coarse spatial scale bathymetry is directly related to the magnitude of un-resolved seafloor slope. Another moderate uncertainty source is the bathymetry uncertainty which is again linked to the magnitude of seafloor slope. On the other hand, seafloor slope algorithms used to compute the seafloor slope values have negligible to small effects (< 1 dB) on slope estimation.

6.4. Results from the first phase of the Backscatter Software Inter-comparison Project

One of the most prevalent issues in seafloor backscatter uncertainty estimation is the absence of standardized methods to compensate for the various corrections. As evident from the user survey (Chapter 2), the majority of the users rely on the third-party software for their processing needs. Obviously, the validity and accuracy of the processing methods cannot be established without active participation from the software developers. The consistency and reliability of processing software results have been questioned in recent studies where the same data set processed with different software tools showed significantly different end results [39]. The study documented in Chapter 5 [208], sought to better understand why these differences exist and worked with the software providers to implement processing protocols to allow the comparison of results from intermediate processing stages without compromising the proprietary nature of the commercial software. A methodology proposed by Schimel et al. [41] was adapted to breakdown the

145

backscatter processing pipeline into intermediate processing stages. Instead of a qualitative comparison between final sonar mosaics, cooperating software developers were invited to provide results of the intermediate processing stages. The two stages that were assessed during this study included BL_0: data as read from the raw data files using snippets (also referred to as full time series) within beams to produce a representative value per beam, and BL_3: data after radiometric corrections but before the removal of angular dependence for mosaicking. The software developers implemented the required changes in their processing methodologies and provided data in "Beam – Ping configuration" with BL_0 and BL_3 reported for each beam along with incidence angle. The breakdown of processing sequence into BL_0 and BL_3 allowed for the inter-comparison of their results after only few discrete corrections and provided a framework for identifying potential causes of the differences between processing solutions. Both BL_0 and BL_3 showed large differences between the various software tools as high as > 10 dB. The differences in BL_0 indicate that software developers have adopted different approaches to reading the raw data. Although, without complete knowledge of the algorithms used by the software developers, it is not possible to describe what exact differences exist between reading of raw data for BL_0, having identified this stage as different between software packages suggests a plausible cause of differences observed between backscatter mosaics in earlier studies and a path to resolution of these differences. This study has shown the applicability and usefulness of the availability of intermediate processing stages for inter-comparison of proprietary software without requiring the software vendors to disclose their proprietary algorithms.

Although the scope of this study focused on developing a method to understand the differences between the software packages, the study also supports the arguments for why it is critical for various sonar manufacturers, commercial and academic software developers, and end users from diverse domains to work together to develop methods that can improve the consistency of backscatter processing. It is evident from this study that agreed upon protocols to test and compare software processing results are desired. This study offers a first step towards implementation of previously proposed processing protocols [41,117]. As software developers provide the results from other intermediate processing stages, it can be envisioned that data test benches can be developed to aid end

146

users in assessing the processing options currently available in processing tools (e.g., [207]). This may serve as a model for collaboration between sonar manufactures, processing solution developers, and end users to work together with the aim of improving the standardization of processing and making the backscatter processing workflow more transparent.

6.5. Recommendations

The science of acoustic seabed classification is developing rapidly [1]. It is expected that seafloor data acquisition and processing techniques will continue to evolve, and the standardization of instruments and methods remains a high priority goal of the seafloor backscatter community. Fisheries acoustics have been developing standardized methods to measure and map fish and plankton in the water column during the last two decades [209,210]. Similar efforts are recommended and are already underway for seafloor backscatter standardization [15].

The inversion of the seafloor backscatter to derive seafloor classes is itself complex and without confidence in the results of the original seafloor backscatter measurement, the problem becomes even more perplexing. The well-known inversion model (APL model) have uncertainties up to 10 dB for rock and gravel bottoms; and approximately 3 dB for well characterized sand and silt bottoms for grazing angles greater than 5° [70]. With quantified estimates of uncertainty in the measured backscatter, the probabilistic estimates of seafloor characteristics become a possibility. For example, one can envision the inverted results of the backscatter to be stated as: 'with 70% confidence we can predict the seafloor to be sand, mud, rock, etc.'

The sources of uncertainty in seafloor backscatter encompass a large spectrum, from those that are well quantified, to those that are poorly quantified. In uncertainty analyses studies, it is common to assume that systematic uncertainties are negligible. However, several challenges remain in identifying and addressing the systematic uncertainty in seafloor backscatter measurements. Theoretically, the systematic uncertainty of a measurement can be quantified if concomitant high accuracy test methods are available, or if test standards exist. The complete characterization of systematic uncertainty of backscatter measurements still needs further work. Methods to empirically infer the

147

effect of the sonar hardware and processing techniques on final backscatter results need improvement. For example, poor selection of sonar settings (e.g., user induced errors) or poor implementation of corrections (e.g., manufacturer induced 'methodological' errors during acquisition or processing), are hard to detect and correct during the processing stage by the end user. Multibeam sonars can also have several device specific sources of error, e.g., heating of the boards, acoustic covers, defective installation etc. These systematic uncertainties are thought to be the most dominant cause of uncertainty in seafloor backscatter measurements and alarmingly cannot be generalized as they vary on a case-by-case basis. Several of these systematic uncertainty sources were identified in Chapter 3 and approaches were devised to decrease the impact of two of the most important uncertainty sources: seafloor slope in Chapter 4 and processing uncertainty in Chapter 5.

Several recommendations are identified to improve upon the uncertainty estimates of the seafloor backscatter developed here:

1. Sonar manufacturers are encouraged to provide detailed multibeam characteristics (e.g., source level, pulse length, beam patterns, etc.) accompanied with their accurate definitions and uncertainty estimates.

2. Better quantification of environment and seafloor related uncertainty sources is desired. Two of the uncertainty sources that need critical improvement include the uncertainty estimation of the seafloor slope, and the transmission loss. Both of these uncertainty sources require collection of additional data (i.e., high-resolution bathymetry and water column oceanographic parameters).

3. Backscatter metadata protocols should be developed and implemented. The backscatter end products (e.g., mosaics and angular response curves) can be obtained through a variety of methods. Information about the origin of the backscatter samples, range of incidence angles, number of samples and the range of azimuth of survey lines, and corrections applied during processing should be included in the metadata to accompany backscatter results. This will convey the context in which the backscatter data were collected and processed to produce the reported results.

4. Ideally, backscatter acquisition and processing protocols should become more standardized. In particular, it would be beneficial to develop standards that convey information to the end user concerning the various acquisition and processing steps that were used.

5. In the absence of implementation details about the algorithms required for various corrections of backscatter data (e.g., area, transmission loss, beam patterns etc.), this dissertation proposes a comparison methodology to enable comparison of results at various stages of backscatter processing. Currently, not all software tools provide users the ability to extract results of all intermediate processing steps. Collaborative efforts with software manufacturers reported in Chapter 5 should continue in order to provide more transparency into the processing pipeline at intermediate processing steps. This approach will be attractive to software vendors as they will not have to divulge the details of their algorithms, but still provide end users a way to identify the reasons for potential differences in the output of various processing methods.

6. This dissertation did not provide details of the uncertainty propagation to backscatter end-products. Uncertainty propagation is a well-developed field and with improvements in the understanding of the uncertainty sources, the next logical step would be to develop tools for complete seafloor backscatter uncertainty propagation.

7. The major goal of this study is the building of a framework under which seafloor backscatter uncertainty can be assessed and quantified. The empirical studies described here were limited to a few representative sensors and environmental conditions. However, the overall treatment and approach to uncertainty estimation are applicable to a broader range of multibeam sonars and environmental conditions. To calculate the total uncertainty of the estimate, the individual uncertainty sources must first be determined. A comprehensive list of these sources has been built through this study. However, as the new MBES and processing tools are introduced, uncertainty quantification will need to be re-visited.

REFERENCES

1. ICES Acoustic seabed classification of marine physical and biological landscapes. ICES Cooperative Research Report No. 286. 183 pp. 2007.
2. Kenny, A.J.; Cato, I.; Desprez, M.; Fader, G.; Schüttenhelm, R.T.E.; Side, J. An overview of seabed-mapping technologies in the context of marine habitat classification. *ICES J. Mar. Sci.* **2003**, *60*, 411–418.
3. Anderson, J.T.; Van Holliday, D.; Kloser, R.; Reid, D.G.; Simard, Y. Acoustic seabed classification: current practice and future directions. *ICES J. Mar. Sci.* **2008**, *65*, 1004–1011.
4. Hunkins, K.L.; Ewing, M.; Heezen, B.C.; Menzies, R.J. Biological and Geological observations on the first photographs of the Arctic Ocean Deep sea floor. *Limnol. Oceanogr.* **1960**, *5*, 154–161.
5. Pickrill, R.A.; Kostylev, V.E. Habitat Mapping and National Seafloor Mapping Strategies in Canada. *Geol Assoc Can. Spec Pap* **2007**, *47*, 449–462.
6. Waddington, T.R.; Hart, K. *Tools and Techniques for the Acquisition of Estuarine Benthic Habitat Data*; Prepared for NOAA Coastal Services Center; Charleston, SC, 2003;
7. Fornshell, J.A.; Tesei, A. The Development of SONAR as a Tool in Marine Biological Research in the Twentieth Century. *Int. J. Oceanogr.* **2013**.
8. Farr, H.K. Multibeam bathymetric sonar: Sea beam and hydro chart. *Mar. Geod.* **1980**, *4*, 77–93.
9. de Moustier, C. Beyond bathymetry: Mapping acoustic backscattering from the deep seafloor with Sea Beam. *J. Acoust. Soc. Am.* **1986**, *79*, 316–331.
10. Tyce, R.C. Deep Seafloor Mapping Systems - A Review. *Mar. Technol. Soc. J.* **1986**, *20*, 4–16.
11. Mayer, L.A. Frontiers in Seafloor Mapping and Visualization. *Mar. Geophys. Res.* **2006**, *27*, 7–17.
12. Calder, B.R.; Mayer, L.A. Automatic processing of high-rate, high-density multibeam echosounder data. *Geochem. Geophys. Geosystems* **2003**, *4*.
13. Hughes Clarke, J.E.; Mayer, L.A.; Wells, D.E. Shallow-water imaging multibeam sonars: A new tool for investigating seafloor processes in the coastal zone and on the continental shelf. *Mar. Geophys. Res.* **1996**, *18*, 607–629.
14. Brown, C.J.; Blondel, P. Developments in the application of multibeam sonar backscatter for seafloor habitat mapping. *Appl. Acoust.* **2009**, *70*, 1242–1247.
15. Lurton, X.; Lamarche, G.; Brown, C.; Lucieer, V.; Rice, G.; Schimel, A.C.G.; Weber, T.C. Backscatter measurements by seafloor-mapping sonars. Guidelines and recommendations. Geohab report. 2015.
16. Cochrane, N.A.; Li, Y.; Melvin, G.D. Quantification of a multibeam sonar for fisheries assessment applications. *J. Acoust. Soc. Am.* **2003**, *114*, 745–758.

17. Brothers, L.L.; Dover, C.L.V.; German, C.R.; Kaiser, C.L.; Yoerger, D.R.; Ruppel, C.D.; Lobecker, E.; Skarke, A.D.; Wagner, J.K.S. Evidence for extensive methane venting on the southeastern U.S. Atlantic margin. *Geology* **2013**, *41*, 807–810.

18. Weber, T.C.; Mayer, L.; Jerram, K.; Beaudoin, J.; Rzhanov, Y.; Lovalvo, D. Acoustic estimates of methane gas flux from the seabed in a 6000 km ^{2} region in the Northern Gulf of Mexico. *Geochem. Geophys. Geosystems* **2014**, *15*, 1911–1925.

19. Lurton, X. *An Introduction to Underwater Acoustics: Principles and Applications*; Geophysical Sciences; 2nd ed.; Springer-Verlag: Berlin Heidelberg, 2010; ISBN 978-3-540-78480-7.

20. Malzone, C.; Lockhart, D.; Meurling, T.; Baldwin, M. The progression and impact of the latest generation of multibeam acoustics upon multidisciplinary hydrographic-based applications. *Underw. Technol.* **2008**, *27*, 151–160.

21. Goff, J.A.; Orange, D.L.; Mayer, L.A.; Hughes Clarke, J.E. Detailed investigation of continental shelf morphology using a high-resolution swath sonar survey: the Eel margin, northern California. *Mar. Geol.* **1999**, *154*, 255–269.

22. Wildish, D.J.; Hughes Clarke, J.E.; Pohle, G.W.; Hargrave, B.T.; Mayer, L.M. Acoustic detection of organic enrichment in sediments at a salmon farm is confirmed by independent groundtruthing methods. *Mar. Ecol. Prog. Ser.* **2004**, *267*, 99–105.

23. Simons, D.G.; Snellen, M. A Bayesian approach to seafloor classification using multi-beam echo-sounder backscatter data. *Appl. Acoust.* **2009**, *70*, 1258–1268.

24. Brown, C.J.; Smith, S.J.; Lawton, P.; Anderson, J.T. Benthic habitat mapping: A review of progress towards improved understanding of the spatial ecology of the seafloor using acoustic techniques. *Estuar. Coast. Shelf Sci.* **2011**, *92*, 502–520.

25. Urick, R.J. *Principles of Underwater Sound 3rd Edition*; Originated 1983 edition.; Peninsula Pub: Los Altos, Calif, 1983; ISBN 978-0-932146-62-5.

26. Jackson, D.R.; Richardson, M.D. *High-Frequency Seafloor Acoustics*; Springer Science & Business Media: New York, 2007; ISBN 978-0-387-34154-5.

27. Hamilton, E.L. Prediction of Deep-Sea Sediment Properties: State-of-the-Art. In *Deep-Sea Sediments: Physical and Mechanical Properties*; Inderbitzen, A.L., Ed.; Marine Science; Springer US: Boston, MA, 1974; pp. 1–43 ISBN 978-1-4684-2754-7.

28. Hamilton, E.L. Geoacoustic Models of the Sea Floor. In *Physics of Sound in Marine Sediments*; Hampton, L., Ed.; Marine Science; Springer US: Boston, MA, 1974; pp. 181–221 ISBN 978-1-4684-0838-6.

29. Bachman, R.T. Acoustic and physical property relationships in marine sediment. *J. Acoust. Soc. Am.* **1985**, *78*, 616–621.

30. Ferrini, V.L.; Flood, R.D. The effects of fine-scale surface roughness and grain size on 300 kHz multibeam backscatter intensity in sandy marine sedimentary environments. *Mar. Geol.* **2006**, *228*, 153–172.

31. Fonseca, L.; Mayer, L. Remote estimation of surficial seafloor properties through the application Angular Range Analysis to multibeam sonar data. *Mar. Geophys. Res.* **2007**, *28*, 119–126.

32. Jackson, D.R.; Winebrenner, D.P.; Ishimaru, A. Application of the composite roughness model to high-frequency bottom backscattering. *J. Acoust. Soc. Am.* **1986**, *79*, 1410–1422.

33. Hughes Clarke, J. Toward remote seafloor classification using the angular response of acoustic backscattering: a case study from multiple overlapping GLORIA data. *IEEE J. Ocean. Eng.* **1994**, *19*, 112–127.
34. Orpin, A.R.; Kostylev, V.E. Towards a statistically valid method of textural sea floor characterization of benthic habitats. *Mar. Geol.* **2006**, *225*, 209–222.
35. Fonseca, L.; Brown, C.; Calder, B.; Mayer, L.; Rzhanov, Y. Angular range analysis of acoustic themes from Stanton Banks Ireland: A link between visual interpretation and multibeam echosounder angular signatures. *Appl. Acoust.* **2009**, *70*, 1298–1304.
36. Turgut, A. Inversion of bottom/subbottom statistical parameters from acoustic backscatter data. *J. Acoust. Soc. Am.* **1997**, *102*, 833–852.
37. Foody, G.M.; Atkinson, P.M. *Uncertainty in Remote Sensing and GIS*; John Wiley & Sons, 2003; ISBN 978-0-470-85924-7.
38. Huang, Z.; Siwabessy, J.; Nichol, S.; Anderson, T.; Brooke, B. Predictive mapping of seabed cover types using angular response curves of multibeam backscatter data: Testing different feature analysis approaches. *Cont. Shelf Res.* **2013**, *61–62*, 12–22.
39. Lucieer, V.; Roche, M.; Degrendele, K.; Malik, M.; Dolan, M.; Lamarche, G. User expectations for multibeam echo sounders backscatter strength data-looking back into the future. *Mar. Geophys. Res.* **2018**, *39*, 23–40.
40. Hughes Clarke, J.E.; Iwanowska, K.K.; Parrott, R.; Duffy, G.; Lamplugh, M.; Griffin, J. Inter-calibrating multi-source, multi-platform backscatter data sets to assist in compiling regional sediment type maps : Bay of Fundy. **2008**, 23.
41. Schimel, A.C.G.; Beaudoin, J.; Parnum, I.M.; Le Bas, T.; Schmidt, V.; Keith, G.; Ierodiaconou, D. Multibeam sonar backscatter data processing. *Mar. Geophys. Res.* **2018**, *39*, 121–137.
42. Hughes Clarke, J.E. Optimal use of multibeam technology in the study of shelf morphodynamics. In *Sediments, Morphology and Sedimentary Processes on Continental Shelves: Advances in Technologies, Research and Applications*; Li, M.Z., Sherwood, C.R., Hill, P.R., Eds.; John Wiley & Sons, 2012 ISBN 978-1-4443-5082-1.
43. Lanzoni, J.C.; Weber, T.C. High-resolution calibration of a multibeam echo sounder. In Proceedings of the OCEANS 2010 MTS/IEEE SEATTLE; 2010; pp. 1–7.
44. Hiroji, A.D. Extracting Sonar Relative Beam Patterns for Multi-Sector Mulitbeam Sonar. PhD Dissertation, University of New Brunswick, Department of Geodesy and Geomatics Engineering.: Fredericton, Canda, 2016.
45. Lanzoni, J.C.; Weber, T.C. Calibration of multibeam echo sounders: a comparison between two methodologies. In Proceedings of the Meetings on Acoustics; 2012; Vol. 17.
46. Beaudoin, J.; Clarke, J.E.; Ameele, E.V. den; Gardner, J. Geometric and Radiometric Correction of Multibeam Backscatter Derived from Reson 8101 Systems. *Can. Hydrogr. Conf.* **2002**.
47. de Moustier, C. Inference of manganese nodule coverage from Sea Beam acoustic backscattering data. *Geophysics* **1985**, *50*, 989.
48. Davies, J.; Baxter, J.; Bradley, M. *Marine monitoring handbook, March 2001*; Joint nature conservation committee: S.l., 2001;

49. Lamarche, G.; Lurton, X.; Verdier, A.-L.; Augustin, J.-M. Quantitative characterisation of seafloor substrate and bedforms using advanced processing of multibeam backscatter—Application to Cook Strait, New Zealand. *Cont. Shelf Res.* **2011**, *31*, S93–S109.

50. Lucieer, V.; Lamarche, G. Unsupervised fuzzy classification and object-based image analysis of multibeam data to map deep water substrates, Cook Strait, New Zealand. *Cont. Shelf Res.* **2011**, *31*, 1236–1247.

51. Che Hasan, R.; Ierodiaconou, D.; Laurenson, L. Combining angular response classification and backscatter imagery segmentation for benthic biological habitat mapping. *Estuar. Coast. Shelf Sci.* **2012**, *97*, 1–9.

52. Hill, N.A.; Lucieer, V.; Barrett, N.S.; Anderson, T.J.; Williams, S.B. Filling the gaps: Predicting the distribution of temperate reef biota using high resolution biological and acoustic data. *Estuar. Coast. Shelf Sci.* **2014**, *147*, 137–147.

53. Faure, K.; Greinert, J.; Pecher, I.A.; Graham, I.J.; Massoth, G.J.; De Ronde, C.E.J.; Wright, I.C.; Baker, E.T.; Olson, E.J. Methane seepage and its relation to slumping and gas hydrate at the Hikurangi margin, New Zealand. *N. Z. J. Geol. Geophys.* **2006**, *49*, 503–516.

54. Bertels, L.; Houthuys, R.; Deronde, B.; Janssens, R.; Verfaillie, E.; Van Lancker, V. Integration of Optical and Acoustic Remote Sensing Data over the Backshore–Foreshore–Nearshore Continuum: A Case Study in Ostend (Belgium). *J. Coast. Res.* **2012**, 1426–1436.

55. Colenutt, A.; Mason, T.; Cocuccio, A.; Kinnear, R.; Parker, D. Nearshore substrate and marine habitat mapping to inform marine policy and coastal management. *J. Coast. Res.* **2013**, *65*, 1509–1514.

56. Lucieer, V.; Huang, Z.; Siwabessy, J. Analyzing Uncertainty in Multibeam Bathymetric Data and the Impact on Derived Seafloor Attributes. *Mar. Geod.* **2016**, *39*, 32–52.

57. Müller, R.D.; Qin, X.; Sandwell, D.T.; Dutkiewicz, A.; Williams, S.E.; Flament, N.; Maus, S.; Seton, M. The GPlates Portal: Cloud-Based Interactive 3D Visualization of Global Geophysical and Geological Data in a Web Browser. *PLOS ONE* **2016**, *11*, e0150883.

58. Diez, S.; Sorribas, J. Bedform Mapping: Multibeam Data Processing, Metadata and Spatial Data Services. *Atlas Bedforms West. Mediterr.* **2017**, 3.

59. Lecours, V. Quantifying the effects of variable selection, spatial scale and spatial data quality in marine benthic habitat mapping - Memorial University Research Repository. PhD Dissertation, Memorial University of Newfoundland, 2016.

60. Lechner, A.M.; Langford, W.T.; Jones, S.D.; Bekessy, S.A.; Gordon, A. Investigating species–environment relationships at multiple scales: Differentiating between intrinsic scale and the modifiable areal unit problem. *Ecol. Complex.* **2012**, *11*, 91–102.

61. Goff, J.A.; Olson, H.C.; Duncan, C.S. Correlation of side-scan backscatter intensity with grain-size distribution of shelf sediments, New Jersey margin. *Geo-Mar. Lett.* **2000**, *20*, 43–49.

62. Collier, J.S.; Brown, C.J. Correlation of sidescan backscatter with grain size distribution of surficial seabed sediments. *Mar. Geol.* **2005**, *214*, 431–449.

63. Diesing, M.; Green, S.L.; Stephens, D.; Lark, R.M.; Stewart, H.A.; Dove, D. Mapping seabed sediments: Comparison of manual, geostatistical, object-based image analysis and machine learning approaches. *Cont. Shelf Res.* **2014**, *84*, 107–119.

64. Schimel, A.; Beaudoin, J.; Gaillot, A.; Keith, G.; Le Bas, T.; Parnum, I.M.; Schmidt, V. Chapter 7: processing backscatter data: from datagrams to angular responses and mosaics. In *Backscatter measurements by seafloor mapping sonars. Guidelines and Recommendations,* .; pp. 133–164.

65. Carvalho, R. de C.; Junior, A.M. de O.; Clarke, J.E.H. Proper environmental reduction for attenuation in multi-sector sonars. In Proceedings of the 2013 IEEE/OES Acoustics in Underwater Geosciences Symposium; 2013; pp. 1–6.

66. Hughes Clarke, J.E. Optimal Use of Multibeam Technology in the Study of Shelf Morphodynamics. In *Sediments, Morphology and Sedimentary Processes on Continental Shelves*; John Wiley & Sons, Ltd, 2013; pp. 1–28 ISBN 978-1-118-31117-2.

67. University of Bath; Roche, M.; Baeye, M.; Bisschop, J.D.; Degrendele, K.; Mol, L.D.; Papili, S.; Lopera, O.; Lancker, V.V. Backscatter stability and influence of water column conditions: estimation by multibeam echosounder and repeated oceanographic measurements, Belgian part of the North Sea. In Proceedings of the Seabed and Sediment Acoustics: Measurements and Modelling; Institute of Acoustics: Bath, 2015; pp. 74–84.

68. Rice, G.; Cooper, R.; Degrendele, K.; Gutierrez, F.; Le Bouffant, N.; Roche, M. Chapter 5—Acquisition: best practice guide. In *Backscatter measurements by seafloor mapping sonars. Guidelines and Recommendations,* .; p. pp 106–132.

69. Gueriot, D.; Chedru, J.; Daniel, S.; Maillard, E. The patch test: a comprehensive calibration tool for multibeam echosounders. In Proceedings of the OCEANS 2000 MTS/IEEE Conference and Exhibition. Conference Proceedings (Cat. No.00CH37158); 2000; Vol. 3, pp. 1655–1661 vol.3.

70. APL-UW *APL-UW High-Frequency Ocean Environmental Acoustic Models Handbook, Ch. IV: Bottom*; 1994;

71. Malik, M.; Mayer, L.; Weber, T.; Calder, B.; Huff, L. Challenges of defining uncertainty in multibeam sonar derived seafloor backscatter.; Corfu, Greece, 2013.

72. Fonseca, L.; Calder, B. Geocoder: An Efficient Backscatter Map Constructor. In Proceedings of the U.S. Hydrographic Conference (US Hydro); San Diego, CA, USA, 2005.

73. Fonseca, L.; Brown, C.; Calder, B.; Mayer, L.; Rzhanov, Y. Angular range analysis of acoustic themes from Stanton Banks Ireland: A link between visual interpretation and multibeam echosounder angular signatures. *Appl. Acoust.* **2009**, *70*, 1298–1304.

74. Parnum, I. Benthic habitat mapping using multibeam sonar systems. PhD Dissertation, Curtin University, 2007.

75. Hamilton, L. j.; Parnum, I. Acoustic seabed segmentation from direct statistical clustering of entire multibeam sonar backscatter curves. *Cont. Shelf Res.* **2011**, *31*, 138–148.

76. Hughes Clarke, J.E.; Danforth, B.W.; Valentine, P. Areal seabed classification using backscatter angular response at 95kHz. *High Freq. Seafloor Acoust. SACLANTCEN Conf. Proc. CP-45 1997 Pp 243-250* **1997**.

77. Chenadec, G.L.; Boucher, J.; Lurton, X. Angular Dependence of K-Distributed Sonar Data. *IEEE Trans. Geosci. Remote Sens.* **2007**, *45*, 1224–1235.

78. Hellequin, L.; Boucher, J.-; Lurton, X. Processing of high-frequency multibeam echo sounder data for seafloor characterization. *IEEE J. Ocean. Eng.* **2003**, *28*, 78–89.

79. Dartnell, P.; Gardner, J.V. Predicting Seafloor Facies from Multibeam Bathymetry and Backscatter Data. *Photogramm. Eng. Remote Sens.* **2004**, *9*, 1081–1091.

80. Pace, N.G.; Gao, H. Swath seabed classification. *IEEE J. Ocean. Eng.* **1988**, *13*, 83–90.

81. Tamsett, D. Sea-bed characterisation and classification from the power spectra of side-scan sonar data. *Mar. Geophys. Res.* **1993**, *15*, 43–64.

82. Lurton, X.; Dugelay, S.; Augustin, J.M. Analysis of multibeam echo-sounder signals from the deep seafloor. In Proceedings of the Proceedings of OCEANS'94; 1994; Vol. 3, p. III/213-III/218 vol.3.

83. Pace, N.G.; Dyer, C.M. Machine Classification of Sedimentary Sea Bottoms. *IEEE Trans. Geosci. Electron.* **1979**, *17*, 52–56.

84. Reed, T.B.; Hussong, D. Digital image processing techniques for enhancement and classification of SeaMARC II side scan sonar imagery. *J. Geophys. Res. Solid Earth* **1989**, *94*, 7469–7490.

85. Imen, K.; Fablet, R.; Boucher, J.-; Augustin, J.- Statistical discrimination of seabed textures in sonar images using co-occurrence statistics. In Proceedings of the Europe Oceans 2005; 2005; Vol. 1, pp. 605-610 Vol. 1.

86. Lucieer, V.; Hill, N.A.; Barrett, N.S.; Nichol, S. Do marine substrates 'look' and 'sound' the same? Supervised classification of multibeam acoustic data using autonomous underwater vehicle images. *Estuar. Coast. Shelf Sci.* **2013**, *117*, 94–106.

87. Linnett, L.M.; Clarke, S.J.; Graham, C.; Langhorne, D.N. Remote sensing of the sea-bed using fractal techniques. *Electron. Commun. Eng. J.* **1991**, *3*, 195–203.

88. Carmichael, D.R.; Linnett, L.M.; Clarke, S.J.; Calder, B.R. Seabed classification through multifractal analysis of sidescan sonar imagery. In Proceedings of the Sonar and Navigation IEE Proceedings - Radar; 1996; Vol. 143, pp. 140-.

89. Stanton, T.K. Volume scattering: Echo peak PDF. *J. Acoust. Soc. Am.* **1985**, *77*, 1358–1366.

90. Alexandrou, D.; Moustier, C. de Adaptive noise canceling applied to Sea Beam sidelobe interference rejection. *IEEE J. Ocean. Eng.* **1988**, *13*, 70–76.

91. Foster, S.D.; Hosack, G.R.; Hill, N.A.; Barrett, N.S.; Lucieer, V.L. Choosing between strategies for designing surveys: autonomous underwater vehicles. *Methods Ecol. Evol.* **2014**, *5*, 287–297.

92. Hamid, U.; Qamar, R.A.; Waqas, K. Performance comparison of time-domain and frequency-domain beamforming techniques for sensor array processing. In Proceedings of the Proceedings of 2014 11th International Bhurban Conference on Applied Sciences Technology (IBCAST) Islamabad, Pakistan, 14th - 18th January, 2014; 2014; pp. 379–385.

93. Lucieer, V.L. The application of automated segmentation methods and fragmentation statistics to characterise rocky reef habitat. *J. Spat. Sci.* **2007**, *52*, 81–91.

94. Diesing, M.; Mitchell, P.; Stephens, D. Image-based seabed classification: what can we learn from terrestrial remote sensing?; 2016.

95. Lucieer, V.L.; Siwabessy, J.W.; Huang, Z.; Hayes, K. Multi-scale image segmentation of multibeam backscatter data for benthic monitoring. In Proceedings of the GeoHab (Maine Geological and Biological Habitat Mapping); 2014; p. 62.

96. Lucieer, V.L. Object-oriented classification of sidescan sonar data for mapping benthic marine habitats. *Int. J. Remote Sens.* **2008**, *29*, 905–921.

97. Kraft, B.J.; Fonseca, L.; Mayer, L.A.; McGillicuddy, G.; Ressler, J.; Henderson, J.; Simpkin, P.G. In situ measurement of sediment acoustic properties and relationship to multibeam backscatter. *J. Acoust. Soc. Am.* **2004**, *115*, 2401–2402.

98. Anderson, J.T.; International Council for the Exploration of the Sea *Acoustic seabed classification of marine physical and biological landscapes*; Copenhagen, Denmark : International Council for the Exploration of the Sea, 2007;

99. Hare, R.; Godin, A.; Mayer, L.A. Accuracy estimation of Canadian swath (multibeam) and sweep (multitransducer) sounding systems. Canadian Hydrographic Service Internal Report 1995.

100. Hare, R. Error budget analysis for US Naval Oceanographic Office (NAVOCEANO) hydrographic survey systems. 2001.

101. Calder, B.R.; Mayer, L.A. Automatic processing of high-rate, high-density multibeam echosounder data. *Geochem. Geophys. Geosystems* **2003**, *4*, 1048.

102. Lurton, X.; Augustin, J. A Measurement Quality Factor for Swath Bathymetry Sounders. *IEEE J. Ocean. Eng.* **2010**, *35*, 852–862.

103. Hasan, R.C.; Ierodiaconou, D.; Laurenson, L.; Schimel, A. Integrating Multibeam Backscatter Angular Response, Mosaic and Bathymetry Data for Benthic Habitat Mapping. *PLOS ONE* **2014**, *9*, e97339.

104. Brown, C.J.; Smith, S.J.; Lawton, P.; Anderson, J.T. Benthic habitat mapping: A review of progress towards improved understanding of the spatial ecology of the seafloor using acoustic techniques. *Estuar. Coast. Shelf Sci.* **2011**, *92*, 502–520.

105. Lacharité, M.; Brown, C.J.; Gazzola, V. Multisource multibeam backscatter data: developing a strategy for the production of benthic habitat maps using semi-automated seafloor classification methods. *Mar. Geophys. Res.* **2018**, *39*, 307–322.

106. Rzhanov, Y.; Fonseca, L.; Mayer, L. Construction of seafloor thematic maps from multibeam acoustic backscatter angular response data. *Comput. Geosci.* **2012**, *41*, 181–187.

107. Alevizos, E.; Snellen, M.; Simons, D.; Siemes, K.; Greinert, J. Multi-angle backscatter classification and sub-bottom profiling for improved seafloor characterization. *Mar. Geophys. Res.* **2018**, *39*, 289–306.

108. Fonseca, L.; Calder, B.; Wetzler, M. Experiments for Multibeam Backscatter Adjustments on the NOAA Ship Fairweather. In Proceedings of the OCEANS 2006; 2006; pp. 1–4.

109. Gavrilov, A.N.; Parnum, I.M. Fluctuations of Seafloor Backscatter Data From Multibeam Sonar Systems. *IEEE J. Ocean. Eng.* **2010**, *35*, 209–219.

110. Greenaway, S.F.; Weber, T.C. Test methodology for evaluation of linearity of multibeam echosounder backscatter performance. In Proceedings of the OCEANS 2010 MTS/IEEE SEATTLE; 2010; pp. 1–7.

156

111. Brown, C.; Schmidt, V.; Malik, M.; Bouffant, N. Chapter 4—Backscatter measurement by bathymetric echo sounders. In *Backscatter measurements by seafloor mapping sonars. Guidelines and Recommendations, .*

112. de Moustier, C.; Alexandrou, D. Angular dependence of 12-kHz seafloor acoustic backscatter. *J. Acoust. Soc. Am.* **1991**, *90*, 522.

113. IHO International Hydrographic Office Standards for Hydrographic Surveys 5th Edition, Special Publication No. 44 2008.

114. Dyer, I. Statistics of Sound Propagation in the Ocean. *J. Acoust. Soc. Am.* **1970**, *48*, 337–345.

115. Stanic, S.; Kennedy, E. Fluctuations of high-frequency shallow-water seafloor reverberation. *J. Acoust. Soc. Am.* **1992**, *91*, 1967–1973.

116. Peritsky, M.M. Statistical estimation of mean signal strength in a Rayleigh-fading environment. *IEEE Trans. Veh. Technol.* **1973**, *22*, 123–129.

117. Lamarche, G.; Lurton, X. Recommendations for improved and coherent acquisition and processing of backscatter data from seafloor-mapping sonars. *Mar. Geophys. Res.* **2018**, *39*, 5–22.

118. Hammerstad, E. EM Technical Note: Backscattering and Seabed Image Reflectivity 2000.

119. Lanzoni, J.C.; Weber, T.C. A method for field calibration of a multibeam echo sounder. In Proceedings of the OCEANS'11 MTS/IEEE KONA; 2011; pp. 1–7.

120. Rice, G.; Greenaway, S.; Weber, T.; Beaudoin, J.; Beaudoin, J.; Beaudoin, J. Methods for Collecting and Using Backscatter Field Calibration Information for the Reson 7000 Series Multibeam.; Niagara Falls, Canada, 2012.

121. Welton, B. A Field Method for Backscatter Calibration Applied to NOAA's Reson 7125, University of New Hampshire: Durham, NH, 2014.

122. Hellequin, L.; Boucher, J.-; Lurton, X. Processing of high-frequency multibeam echo sounder data for seafloor characterization. *IEEE J. Ocean. Eng.* **2003**, *28*, 78–89.

123. Augustin, J.-; Lurton, X. Image amplitude calibration and processing for seafloor mapping sonars. In Proceedings of the Europe Oceans 2005; 2005; Vol. 1, pp. 698-701 Vol. 1.

124. Llewellyn, K.C. Corrections for Beam Pattern Residuals in Backscatter Imagery from the Kongsberg-Simrad EM300 Multibeam Echosounder. MSc Thesis, University of New Brunswick, Department of Geodesy and Geomatics Engineering: Fredericton, Canda, 2006.

125. Chu, D.; Hufnagle, L.C. Time varying gain (TVG) measurements of a multibeam echo sounder for applications to quantitative acoustics. In Proceedings of the OCEANS 2006; 2006; pp. 1–5.

126. Parnum, I.M.; Gavrilov, A.N. High-frequency multibeam echo-sounder measurements of seafloor backscatter in shallow water: Part 1–Data acquisition and processing. *Underw. Technol.* **2011**, *30*, 3–12.

127. Teng, Y. Sector-specific Beam Pattern Compensation for Multi-sector and Multi-swath Multibeam Sonars. Master, University of New Brunswick, Department of Geodesy and Geomatics Engineering: Fredericton, Canda, 2011.

128. Lehaitre, M.; Delauney, L.; Compère, C. Biofouling and underwater measurements. In *Babin M, Roesler CS, Cullen JJ (Eds) Real-time Coastal Observing Systems for*

Marine Ecosystem Dynamics and Harmful Algal Blooms: theory, instrumentation and modelling - UNESCO Digital Library; pp. 463–493.

129. Rice, G.; Malik, M. *NOAA SHIP NANCY FOSTER EM710 Acceptance Testing With Hydrographic Systems and Technology Programs Multibeam Sonar Acceptance Procedures*; 2015;

130. Hauser, O.; Downs, R.; Rice, G.; Greenaway, S.; Annis, M.; Eisenberg, J.; Malik, M. NOAA's Multibeam Sonar Test Procedure Manual: Formalizing and documenting a procedure to ensure that a new multibeam sonar is properly installed, integrated, and capable of meeting hydrographic standards. In Proceedings of the US Hydrographic Conference; Washington DC, USA, 2015.

131. Foote, K.G.; Chu, D.; Hammar, T.R.; Baldwin, K.C.; Mayer, L.A.; Hufnagle, L.C.; Jech, J.M. Protocols for calibrating multibeam sonar. *J. Acoust. Soc. Am.* **2005**, *117*, 2013–2027.

132. Demer, D.A.; Berger, L.; Bernasconi, M.; Bethke, E.; Boswell, K.; Chu, D.; Domokos, R.; Dunford, A.; Fassler, S.; Gauthier, S.; et al. *Calibration of acoustic instruments.*; International Council for the Exploration of the Sea (ICES), 2015;

133. Heaton, J.L.; Weber, T.C.; Rice, G.; Lurton, X. Testing of an extended target for use in high frequency sonar calibration. *Proc. Meet. Acoust.* **2013**, *19*, 005022.

134. Johannesson, K.A.; Mitson, R.B. *Fisheries Acoustics: A Practical Manual for Aquatic Biomass Estimation*; Food and Agriculture Organization of the United Nations, 1983; ISBN 978-92-5-101449-3.

135. Fusillo, L.; Moustier, C. de; Satriano, J.H.; Zietz, S. In-situ far-field calibration of multibeam sonar arrays for precise backscatter imagery. In Proceedings of the OCEANS 96 MTS/IEEE Conference Proceedings. The Coastal Ocean - Prospects for the 21st Century; 1996; pp. 47-49 suppl.

136. Eleftherakis, D.; Berger, L.; Le Bouffant, N.; Pacault, A.; Augustin, J.-M.; Lurton, X. Backscatter calibration of high-frequency multibeam echosounder using a reference single-beam system, on natural seafloor. *Mar. Geophys. Res.* **2018**, *39*, 55–73.

137. Ladroit, Y.; Lamarche, G.; Pallentin, A. Seafloor multibeam backscatter calibration experiment: comparing 45°-tilted 38-kHz split-beam echosounder and 30-kHz multibeam data. *Mar. Geophys. Res.* **2018**, *39*, 41–53.

138. Lurton, X.; Eleftherakis, D.; Augustin, J.-M. Analysis of seafloor backscatter strength dependence on the survey azimuth using multibeam echosounder data. *Mar. Geophys. Res.* **2018**, *39*, 183–203.

139. Dolan, M.F.J.; Lucieer, V.L. Variation and Uncertainty in Bathymetric Slope Calculations Using Geographic Information Systems. *Mar. Geod.* **2014**, *37*, 187–219.

140. Zhu, S.; Tang, G.; Xiong, L.; Zhang, G. Uncertainty of slope length derived from digital elevation models of the Loess Plateau, China. *J. Mt. Sci.* **2014**, *11*, 1169–1181.

141. Long, D.G.; Skouson, G.B. Calibration of spaceborne scatterometers using tropical rain forests. *IEEE Trans. Geosci. Remote Sens.* **1996**, *34*, 413–424.

142. Prigent, C.; Aires, F.; Jimenez, C.; Papa, F.; Roger, J. Multiangle Backscattering Observations of Continental Surfaces in Ku-Band (13 GHz) From Satellites: Understanding the Signals, Particularly in Arid Regions. *IEEE Trans. Geosci. Remote Sens.* **2015**, *53*, 1364–1373.

143. Seabird Electronics Inc. Application Note No. 6. Determination of Sound Velocity from CTD data. 2004.

144. Beaudoin, J.; Hiebert, J.; Calder, B.R.; Imahori, G. Uncertainty Wedge Analysis: Quantifying the Impact of Sparse Sound Speed Profiling Regimes on Sounding Uncertainty.; Norfolk, VA, USA, 2009; p. 27.

145. Ainslie, M.A.; McColm, J.G. A simplified formula for viscous and chemical absorption in sea water. *J. Acoust. Soc. Am.* **1998**, *103*, 1671–1672.

146. Francois, R.E.; Garrison, G.R. Sound absorption based on ocean measurements. Part II: Boric acid contribution and equation for total absorption. *J. Acoust. Soc. Am.* **1982**, *72*, 1879–1890.

147. Doonan, I.J.; Coombs, R.F.; McClatchie, S. The absorption of sound in seawater in relation to the estimation of deep-water fish biomass. *ICES J. Mar. Sci.* **2003**, *60*, 1047–1055.

148. Kim, Y.S.; Moore, K.; Onstott, G. *Scattering Coefficient Estimation: An Examination of the Narrow-Beam Approximation.*; Kansas University Remote Sensing Lab /Center for Research Inc., 1982; p. 42;.

149. Ulaby, F.T.; Allen, C.T.; Fung, A.K. Method for Retrieving the True Backscattering Coefficient from Measurements with a Real Antenna. *IEEE Trans. Geosci. Remote Sens.* **1983**, *GE-21*, 308–313.

150. Wang, Q.; Gogineni, S. A numerical procedure for recovering scattering coefficients from measurements with wide-beam antennas. *IEEE Trans. Geosci. Remote Sens.* **1991**, *29*, 778–783.

151. Matsumoto, H.; Dziak, R.P.; Fox, C.G. Estimation of seafloor microtopographic roughness through modeling of acoustic backscatter data recorded by multibeam sonar systems. *J. Acoust. Soc. Am.* **1993**, *94*, 2776–2787.

152. Ladroit, Y.; Sintès, C.; Lurton, X.; Garello, R. Extended scatterers model for fast sonar signal simulation. In Proceedings of the 2012 Oceans - Yeosu; 2012; pp. 1–5.

153. Gallaudet, T.C. Shallow water acoustic backscatter and reverberation measurements using a 68-kHz cylindrical array. PhD Dissertation, University of California, San Diego, 2001.

154. QPS Technical Note: Correcting backscatter for seafloor 3D incidence 2014.

155. Mandel, J. *The statistical analysis of experimental data.*; Interscience Publishers: New York, 1964;

156. Bjørnø, L.; Neighbors, T.; Bradley, D. *Applied underwater acoustics*; 2017; ISBN 978-0-12-811247-2.

157. Goodchild, M.F.; Gopal, S. *The Accuracy of spatial databases*; Taylor & Francis: New York NY USA, 1989; ISBN 978-0-85066-847-6.

158. Kiiveri, H.T. Assessing, representing and transmitting positional uncertainty in maps. *Int. J. Geogr. Inf. Sci.* **1997**, *11*, 33–52.

159. Congalton, R. *Quantifying Spatial Uncertainty in Natural Resources: Theory and Applications for GIS and Remote Sensing*; Mowrer, H.T., Congalton, R.G., Eds.; 1 edition.; CRC Press: Chelsea, Mich, 2000; ISBN 978-1-57504-131-5.

160. Zhang, J.; Goodchild, M.F. *Uncertainty in Geographical Information*; CRC Press, 2002; ISBN 978-0-203-47132-6.

161. Malik, M.; Lurton, X.; Mayer, L. A framework to quantify uncertainties of seafloor backscatter from swath mapping echosounders. *Mar. Geophys. Res.* **2018**, *39*, 151–168.

162. Stephens, D.; Diesing, M. A Comparison of Supervised Classification Methods for the Prediction of Substrate Type Using Multibeam Acoustic and Legacy Grain-Size Data. *PLOS ONE* **2014**, *9*, e93950.

163. Kloser, R.J.; Penrose, J.D.; Butler, A.J. Multi-beam backscatter measurements used to infer seabed habitats. *Cont. Shelf Res.* **2010**, *30*, 1772–1782.

164. Amiri-Simkooei, A.; Snellen, M.; Simons, D.G. Riverbed sediment classification using multi-beam echo-sounder backscatter data. *J. Acoust. Soc. Am.* **2009**, *126*, 1724–1738.

165. Neteler, M.; Mitasova, H. *Open Source GIS: A GRASS GIS Approach*; 3rd ed.; Springer US: New York NY USA, 2008; ISBN 978-0-387-35767-6.

166. Horn, B.K.P. Hill shading and the reflectance map. *Proc. IEEE* **1981**, *69*, 14–47.

167. Jones, K.H. A comparison of algorithms used to compute hill slope as a property of the DEM. *Comput. Geosci.* **1998**, *24*, 315–323.

168. Goulden, T.; Hopkinson, C.; Jamieson, R.; Sterling, S. Sensitivity of DEM, slope, aspect and watershed attributes to LiDAR measurement uncertainty. *Remote Sens. Environ.* **2016**, *179*, 23–35.

169. Kongsberg Inc. EM 3002 product description (855-164771 / Rev.E / 20.06.2006) Available online: https://www.km.kongsberg.com/ks/web/nokbg0397.nsf/AllWeb/7C8510CFA3CD21ABC1256CF00052DD1C/$file/164771ae_EM3002_Product_spec_lr.pdf.

170. *QIMERA 1.6.0*; Quality Positioning Services BV (QPS): Zeist, The Netherlands, 2018;

171. *FMGT - Fledermaus Geocoder Toolbox 7.8.0*; Quality Positioning Services BV (QPS): Zeist, The Netherlands, 2018;

172. *ARC MAP 10.3*; Environmental Systems Research Institute - ESRI: Redlands, CA, 2014;

173. Mukherjee, S.; Mukherjee, S.; Bhardwaj, A.; Mukhopadhyay, A.; Garg, R.D.; Hazra, S. Accuracy of Cartosat-1 DEM and its derived attribute at multiple scale representation. *J. Earth Syst. Sci.* **2015**, *124*, 487–495.

174. Buscombe, D.; Grams, P.E.; Kaplinski, M.A. Compositional Signatures in Acoustic Backscatter Over Vegetated and Unvegetated Mixed Sand-Gravel Riverbeds. *J. Geophys. Res. Earth Surf.* **2017**, *122*, 1771–1793.

175. Marks, K.M.; Smith, W.H.F. An uncertainty model for deep ocean single beam and multibeam echo sounder data. *Mar. Geophys. Res.* **2008**, *29*, 239–250.

176. Rice, G.; Greenaway, S. NOAA Ship Fairweather Launch 2017 SAT | Multibeam Advisory Committee Available online: http://mac.unols.org/reports/noaa-ship-fairweather-launch-2017-sat (accessed on Mar 20, 2019).

177. Beaudoin, J.; Johnson, P.; Lurton, X.; Augustin, J.M. SAT and Trial Cruise of the Acoustical Sensors Onboard R/V Falkor. Available online: http://mac.unols.org/sites/mac.unols.org/files/20120904_Falkor_EM710_EM302_report.pdf (accessed on Mar 20, 2019).

178. Dark, S.J.; Bram, D. The modifiable areal unit problem (MAUP) in physical geography. *Prog. Phys. Geogr.* **2007**, *31*, 471–479.

179. Chang, K.; Tsai, B. The Effect of DEM Resolution on Slope and Aspect Mapping. *Cartogr. Geogr. Inf. Syst.* **1991**, *18*, 69.

180. de Moustier, C. State of the Art in Swath Bathymetry Survey Systems. *Int. Hydrogr. Rev.* **1988**.

181. Lamarche, G.; Lurton, X. Recommendations for improved and coherent acquisition and processing of backscatter data from seafloor-mapping sonars. *Mar. Geophys. Res.* **2018**, *39*, 5–22.

182. Dufek, T. Backscatter Analysis of Multibeam Sonar Data in the Area of the Valdivia Fracture Zone using Geocoder in CARIS HIPS&SIPS and IVS3D Fledermaus. MSc Thesis, Hafencity University Hamburg, 2012.

183. Roche, M.; Degrendele, K.; Mol, L.D. Constraints and limitations of MBES Backscatter Strength (BS) measurements for monitoring the seabed. Surveyor and geologist point of view. In Proceedings of the GeoHab (Maine Geological and Biological Habitat Mapping); Rome, Italy, 2013; p. 21.

184. Roche, M.; Degrendele, K.; Vrignaud, C.; Loyer, S.; Le Bas, T.; Augustin, J.-M.; Lurton, X. Control of the repeatability of high frequency multibeam echosounder backscatter by using natural reference areas. *Mar. Geophys. Res.* **2018**, *39*, 89–104.

185. Malik, M. Sources and Impacts of Bottom Slope Uncertainty on Estimation of Seafloor Backscatter from Swath Sonars. *Geosciences* **2019**, *9*, 183.

186. *Teledyne Computer Aided Resource Information System (CARIS) HIPS and SIPS*; Teledyne CARIS Inc.: Fredericton, Canada;

187. Augustin, J. SonarScope® software on-line presentation. Available online: http://flotte.ifremer.fr/fleet/Presentation-of-the-fleet/Logiciels-embarques/SonarScope. (accessed on Jun 6, 2019).

188. Kongsberg Inc. Kongsberg Multibeam Echo Sounder EM Datagram Formats. Available online: https://kmdoc.kongsberg.com/ks/web/nokbg0397.nsf/AllWeb/253E4C58DB98DDA4C1256D790048373B/$file/160692_em_datagram_formats.pdf?OpenElement.

189. Teledyne Reson Teledyne Reson Data Format Definition Document. 7k Data Format, Volue 1, Version 3.01.

190. Gavrilov, A.; Duncan, A.; McCauley, R.; Parnum, I.; Penrose, J.; Siwabessy, P.; Woods, A.J.; Tseng, Y.-T. Characterization of the seafloor in Australia's coastal zone using acoustic techniques. In Proceedings of the Proceedings of the 1st International Conference on Underwater Acoustic Measurements: Technologies & Results; Foundation for Research and Technology, 2005; pp. 1075–1080.

191. Parnum, I.M.; Tyler, E.; Miles, P. Software for rapid visualisation and analysis of multibeam echosounder water column data. In Proceedings of the ICES Symposium on Marine Ecosystem Acoustics; Nantes, France, 2015.

192. *Directive 2008/56/EC of the European Parliament and of the Council of 17 June 2008 establishing a framework for community action in the field of marine environmental policy (Marine Strategy Framework Directive) (Text with EEA relevance)*; 2008; Vol. OJ L;

193. Lucieer, V.; Walsh, P.; Flukes, E.; Butler, C.; Proctor, R.; Johnson, C. *Seamap Australia–A national seafloor habitat classification scheme*; Hobart: Institute for Marine and Antarctic Studies (IMAS), University of …, 2017;

194. Buhl-Mortensen, L.; Buhl-Mortensen, P.; Dolan, M.F.J.; Holte, B. The MAREANO programme – A full coverage mapping of the Norwegian off-shore benthic environment and fauna. *Mar. Biol. Res.* **2015**, *11*, 4–17.

195. Manzella, G.; Griffa, A.; de la Villéon, L.P. *Report on data management best practice and Generic Data and Metadata models. V.2.1 [Deliverable 5.9]*; Ifremer for JERICO-NEXT Project, 2017;

196. Idaszak, R.; Investigator), D.G.T. (Principal; Yi, H.; Christopherson, L.; Stealey, M.J.; Miles, B.; Dash, P.; Couch, A.; Spealman, C.; Horsburgh, J.S.; et al. HydroShare – A Case Study of the Application of Modern Software Engineering to a Large Distributed Federally-Funded Scientific Software Development Project Available online: https://www.taylorfrancis.com/ (accessed on Jun 26, 2019).

197. Hannay, J.E.; MacLeod, C.; Singer, J.; Langtangen, H.P.; Pfahl, D.; Wilson, G. How do scientists develop and use scientific software? In Proceedings of the 2009 ICSE Workshop on Software Engineering for Computational Science and Engineering; 2009; pp. 1–8.

198. Hook, D.; Kelly, D. Testing for trustworthiness in scientific software. In Proceedings of the 2009 ICSE Workshop on Software Engineering for Computational Science and Engineering; 2009; pp. 59–64.

199. Howison, J.; Deelman, E.; McLennan, M.J.; Ferreira da Silva, R.; Herbsleb, J.D. Understanding the scientific software ecosystem and its impact: Current and future measures. *Res. Eval.* **2015**, *24*, 454–470.

200. *Software engineering for science*; Carver, J., Hong, N.P.C., Thiruvathukal, G.K., Eds.; Computational science series; Taylor & Francis, CRC Press: Boca Raton, 2017; ISBN 978-1-4987-4385-3.

201. Hughes Clarke, J.E.; Iwanowska, K.K.; Parrott, R.; Duffy, G.; Lamplugh, M.; Griffin, J. Inter-calibrating multi-source, multi-platform backscatter data sets to assist in compiling regional sediment type maps : Bay of Fundy.; 2008; p. 23.

202. Feldens, P.; Schulze, I.; Papenmeier, S.; Schönke, M.; Schneider von Deimling, J. Improved Interpretation of Marine Sedimentary Environments Using Multi-Frequency Multibeam Backscatter Data. *Geosciences* **2018**, *8*, 214.

203. Pendleton, L.H.; Beyer, H.; Estradivari; Grose, S.O.; Hoegh-Guldberg, O.; Karcher, D.B.; Kennedy, E.; Llewellyn, L.; Nys, C.; Shapiro, A.; et al. Disrupting data sharing for a healthier ocean. *ICES J. Mar. Sci.*

204. Franken, S.; Kolvenbach, S.; Prinz, W.; Alvertis, I.; Koussouris, S. CloudTeams: Bridging the Gap Between Developers and Customers During Software Development Processes. *Procedia Comput. Sci.* **2015**, *68*, 188–195.

205. Mackenzie, B.; Celliers, L.; Assad, L.P. de F.; Heymans, J.J.; Rome, N.; Thomas, J.; Anderson, C.; Behrens, J.; Calverley, M.; Desai, K.; et al. The Role of Stakeholders in Creating Societal Value From Coastal and Ocean Observations. *Front. Mar. Sci.* **2019**, *6*.

206. Legendre, P. Reply to the comment by Preston and Kirlin on "Acoustic seabed classification: improved statistical method." *Can. J. Fish. Aquat. Sci.* **2003**, *60*, 1301–1305.
207. Masetti, Giuseppe; Augustin, J.M.; Malik, M.; Poncelet, C.; Lurton, X.; Mayer, L.A.; Rice, G.; Smith, M. The Open Backscatter Toolchain (OpenBST) project: towards an open-source and metadata-rich modular implementation. In Proceedings of the US Hydro; Biloxi MS, 2019.
208. Malik, M.; Schimel, A.; Masetti, G.; Roche, M.; Deunf, J.L.; Dolan, M.; Beaudoin, J.; Augustin, J.M.; Travis, H.; Parnum, I. Results from the first phase of the Backscatter Software Inter-comparison Project. *Geosci. Submitt.* **2019**.
209. Simmonds, E.J.; International Council for the Exploration of the Sea, C. (Denmark) eng; Williamson, N.J.; Gerlotto, F.; Aglen, A. Acoustic survey design and analysis procedure: a comprehensive review of current practice. **1992**.
210. Maclennan, D. A consistent approach to definitions and symbols in fisheries acoustics. *ICES J. Mar. Sci.* **2002**, *59*, 365–369.